UNIVERSITÀ
DEGLI STUDI
DI PADOVA

Dipartimento di Agronomia Animali Alimenti Risorse Naturali e Ambiente - DAFNAE

SCUOLA DI DOTTORATO DI RICERCA
IN SCIENZE DELLE PRODUZIONI VEGETALI
INDIRIZZO: AGRONOMIA AMBIENTALE
CICLO: XXV

Multiscale Soil Salinity Assessment at the Southern Margin of the Venice Lagoon, Italy

Direttore della Scuola: Ch.mo Prof. Angelo Ramina

Coordinatore d'indirizzo: Ch.mo Prof. Antonio Berti

Supervisore: Ch.mo Prof. Francesco Morari

Dottorando: Elia Scudiero

DATA CONSEGNA TESI
31 gennaio 2013

Declaration

I hereby declare that this submission is my own work and that, to the best of my knowledge and belief, it contains no material previously published or written by another person nor material which to a substantial extent has been accepted for the award of any other degree or diploma of the university or other institute of higher learning, except where due acknowledgment has been made in the text.

Elia Scudiero, January 31st 2013

A copy of the thesis will be available at *http://paduaresearch.cab.unipd.it/*

Dichiarazione

Con la presente affermo che questa tesi è frutto del mio lavoro e che, per quanto io ne sia a conoscenza, non contiene materiale precedentemente pubblicato o scritto da un'altra persona né materiale che è stato utilizzato per l'ottenimento di qualunque altro titolo o diploma dell'università o altro istituto di apprendimento, a eccezione del caso in cui ciò venga riconosciuto nel testo.

Elia Scudiero, 31 gennaio 2013

Una copia della tesi sarà disponibile presso *http://paduaresearch.cab.unipd.it/*

"A nation that destroys its soils destroys itself"

Franklin D. Roosevelt

Table of Contents

Riassunto

L'intrusione salina interessa molte zone costiere del mondo con effetti negativi sulla qualità dell'acqua di falda e del suolo. Per gestire i problemi di salinità è necessario capirne le dinamiche temporali a livello di profilo di suolo e la variabilità spaziale a scala di campo. Tecniche geofisiche, in particolare l'utilizzo della conducibilità elettrica apparente (EC_a), sono state utilizzate negli ultimi decenni per stimare la salinità del suolo e della soluzione circolante. A scala puntuale la bontà delle misure di salinità della soluzione circolante è legata alla giusta interpretazione del rapporto che la lega ad EC_a, alle caratteristiche del suolo e al contenuto idrico. Inoltre, i sensori che misurano l'umidità del suolo spesso forniscono misure falsate in suoli salini e con alto contenuto di argilla e/o sostanza organica. A scala di campo il proximal-sensing può essere utile per caratterizzare vaste porzioni di territorio a partire da un numero relativamente ridotto di campioni di suolo. Spesso la caratterizzazione della salinità non è sufficiente per capire la variabilità spaziale delle rese colturali, che può essere influenzata da altre caratteristiche del suolo. Capendo come la salinità e altre proprietà del suolo influenzano la produttività agraria può essere utile per identificare delle aree in cui apportare interventi agronomici sito-specifici.

L'obiettivo generale di questo lavoro è valutare delle metodologie per monitorare e caratterizzare la salinità del suolo ed altri parametri chimico-fisici del suolo ad essa legati, con l'ausilio di sensori, sia a scala puntuale che di campo. In particolare a scala puntuale si affrontano le problematiche relative all'utilizzo di sensoristica capacitivo-resistiva per stimare il contenuto volumetrico e la salinità della soluzione circolante. Mentre a scala di campo si propongono delle metodologie per caratterizzare la variabilità spaziale della salinità del suolo e di altre proprietà che influenzano la resa di *Zea mais* L. con l'utilizzo di tecniche di proximal-sensing del suolo. Questa tesi riguarda i suoli di un'area di studio interessata da intrusione salina, al margine meridionale della Laguna di Venezia.

La tesi è strutturata in cinque capitoli. Il primo include una *review* sulla metodologia comunemente usata per caratterizzare la salinità del suolo con metodi geofisici sia a scala puntuale che di campo. È inoltre presentata una panoramica introduttiva sulle

problematiche ambientali relative alla zona a sud della Laguna di Venezia. Il secondo capitolo si concentra sulla calibrazione di una sonda (low-cost) capacitivo-resistiva da utilizzare per stime in continuo di contenuto idrico volumetrico e salinità della soluzione circolante. Il terzo capitolo propone una metodologia per ottimizzare schemi di campionamento del suolo sulla base della variabilità spaziale di misure geofisiche. Il quarto capitolo analizza la variabilità spaziale della resa colturale in funzione delle proprietà chimico-fisiche del suolo e propone l'utilizzo di dati di proximal-sensing del suolo ad esse correlati per identificare delle aree di gestione omogenee. Infine, l'ultimo capitolo riporta le conclusioni generali e delle note conclusive sui lavori presentati nella tesi.

Summary

Saltwater intrusion affects many coastlands around the world contaminating fresh-groundwater and decreasing soil quality. In order to manage saline soils one should understand the spatiotemporal dynamics of salinity in the soil profile and its spatial variability at field scale. In the last decades, soil and pore-water salinity have been assessed using geophysical techniques, most commonly with the use of apparent electrical conductivity (EC_a) measurements. At point-scale, pore-water salinity can be estimated once its relationship with EC_a, soil properties, and water content is understood. Moreover, most sensors for water content estimation normally provide biased readings in saline conditions and in soil with high clay and organic carbon contents. At field-scale proximal-sensing can be used to characterize large portions of land from a relatively small number of soil samples. Sometimes, characterizing salinity is however not sufficient to understand crop yield spatial variability, which can be also influenced by other soil properties. Understanding the influence of salinity and other soil properties on crop productivity can be useful in the identification of areas that can be managed site-specifically.

The general aim of this dissertation is to evaluate some sensor-based methodologies for monitoring and characterizing salinity and other related soil properties both at point- and field-scale. In particular, at point-scale the dissertation will deal with the issues regarding the use of capacitive-resistive technology for water content and pore-water salinity estimation. At field-scale some methodologies will be proposed in order to characterize the spatial variability of salinity and other soil properties influencing maize (*Zea mais* L.) yield using soil proximal-sensing. All the material presented in this manuscript regard the soils of an area affected by saltwater intrusion located at the southern edge of the Venice Lagoon (Italy).

The dissertation is structured in five chapters. The first one includes a review on commonly used methodologies for point- and field-scale salinity assessment. An overview on the environmental issues concerning the coastland at the southern margin of the Venice Lagoon is also presented. The second chapter deals with the calibration of a low-cost capacitance-resistance probe for simultaneous monitoring of soil water content and

salinity. In the third chapter an EC_a-directed soil sampling scheme optimization procedure is proposed. The forth chapter analyzes maize yield as a function of soil chemical and physical properties and investigates on the use of soil-proximal sensing correlated to soil spatial variability for site-specific management units. The final chapter presents the general conclusions of the work.

Chapter 1

General Introduction

1. Soil salinity, salt water intrusion and field scale assessment of soil salinity

The term salinity refers to the presence of the major dissolved inorganic solutes (basically Na^+, Mg^{2+}, Ca^{2+}, K^+, Cl^-, SO_4^{2-}, HCO_3^-, NO_3^-, and CO_3^{2-}) in the soil (Rhoades et al., 1999). The salinity of a solution can be quantified in terms of its electrical conductivity (*EC*; dS m^{-1}), which is strictly related to the total concentration of dissolved salts, with 1 dS m^{-1} being approximately equivalent to 10 meq L^{-1} at 25°C (Richards and US Salinity Laboratory Staff, 1954).

High soil salinity values can result in plant stress which, in severe cases, could even lead to crop failure. When soil solution is too concentrated in salts, the osmotic potential is reduced, and it becomes harder for plants to extract water from the soil-matrix. Specific-ion toxicity could also occur (e.g. Na^+ toxicity). Moreover, soil salinity can unbalance the nutritional equilibrium of plants. Finally, soil salinity may in certain cases influence soil structure: high levels of sodium can cause soil deflocculation of soil colloids (i.e. clays and soil organic matter), which influences soil permeability and tilth.

Salinity accumulates in soils as a consequence of various processes, which take place according to geomorphological settings and local climate (Corwin et al., 2012). In arid and semi-arid environments, where precipitation is minimal, salts accumulate as a consequence of the evapotranspiration process (ET): when soil-water flows upwards, salts are transported from the groundwater to the rootzone. The shallower the groundwater, then the closer to the soil surface salts can accumulate. Irrigation and precipitation can, however, leach down salts. Specifically, in environments (e.g. the one discussed in this dissertation) where yearly precipitations are larger than the amount of water lost by ET, salts accumulate during dry and semi-dry summers and then leach down during rainy fall and spring seasons. Nevertheless, when water table is very shallow, considerable amounts of salts can be transported to the rootzone by the ET process during summer, limiting therefore plant production (Corwin et al., 2012). The amount of salts that are transported into the rootzone depends much on the salinity of the groundwater, soil type (e.g. texture), and plant type.

Salts found in groundwater are generally originated by dissolution from rocks. The spatial distribution of saline groundwater is however dependent on many factors: it could be

either originated locally or be transported into a place via several processes, such as irrigation, excessive fertilization, and, along the coastlines, by saltwater intrusion.

Saltwater intrusion is a common process along coastlands. As reported by (Tóth et al., 2008), the coastland around the Venice Lagoon, is particularly affected by this phenomenon. Saltwater intrusion acts according to the Ghyben-Herzberg relation (Bear, 1988). In areas below sea level, where land is continuously drained by pumping stations, the situation resembles what shown in Fig. 1.1: the fresh-groundwater / saline-groundwater interface upshifts towards the soil surface (Bear, 1988).

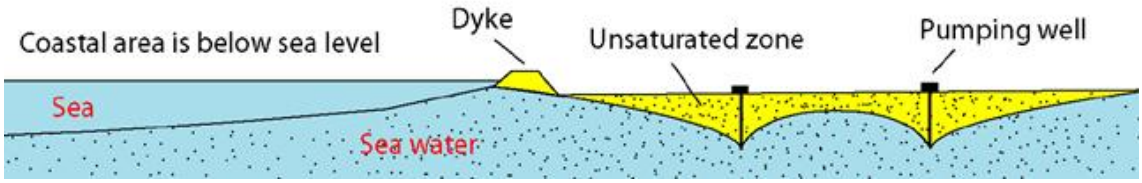

Figure 1.1. Upshift of the freshwater / saltwater interface in a coastal area lying below sea level and in need of continuous draining. Modified after Bear (1988).

Soil salinity is generally determined measuring the electrical conductivity of aqueous extracts of saturated soil-pastes (EC_e) or of other soil to water ratios extracts (e.g. 1:2 and 1:5 ratios, as advised in (Ministero delle Politiche Agricole e Forestali, 1998)). However, such determination methods are destructive, time-consuming, and not representative of the real salinity status of soils at actual field conditions (Rhoades et al., 1999). To determine the real state (i.e. at actual soil water contents) of stress affecting crops and to monitor fluxes of salts (e.g. upward fluxes through the soil profile) the electrical conductivity of the pore-water (EC_p) should be measured. Although such piece of information is very important it has not been frequently used as unpractical to assess at point scale and nearly impossible at field scale. Soil water can be extracted with microlysimeters, which are generally installed through the soil profile. With such implementation, pore-water is extracted whenever negative pressure is forced into the microlysimeters. This procedure is quite reliable at medium to high soil water contents, but clearly cannot provide continuous measures, as it would be too time-expensive. Sensors directly measuring EC_p are available, (i.e. the one described by (Rhoades and

Oster, 1986)), but not reliable, as they are not accurate in time, and sensitivity when changes in EC_p are small. Sensors that indirectly estimate EC_p with continuous measurements are also available. These types of sensors provide readings of the bulk (or apparent) soil electrical conductivity (EC_a), which varies according to EC_p, soil moisture, and soil type. Therefore, soil solution, solid soil particles, and chargeable surface of soil colloids, all contribute to the conductance measured as EC_a (Corwin, 2003). According to (Rhoades et al., 1989), three pathways of current flow contribute to the EC_a measurement (Fig. 1.2): current through the soil solution in the large pores (*the liquid phase pathway*); current through the soil particles that are in continuous and direct contact with one another (*the solid pathway*); and current through exchange complexes on the surface of soil colloids (*the soil-liquid phase pathway*). Rhoades et al. (Rhoades et al., 1989) showed positive significant correlations between EC_a with soil water content, EC_p, and clay content.

As consequence of such complexity, EC_a values are not only a function of pore-water salinity but of several other soil physical and chemical properties, including soil water content, texture, organic carbon content, and bulk density (Corwin and Lesch, 2005).

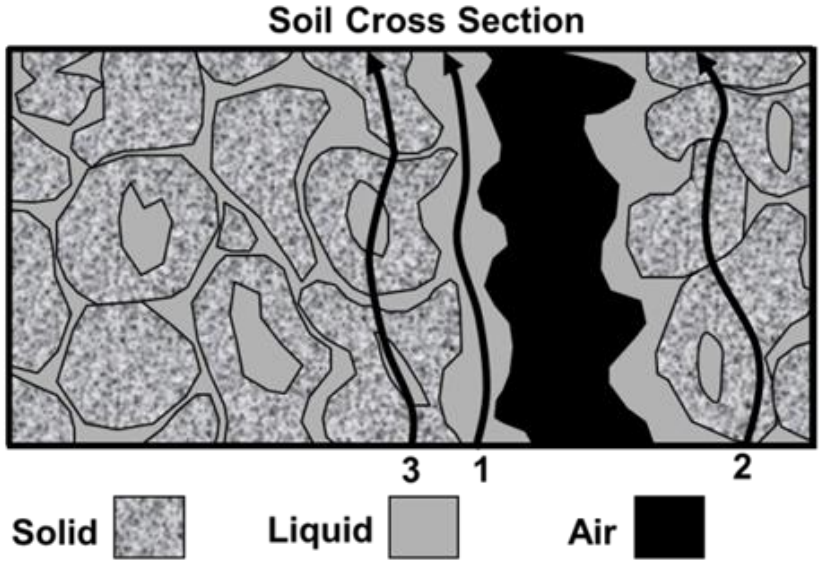

Figure 1.2. Schematic representation of the three conductance pathways of apparent soil electrical conductivity in an unsaturated soil: 1, *the liquid phase pathway*; 2, *the soil pathway*; 3, *the soil-liquid phase pathway*. Modified from Rhoades et al. (1989).

Several models have been developed to estimate EC_p from EC_a readings, at known water contents. A comparison between various models to determine EC_p can be found in (Amente et al., 2000; Friedman, 2005; Hamed and Magnus Berndtsson, 2003; Persson, 2002). At point scale, EC_a is commonly monitored either with time domain reflectometry (TDR) (Dalton et al., 1984) or electrical resistivity (ER) (Rhoades et al., 1999) techniques. The recent development of inexpensive multisensor probes, providing soil moisture and EC_a data, has contributed on making easy to continuously assess EC_p.

2. Implementing field-scale EC_a surveys in precision agriculture

Field surveys of EC_a have been used in the last 25 years, to assess the spatial distribution of soil salinity. Mobile ER and electromagnetic induction (EMI) are most commonly used techniques (Corwin and Lesch, 2005). However, as mentioned earlier, salinity is not the only soil property contributing to the spreading of electrical current through soil. EC_a values have in fact been correlated to many soil properties. The kinds of correlations that can be highlighted depend much on the type of soil sensed and on its location. Corwin and Lesch (Corwin and Lesch, 2005) propose a list of studies in which EC_a measurements were used to directly or indirectly assess the spatial distribution of specific soil properties (Table 1.1).

Table 1.1. List of the soil properties assessed by EC_a measurements as reported by Corwin and Lesch (2005).

Directly measured soil properties	**Indirectly measured soil properties**
Salinity (and nutrients, e.g. NO_3^-)	Organic matter related (including soil organic carbon, and organic chemical plumes)
Water content	Cation exchange capacity
Texture-related (e.g. sand, clay, depth to claypans or sand layers)	Leaching
Bulk density related (e.g. compaction)	Groundwater recharge
	Herbicide partition coefficients
	Soil map unit boundaries
	Corn rootworm distributions
	Soil drainage classes

In precision agriculture, EC_a is often used in order to describe the spatial distribution of soil properties influencing yield. Unfortunately, yield inconsistently correlates with EC_a because it is influenced by soil factors other than those characterizing the EC_a values; and because of a temporal component of yield variability that is inefficiently represented by a state variable such as EC_a (Corwin and Lesch, 2003).

Typical implementations of EC_a in precision agriculture include (Corwin, 2008): *a)* EC_a directed soil sampling schemes optimizations and *b)* delineation of Site-Specific Management Units (SSMUs).

As stated by (Corwin et al., 2010), EC_a-directed soil sampling is advised for characterizing spatial variability on the basis that when EC_a correlates with soil properties, then a field-

scale EC_a surveys can be used to identify locations that represent the range and the variability of those soil properties in the area considered. Some examples of EC_a-directed soil sampling scheme delineation can be found in (Castrignanò et al., 2008), (Corwin et al., 2003b), (Lesch, 2005), and (Corwin et al., 2010).

The use of Site-Specific Management Units could help on improving the soil quality in those areas in which crop production is limited by adverse levels of several edaphic factors (e.g. salinity, pH, texture, etc.) (Robert, 2002). In fact, site-specific crop management aims to manage the soil, pests and crops based upon spatial variation within a field (Larson and Robert, 1991; Van Uffelen et al., 1997) by applying resources (water, fertilizers, etc.) when, where, and in the needed amount (Corwin and Lesch, 2010). Therefore a SSMU can be defined as a portion of land that is managed the same in order to achieve the same goal (Corwin et al., 2008). It could seem legitimate to delineate SSMUs on the base of yield maps or estimates. However, yield spatial variation is affected by a large range of factors, such as topographic, edaphic, biological, meteorological, and anthropogenic factors. For practical reasons, only a limited portion of these factors can be managed in order to increase crop productivity. Therefore, as suggested by (Corwin and Lesch, 2010), a simplified and effective way of designing SSMUs is to analyze the effect of a single factor class on yield spatial variability. As a matter of fact, the extent of yield variation related to edaphic properties can be considerably large (Corwin et al., 2003a; Vitharana et al., 2008). Furthermore, relatively non-expensive interventions (e.g. fertilization, controlled leaching, use of soil improvers, etc.) can be carried out on soil properties to improve soil productivity and/or quality.

As seen earlier, the spatial characterization of edaphic properties can be achieved with spatial EC_a measurements (Corwin and Lesch, 2005). When EC_a does not fully describe the soil variability which influences yield, other types of proximal sensors could be complementarily used. Proximal sensors are very popular in soil science as they allow gaining a very large amount of information on study areas with little time and cost. Moreover, such measures are nondestructive and the sensors are generally easy to operate. Indeed, several types of sensors have recently been used to provide ancillary data in order to characterize large areas on the basis of a limited number of soil samples

(Adamchuk et al., 2004; Mulder et al., 2011; Viscarra Rossel et al., 2011), including optical sensors (Ben-Dor et al., 2009), radiometric sensors (Lunt et al., 2005), mechanical sensors (Hemmat and Adamchuk, 2008), acoustic and pneumatic sensors (Adamo et al., 2004; Clement and Stombaugh, 2000; Liu et al., 1993), and electrochemical sensors (Sethuramasamyraja et al., 2008; Viscarra Rossel and Walter, 2004).

Some recent studies on the delineation of SSMUs guided by ancillary data from proximal sensors can be found in (Corwin et al., 2003a), (Li et al., 2007a; Li et al., 2007b), (Vitharana et al., 2008), (Johnson et al., 2008), and (Morari et al., 2009). Generally SSMUs are designed on the basis of a single soil sensor type data, which generally correlates only to a limited amount of soil properties.

In this dissertation, along with EC_a, bare-soil reflectance will be considered as complementary ancillary information, both in the visible (400-700 nm) and near-infrared (700-2500 nm) regions. Sensors measuring reflectance emit radiation directed toward the soil. A portion of that radiation is reflected back to the sensor. The remaining portion of the radiation is mainly adsorbed by the components of the soil (e.g. soil water, chemical bounds of the soil particles, etc.).

Soil reflectance in the visible range is closely related to soil color and water content (Post et al., 2000). As a matter of fact, high water content will increase the color intensity (Ellis and Mellor, 1995; Post et al., 2000). Soil color has been widely studied in the past and been connected to many soil properties (Torrent and Barron, 1993). Dark soils are generally characterized by high organic matter content and/or iron oxides (FitzPatrick, 1986; Leone and Escadafal, 2001). A lighter color, on the other side, can be used to identify areas rich in carbonate (Ellis and Mellor, 1995), or areas affected by high salinity (Metternicht and Zinck, 2003), or sandy areas (Goovaerts and Kerry, 2010; Rizzetto et al., 2002).

The near-infrared reflectance of soil is primarily related to the presence of OH, CH, and NH groups (Gomez et al., 2008). Nevertheless, near-infrared reflectance has been correlated with a wide range of soil properties, including total C, total N, water content, and texture (Chang et al., 2001; Viscarra Rossel et al., 2006). An improved benefit on

describing soil properties comes when visible and near-infrared data are joined. The use of these two ranges of wavelengths allowed predicting the spatial distribution of soil organic carbon (Gomez et al., 2008; Zhang et al., 2012) as well as soil color (Singh et al., 2004).

3. The southern margin of the Venice Lagoon: an endangered delta plain environment

Alike many delta plains around the world, the area south of the Venice Lagoon (Italy) is a precarious environment subject to both natural changes and anthropogenic pressure. Previous studies highlighted a number of critical problems affecting this low-lying area, including land subsidence, periodic flooding during severe winter storms, and saltwater intrusion (Carbognin et al., 2005a; Carbognin et al., 2006; Gambolati et al., 2005; Teatini et al., 2005; Tosi et al., 2009). The area is part of the greater Po and Adige rivers delta plain. The Po used to flow in the area but migrated down south as the shoreline moved eastward in the last 6000 years (Fig. 1.3) leaving behind many highly permeable sandy drifts consisting on ancient river forks (i.e. paleochannels). These paleochannels are generally orientated towards the Lagoon (Carbognin and Tosi, 2003; Rizzetto et al., 2002; Rizzetto et al., 2003).

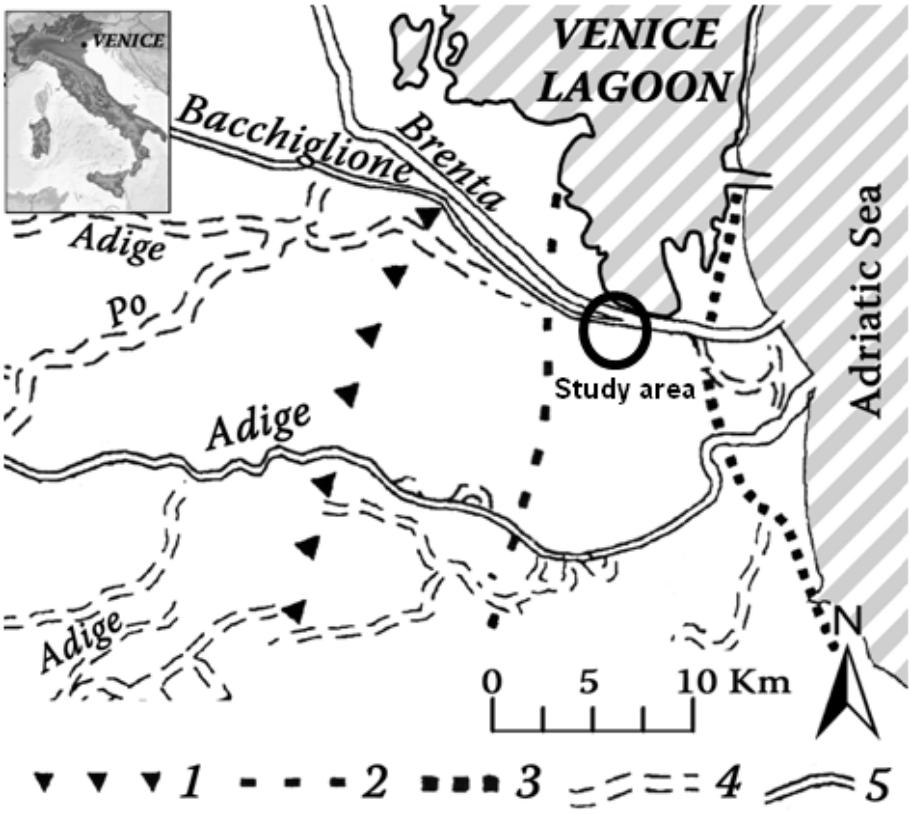

Figure 1.3. Map of the southern catchment of the Venice Lagoon. The coastline headway around (1) 5-6000 years B.P., (2) 4500 years B.P., and (3) 500 years B.P. The (4) past and (5) current locations of the larger rivers flowing in the area are highlighted. Modified after Rizzetto et al. (2002).

Saltwater intrusion and related soil salinization are potentially a major threat for agriculture. Such risk could be amplified by the combined future effects of land subsidence and sea-level rise. (Carbognin and Tosi, 2003; Carbognin et al., 2005b; De Franco et al., 2009; Rizzetto et al., 2003) showed that saline water may extend inshore up to 20 km far from the Adriatic Sea coastline, and that the saltwater plume is observed from the near ground surface down to 100 m depth. Moreover, the presence of the paleochannels could serve as preferential flow for the saltwater to intrude into the agricultural lands from the Venice Lagoon, the Adriatic Sea, and the various rivers and canals flowing in the area as reported by (Abarca et al., 2006) for the Llobregat delta plain in Spain.

Great portions of the Po and Adige delta plains were reclaimed from the 1890s to the 1960s and are nowadays kept constantly drained by the activity of several pumping stations allocated in the area. At the southern margin of the Lagoon, pumps control the height of the water table generally maintaining it very shallow (<1 m) in order to make rainfed farming possible. However being the area characterized by high spatial variability in both elevation and texture/water retention capacity, it is likely that water stress may occur in crops, in areas characterized by sandy soils and deep water table.

4. An introductory note on the study site

The study site (Fig. 1.4) was located at Ca' Bianca, Chioggia, Venice, Italy (45°10'57"N; 12°13'55"E; UTM, WGS84). The site is located at the southern margins of the Lagoon of Venice, North-East of Italy; in proximity to the Brenta and Bacchiglione Rivers; and approximately 7 km afar the Adriatic Sea shoreline. A draining house operates at the NW corner of the study area keeping it reclaimed; and reversing the drainage water into the Morto Canal, which then discharges its waters into the Bacchiglione River.

The original size of the study site was ca. 28 ha; however, even if the preliminary studies of this dissertation regarded the entire site (see Chapter 3), ca. 7 ha in the South Eastern corner were not sowed in 2010 and were thus removed from subsequent research (see Chapter 4). The field is cropped on maize (*Zea mais* L.) and harvested for grain.

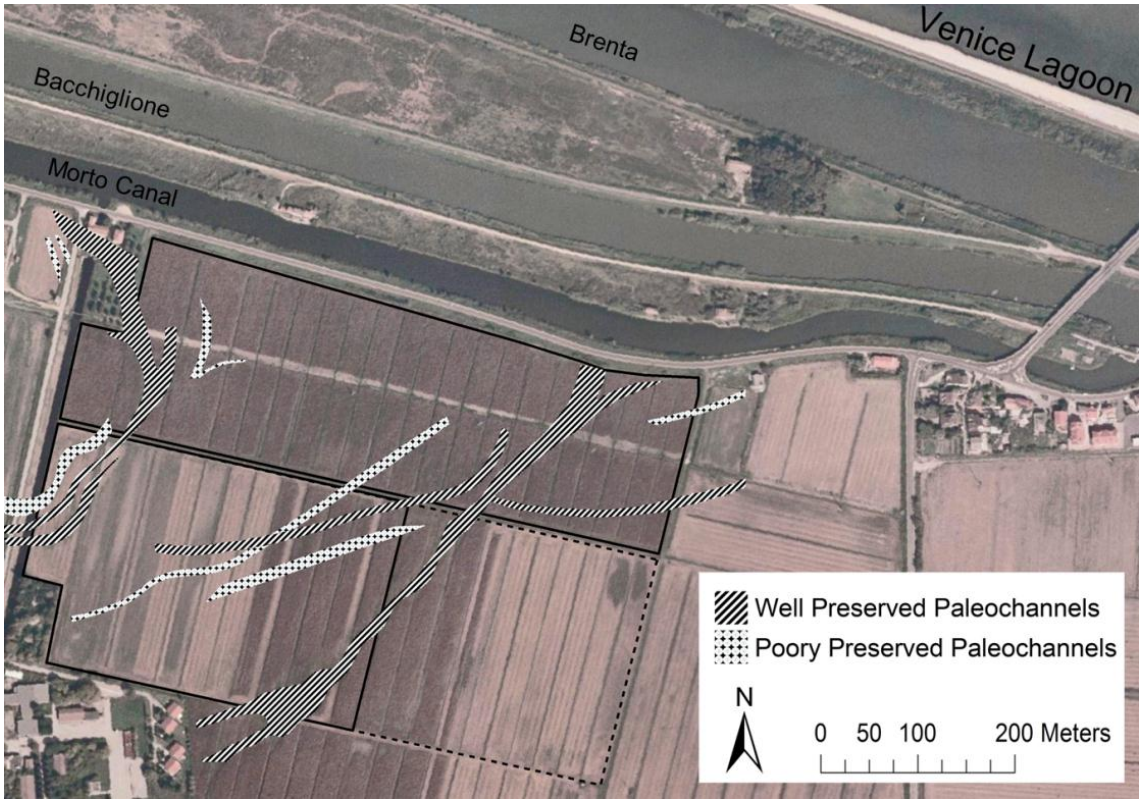

Figure 1.4. Aerial image of the study area at the southern margin of the Venice Lagoon, Italy; with a highlight on the paleochannels crossing it. The dashed line represents the portion of the study site that was not sowed in 2010.

Previous research conducted at the southern margin of the Venice Lagoon (Viezzoli et al., 2010) showed low bulk resistance values (Ωm = S m^{-1}) in the 0-5m soil increment in the study site, suggesting that this particular portion of land could be heavily affected by saltwater intrusion (Fig. 1.5). This evidence confirms the values displayed on the Venice Province salinity map (Vitturi et al., 2008) which indicates the study area as "very saline".

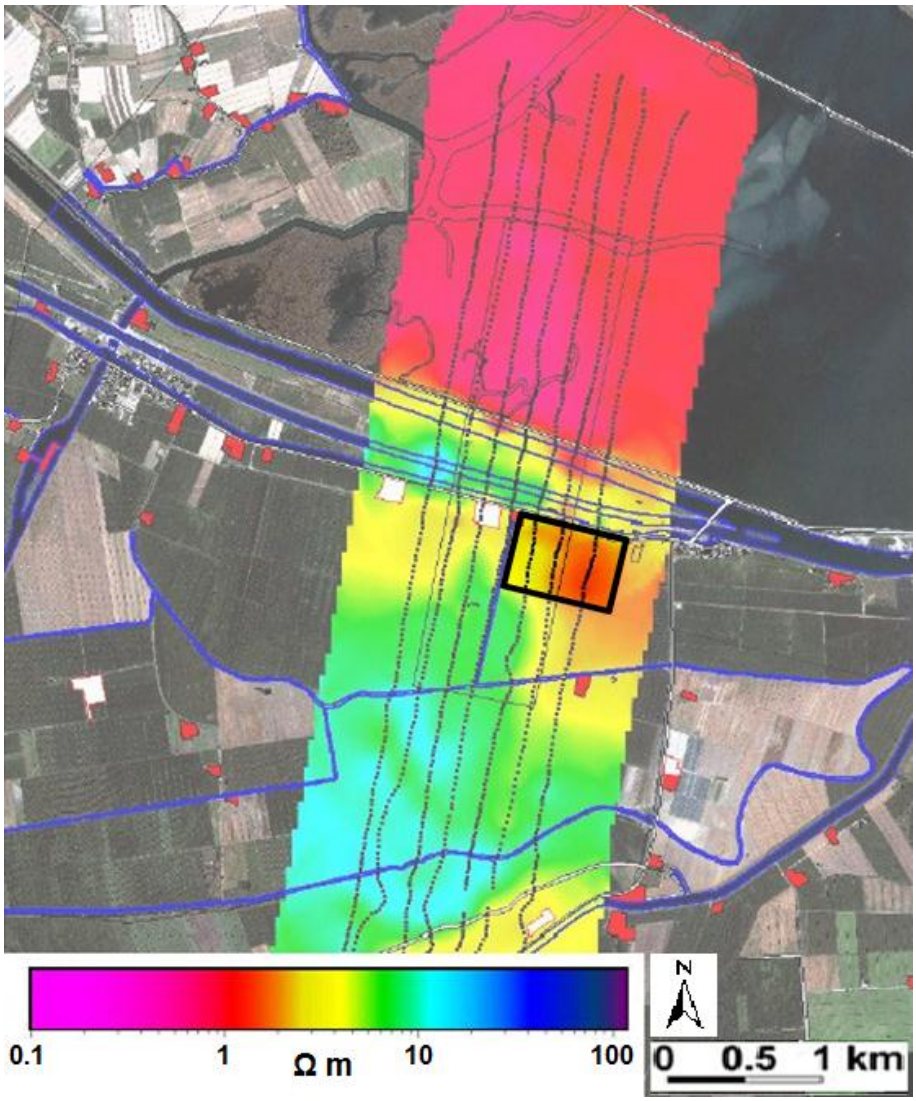

Figure 1.5. Airborne electromagnetics measuring soil apparent resistance (Ω m) in the 0-5 m soil increment; modified from (Viezzoli et al., 2010). The study area is highlighted.

5. Objectives

This dissertation aims to propose a set of tools and methodological approaches for salinity assessment at point- and field-scale, in a site characterized by a high heterogeneity of the geomorphological settings, typical of southern margin of the Venice Lagoon, Italy.

Firstly, the point-scale objectives of this work were to:

i) Investigate the relation between bulk electrical conductivity (EC_a) vs. pore-water electrical conductivity (EC_p), water content, and soil properties. In particular this work will focus on the interpretation of EC_a readings made with a two-array ER probe over a wide range of soil water contents and EC_p values on a set of five contrasting soil. Moreover, soil water content will be estimated from dielectric readings made with a capacitance probe. Capacitance probes are known for being very low-cost systems to determine the soil complex permittivity. However their readings are often biased by the high electrical conductivity of saline soils, or soils containing large amounts of colloids (i.e. clay and organic matter with chargeable surfaces) (Pardossi et al., 2009).

ii) Develop a reliable methodology for sensor-based continuous EC_p monitoring. In particular, some models found in the literature were tested. The fitting parameters of these models will be related to soil properties in order to reformulate each model with a "general" equation, applicable to a wide range of soils.

Secondly, the field-scale objectives of this work were to:

iii) Characterize the spatial distribution of soil salinity (and other relevant soil properties) using soil proximal-sensing methods. In the study site, the soil sampling scheme will be optimized according to the spatial measurements of EC_a, to ease the spatial characterization of salinity and the other soil properties commonly influencing the electrical conduction through the soil.

iv) Quantify the influence of salinity and other soil properties on maize yield. Especially in areas characterized by contrasting geomorphological settings, several soil characteristics are likely to influence crop yield at once. Moreover, Site-Specific Management Units (SSMUs) will be delineated and validated according to soil spatial variability and yield

spatio-temporal variability. The SSMU delineation methodology that will be proposed could be used both to identify areas of interest (e.g. saline areas) and to plan sustainable and profitable site-specific managing strategies.

6. References

Abarca, E., E. Vázquez-Suñé, J. Carrera, B. Capino, D. Gámez and F. Batlle. 2006. Optimal design of measures to correct seawater intrusion. Water Resour. Res. 42:W09415.

Adamchuk, V.I., J. Hummel, M. Morgan and S. Upadhyaya. 2004. On-the-go soil sensors for precision agriculture. Comput. Electron. Agric. 44:71-91.

Adamo, F., G. Andria, F. Attivissimo and N. Giaquinto. 2004. An acoustic method for soil moisture measurement. Instrumentation and Measurement, IEEE Transactions on 53:891-898.

Amente, G., J.M. Baker and C.F. Reece. 2000. Estimation of soil solution electrical conductivity from bulk soil electrical conductivity in sandy soils. Soil Sci. Soc. Am. J. 64:1931-1939.

Bear, J. 1988. Dynamics of fluids in porous media. Dover publications, New York, NY, USA.

Ben-Dor, E., S. Chabrillat, J. Demattę, G. Taylor, J. Hill, M. Whiting and S. Sommer. 2009. Using imaging spectroscopy to study soil properties. Remote Sens. Environ. 113:S38-S55.

Carbognin, L. and L. Tosi. 2003. Il progetto ISES per l'analisi dei processi di intrusione salina e subsidenza nei territori meridionali delle province di padova e venezia. Istituto Per Lo Studio Della Dinamica Delle Grandi Masse, CNR, Rome, Italy.

Carbognin, L., P. Teatini and L. Tosi. 2005a. Land subsidence in the venetian area: Known and recent aspects. Giornale Di Geologia Applicata 1:5-11.

Carbognin, L., F. Rizzetto, L. Tosi, P. Teatini and G. Gasparetto-Stori. 2005b. L'intrusione salina nel comprensorio lagunare veneziano. il bacino meridionale. Giornale Di Geologia Applicata 2:119-124.

Carbognin, L., G. Gambolati, M. Putti, F. Rizzetto, P. Teatini and L. Tosi. 2006. Soil contamination and land subsidence raise concern in the Venice watershed, Italy. Management of Natural Resources, Sustainable Development and Ecological Hazards.Vol.99: 691-700.

Castrignanò, A., F. Morari, C. Fiorentino, C. Pagliarin and S. Brenna. 2008. Constrained optimization of spatial sampling in skeletal soils using EMI data and continuous simulated annealing. *In*. 1st global workshop on high resolution digital soil sensing & mapping, Sydney, Australia. 5-8 February 2008 2008.

Chang, C.W., M.J. Mausbach, D.A. Laird and C.R. Hurburgh. 2001. Near-infrared reflectance spectroscopy–Principal components regression analyses of soil properties. Soil Sci. Soc. Am. J. 65:480-490.

Clement, B. and T. Stombaugh. 2000. Continuously-measuring soil compaction sensor development. p. 1-15. *In* Continuously-measuring soil compaction sensor development. 2000 ASAE annual international meeting, Milwaukee, Wisconsin, USA, 9-12 July 2000. 2000. American Society of Agricultural Engineers, .

Corwin, D.L., S.M. Lesch, E. Segal, T.H. Skaggs and S.A. Bradford. 2010. Comparison of sampling strategies for characterizing spatial variability with apparent soil electrical conductivity directed soil sampling. J. Environ. Eng. Geophys. 15:147-162.

Corwin, D.L., S.M. Lesch, P.J. Shouse, R. Soppe and J.E. Ayars. 2008. 16 delineating site-specific management units using geospatial ECa measurements. *In* B.J. Allred, J.J. Daniels and Reza Eshani M. (eds.) Handbook of Agricultural Geophysics 247. CRC Press, Taylor & Francis Group, New York, NY, USA.

Corwin, D. 2008. Past, present, and future trends of soil electrical conductivity measurements using geophysical methods. p. 17-44. *In* B.J. Allred, J.J. Daniels and Reza Eshani M. (eds.) Handbook of agricultural geophysics. CRC Press. Taylor & Francis Group, New York, NY, USA.

Corwin, D. 2003. Soil salinity measurement. Encyclopedia of Water Science.Marcel Dekker, New York, NY, USA.

Corwin, D. and S. Lesch. 2010. Delineating site-specific management units with proximal sensors. Geostatistical Applications for Precision Agriculture139-165.

Corwin, D. and S. Lesch. 2005. Apparent soil electrical conductivity measurements in agriculture. Comput. Electron. Agric. 46:11-43.

Corwin, D. and S. Lesch. 2003. Application of soil electrical conductivity to precision agriculture. Agron. J. 95:455-471.

Corwin, D., S. Lesch and D. Lobell. 2012. Laboratory and field measurements. p. 295-341. *In* W. Wallender and K. Tanji (eds.) Agricultural salinity assessment and management. ASCE manual and reports on engineering practice no. 71 2nd ed. ASCE, Reston, VA, USA.

Corwin, D., S. Lesch, P. Shouse, R. Soppe and J. Ayars. 2003a. Identifying soil properties that influence cotton yield using soil sampling directed by apparent soil electrical conductivity. Agron. J. 95:352-364.

Corwin, D., S. Kaffka, J. Hopmans, Y. Mori, J. Van Groenigen, C. Van Kessel, S. Lesch and J. Oster. 2003b. Assessment and field-scale mapping of soil quality properties of a saline-sodic soil. Geoderma 114:231-259.

Dalton, F.N., W.N. Herkelrath, D.S. Rawlins and J.D. Rhoades. 1984. Time-domain reflectometry: Simultaneous measurement of soil water content and electrical conductivity with a single probe. Science 224:989-990.

De Franco, R., G. Biella, L. Tosi, P. Teatini, A. Lozej, B. Chiozzotto, M. Giada, F. Rizzetto, C. Claude and A. Mayer. 2009. Monitoring the saltwater intrusion by time lapse electrical resistivity tomography: The Chioggia test site (Venice Lagoon, Italy). J. Appl. Geophys. 69:117-130.

Ellis, S. and A. Mellor. 1995. Soils and environment. Routledge, London, UK.

FitzPatrick, E.A. 1986. An introduction to soil science. Longman Scientific & Technical Group UK, Longman, Harlow, UK.

Friedman, S.P. 2005. Soil properties influencing apparent electrical conductivity: A review. Comput. Electron. Agric. 46:45-70.

Gambolati, G., M. Putti, P. Teatini, M. Camporese, S. Ferraris, G.G. Stori, V. Nicoletti, S. Silvestri, F. Rizzetto and L. Tosi. 2005. Peat land oxidation enhances subsidence in the Venice watershed. EOS Transactions, American Geophysical Union 86(23): 217‑224.

Gomez, C., R.A. Viscarra Rossel and A.B. McBratney. 2008. Soil organic carbon prediction by hyperspectral remote sensing and field VIS-NIR spectroscopy: An Australian case study. Geoderma 146:403-411.

Goovaerts, P. and R. Kerry. 2010. Using ancillary data to improve prediction of soil and crop attributes in precision agriculture. Geostatistical Applications for Precision Agriculture167-194.

Hamed, Y.P. and R. Magnus Berndtsson. 2003. Soil solution electrical conductivity measurements using different dielectric techniques. Soil Sci. Soc. Am. J. 67:1071-1078.

Hemmat, A. and V. Adamchuk. 2008. Sensor systems for measuring soil compaction: Review and analysis. Comput. Electron. Agric. 63:89-103.

Johnson, C.K., R.A. Drijber, B.J. Wienhold and J.W. Doran. 2008. Productivity zones based on bulk soil electrical conductivity. p. 263-272. *In* B.J. Allred, J.J. Daniels and M. Reza Ehsani (eds.) Handbook of agricultural geophysics. CRC Press, Taylor & Francis Group,, New York, NY, USA.

Larson, W. and P. Robert. 1991. Farming by soil. Soil Management for Sustainability. Soil and Water Conserv.Soc., Ankeny, IA, USA.

Leone, A. and R. Escadafal. 2001. Statistical analysis of soil color and spectroradiometric data for hyperspectral remote sensing of soil properties (example in a southern Italy Mediterranean ecosystem). Int. J. Remote Sens. 22:2311-2328.

Lesch, S. 2005. Sensor-directed response surface sampling designs for characterizing spatial variation in soil properties. Comput. Electron. Agric. 46:153-179.

Li, Y., Z. Shi and F. Li. 2007a. Delineation of site-specific management zones based on temporal and spatial variability of soil electrical conductivity. Pedosphere 17:156-164.

Li, Y., Z. Shi, F. Li and H.Y. Li. 2007b. Delineation of site-specific management zones using fuzzy clustering analysis in a coastal saline land. Comput. Electron. Agric. 56:174-186.

Liu, W., L. Gaultney and M.T. Morgan. 1993. Soil texture detection using acoustical methods. *In* Soil texture detection using acoustical methods. American society of agricultural engineers. meeting, 1993. Madison, Wisconsin, USA.

Lunt, I., S. Hubbard and Y. Rubin. 2005. Soil moisture content estimation using ground-penetrating radar reflection data. Journal of Hydrology 307:254-269.

Metternicht, G. and J. Zinck. 2003. Remote sensing of soil salinity: Potentials and constraints. Remote Sens. Environ. 85:1-20.

Ministero delle Politiche Agricole e Forestali. 1998. Metodi di analisi fisica del suolo. Franco Angeli Editore, Milan, Italy.

Morari, F., A. Castrignanņ and C. Pagliarin. 2009. Application of multivariate geostatistics in delineating management zones within a gravelly vineyard using geo-electrical sensors. Comput. Electron. Agric. 68:97-107.

Mulder, V., S. De Bruin, M. Schaepman and T. Mayr. 2011. The use of remote sensing in soil and terrain mapping--A review. Geoderma 162: 1-19.

Pardossi, A., L. Incrocci, G. Incrocci, F. Malorgio, P. Battista, L. Bacci, B. Rapi, P. Marzialetti, J. Hemming and J. Balendonck. 2009. Root zone sensors for irrigation management in intensive agriculture. Sensors 9:2809-2835.

Persson, M. 2002. Evaluating the linear dielectric constant-electrical conductivity model using time-domain reflectometry. Hydrological Sciences Journal 47:269-277.

Post, D., A. Fimbres, A. Matthias, E. Sano, L. Accioly, A. Batchily and L. Ferreira. 2000. Predicting soil albedo from soil color and spectral reflectance data. Soil Sci. Soc. Am. J. 64:1027-1034.

Rhoades, J.D., F. Chanduvi and S.M. Lesch. 1999. Soil salinity assessment: Methods and interpretation of electrical conductivity measurements. Food & Agriculture Organization of the UN (FAO), Rome, Italy.

Rhoades, J. and J. Oster. 1986. Solute content. p. 985-1006. *In* A. Klute (ed.) Methods of soil analysis. part 1. physical and mineralogical methods. SSSA Book Series 5.1 ed. American Society of Agronomy, Inc., Madison, Wisconsin, USA.

Rhoades, J., N. Manteghi, P. Shouse and W. Alves. 1989. Soil electrical conductivity and soil salinity: New formulations and calibrations. Soil Sci. Soc. Am. J. 53:433-439.

Richards, L.A. and US Salinity Laboratory Staff. 1954. USDA handbook no. 60. Diagnosis and improvement of saline and alkali soils. U.S. Governament Prnting Office, Washington, D.C., USA.

Rizzetto, F., L. Tosi, M. Bonardi, P. Gatti, A. Fornasiero, G. Gambolati, M. Putti and P. Teatini. 2002. Geomorphological evolution of the southern catchment of the Venice lagoon (Italy): The Zennare basin. Scientific Research and Safeguarding of Venice, Corila Research Program: 2001 Results, Venice, Italy.

Rizzetto, F., L. Tosi, L. Carbognin, M. Bonardi, P. Teatini, E. Servat, W. Najem, C. Leduc and A. Shakeel. 2003. Geomorphic setting and related hydrogeological implications of the coastal plain south of the Venice Lagoon, Italy. IAHS Publ. Wallingford, UK.

Robert, P. 2002. Precision agriculture: A challenge for crop nutrition management. Plant Soil 247:143-149.

Sethuramasamyraja, B., V. Adamchuk, A. Dobermann, D. Marx, D. Jones and G. Meyer. 2008. Agitated soil measurement method for integrated on-the-go mapping of soil pH, potassium and nitrate contents. Comput. Electron. Agric. 60:212-225.

Singh, D., I. Herlin, J.P. Berroir, E. Silva and M. Simoes Meirelles. 2004. An approach to correlate NDVI with soil color for erosion process using NOAA/AVHRR data. Advances in Space Research 33:328-332.

Teatini, P., L. Tosi, T. Strozzi, L. Carbognin, U. Wegmüller and F. Rizzetto. 2005. Mapping regional land displacements in the Venice coastland by an integrated monitoring system. Remote Sens. Environ. 98:403-413.

Torrent, J. and V. Barron. 1993. Laboratory measurement of soil color: Theory and practice. SSSA Special Publication 31:21-21.Madison, WI, USA

Tosi, L., P. Teatini, L. Carbognin and G. Brancolini. 2009. Using high resolution data to reveal depth-dependent mechanisms that drive land subsidence: The Venice coast, Italy. Tectonophysics 474:271-284.

Tóth, G., L. Montanarella and E. Rusco. 2008. Updated map of salt affected soils in the European union. p. 61-74. *In* G. Tóth, L. Montanarella and E. Rusco (eds.) Threats to soil quality in Europe EUR 23438 –Scientific and technical research series. Office for Official Publications of the European Communities, Luxembourg.

Van Uffelen, C., J. Verhagen and J. Bouma. 1997. Comparison of simulated crop yield patterns for site-specific management. Agricultural Systems 54:207-222.

Viezzoli, A., L. Tosi, P. Teatini and S. Silvestri. 2010. Surface water–groundwater exchange in transitional coastal environments by airborne electromagnetics: The Venice Lagoon example. Geophys. Res. Lett. 37:L01402.

Viscarra Rossel, R., V. Adamchuk, K. SUDDUTH, N. Mckenzie and C. Lobsey. 2011. Proximal soil sensing: An effective approach for soil measurements in space and time. Adv. Agron. 113:237-282.

Viscarra Rossel, R. and C. Walter. 2004. Rapid, quantitative and spatial field measurements of soil pH using an ion sensitive field effect transistor. Geoderma 119:9-20.

Viscarra Rossel, R., D. Walvoort, A. McBratney, L. Janik and J. Skjemstad. 2006. Visible, near infrared, mid infrared or combined diffuse reflectance spectroscopy for simultaneous assessment of various soil properties. Geoderma 131:59-75.

Vitharana, U.W.A., M. Van Meirvenne, D. Simpson, L. Cockx and J. De Baerdemaeker. 2008. Key soil and topographic properties to delineate potential management classes for precision agriculture in the European loess area. Geoderma 143:206-215.

Vitturi, A., P. Giandon, V. Bassan and F. Ragazzi. 2008. I suoli della provincia di Venezia. Provincia di Venezia e Arpav, Venezia, Italy.

Zhang, W., K. Wang, H. Chen, X. He and J. Zhang. 2012. Ancillary information improves kriging on soil organic carbon data for a typical karst peak cluster depression landscape. J. Sci. Food Agric. 92: 1094-1102.

Chapter 2

Simultaneous Monitoring of Soil Water Content and Salinity with a Low-Cost Capacitance-Resistance Probe

Frequently Used Symbols

θ volumetric water content

ε_r soil complex permittivity

EC_a bulk electrical conductivity

EC_p pore-water electrical conductivity

EC_w electrical conductivity of the solution used to wet the soil

EC_s electrical conductivity of the solid phase

EC_e electrical conductivity of aqueous extract of saturated soil-paste

1. Introduction

Coastal farmlands are often threatened by saltwater contamination that poses a serious risk for drinking water quality and agricultural activities. To control and evaluate the hazard of soil salinity, accurate measurements of soil water content and solute concentrations are needed. The term salinity refers to the presence of the major dissolved inorganic solutes (basically Na^+, Mg^{2+}, Ca^{2+}, K^+, Cl^-, SO_4^{2-}, HCO_3^-, NO_3^-, and CO_3^{2-} ions) in the soil(Rhoades et al., 1999). The salinity of a solution can be quantified in terms of its electrical conductivity (EC; $dS \cdot m^{-1}$), which is strictly related to the total concentration of dissolved salts, with 1 dS m^{-1} being approximately equivalent to 10 $meq \cdot L^{-1}$ at 25 °C (Richards and US Salinity Laboratory Staff, 1954). Soil salinity is generally determined by measuring the electrical conductivity of aqueous extracts of saturated soil-pastes (EC_e) or of other soil to water ratio extracts. However, such methods of investigation are destructive, time-consuming, and usually not representative of the real salinity status of soils in field conditions (Rhoades et al., 1999). To determine the real (*i.e.*, at actual soil water contents) stress conditions affecting crops and to monitor fluxes of salts (e.g., upward fluxes in the vadose zone) the electrical conductivity of the pore-water (EC_p) should be measured instead. Multi-sensor probes have recently been developed in order to assess water content and electrical conductivity with continuous and non-destructive measurements.

2. Materials and Methods

2.1. The study site

The capacitance (dielectric) technique has been widely used to estimate soil volumetric water content (θ) (Fares and Polyakov, 2006). Capacitance sensors induce an alternating electric field in the surrounding medium. The total complex impedance is obtained by quantifying the voltage and the current induced by the electric field on the sensor electrodes. The impedance is related to the complex permittivity (or dielectric constant; ε_r) of the surrounding medium. The volume of the induced electric field depends mainly on the size and shape of the sensor electrodes. Moreover, the electric field decays rapidly, being inversely proportional to the square of the distance. Topp *et al.* (1980) noticed a strict correlation between ε_r measured by time domain reflectometry (TDR) and soil water content. They therefore proposed an empirical third-degree polynomial in ε_r to calculate θ. The complex permittivity of the soil measured by dielectric sensors is the sum of soil real (ε') and imaginary (ε'') permittivity (dielectric loss):

$$\varepsilon_r = \varepsilon' - j \times \varepsilon'' \qquad (2.1)$$

where $j^2 = -1$. The value of θ is related to ε' only. On the other hand, ε'' changes according to soil salinity, soil temperature (T), and the operating frequency of the sensor (Friedman, 2005; Kelleners et al., 2004a; Kelleners et al., 2004b; Rosenbaum et al., 2011; Saito et al., 2008; Wilczek et al., 2012). Especially in low-cost sensors working at low frequencies (<1 GHz), the contribution of ε'' in saline soils cannot be ignored (Fares and Polyakov, 2006; Pardossi et al., 2009; Schwank and Green, 2007). It is therefore essential to consider the influence of ε'' in ε_r measurements in order to gain correct θ estimations.

2.2. Pore-Water Electrical Conductivity Assessment

The determination of the pore-water electrical conductivity is a difficult task as it cannot be directly related to any sensor output. Typically sensors measure soil bulk (or apparent)

electrical conductivity (EC_a), which is the combination of the contributions of the three phases constituting soils: solid, water and air (Allred et al., 2008; Friedman, 2005). According to Corwin (2008), three pathways of current flow contribute to the EC_a measurement: current through the pore water solution (*the liquid phase pathway*); current through exchange complexes on the surface of soil colloids (*the soil-liquid phase pathway*); and current through the soil particles that are in direct contact (*the solid pathway*). EC_a can be estimated from ε_r readings (Dalton et al., 1984) or from the electrical resistance that soil opposes to an alternating electric current (Allred et al., 2008; Corwin, 2008). EC_p and EC_a are strictly correlated, indeed an increase of ions in the matrix solution leads to an increase of EC_a values (Rhoades et al., 1976; Rhoades et al., 1989b; Saito et al., 2008).

Several models to estimate EC_p from EC_a have been developed in the last sixty years, based on empirical relations as well as on theoretical assumptions. Models are usually based on the empirical relationship between EC_a and θ at constant EC_p values, where the magnitude of EC_a varies according to the tortuosity of the electrical current paths (depending on soil texture, density and particle geometry, particle pore distribution, and organic matter content). Tortuosity can be expressed in terms of a soil transmission factor (π) (Heimovaara et al., 1995; Mualem and Friedman, 1991; Rhoades et al., 1976) or soil-type-related parameters (Archie, 1942; Hilhorst, 2000; Malicki and Walczak, 1999).

Recent development of low-cost multi-sensor probes could make such EC_p models implementable for continuous monitoring purposes. However, since most of the EC_p models are calibrated in limited soil conditions (Friedman, 2005; Hamed and Magnus Berndtsson, 2003; Persson, 2002), new relationships between variables and soil properties must be defined to extend their applicability to a wider range of soils.

The general aim of this study was to calibrate a multi-sensor probe for monitoring soil volumetric water content and soil water electrical conductivity in a heterogeneous saline coastal area. The specific objectives were: (*i*) to develop a procedure to simultaneously calibrate θ and EC_p; (*ii*) to test different models for EC_p; and (*iii*) to develop general functions to extend EC_p model application to a wide range of soils, even in critical saline conditions.

3. Materials and Methods

3.1. Decagon ECH_2O-5TE Probe

The sensor used in this experiment was an ECH_2O-5TE probe (hereafter simply referred to as 5TE). 5TE is a multifunction sensor measuring ε_r, EC_a, and T (Decagon Devices Inc., Pullman, WA, USA). A detailed description of the 5TE can be found in Bogena *et al.* (2010) and Campbell and Greenway (2005). The probe is a fork-type sensor (0.1 m in length, 0.032 m in height). Two of the three tines host the dielectric sensor. The capacitance sensor supplies a 70 MHz electromagnetic wave to the prongs that charge according to the dielectric of the soil surrounding the sensor. The reference soil volume is *ca.* $3 \times 10^{-4} \cdot m^3$. A charge is consequently stored in the prongs and it is proportional to the soil dielectric. Previous versions of dielectric sensors by Decagon Devices operate at lower frequencies (e.g., ECHO10 probe, 5 MHz). The increase of operating frequency has led to a higher salinity tolerance (Kelleners et al., 2004b; Pardossi et al., 2009; Saito et al., 2008). In fact ε_r measurement with 5TE should not be affected by soil salinity up to EC_e values of 10 $dS \cdot m^{-1}$ (Kizito et al., 2008).

The bulk electrical conductivity is measured with a two-sensor array. The array consists of two screws placed on two of the sensor tines. An alternating electrical current is applied on the two screws and the resistance between them is measured. The sensor measures electrical conductivity up to 23.1 dS m^{-1} with 10% accuracy; however a user calibration is suggested above 7 $dS \cdot m^{-1}$. Temperature is measured with a surface-mounted thermistor reading the temperature on the surface of one of the prongs.

3.2. Soil Sampling

Soil samples from a coastal farmland affected by saltwater intrusion (Keesstra et al., 2012) were cored for the calibration of the 5TE probe. The site is located at Ca' Bianca, Chioggia (12°13'55.218"E; 45°10'57.862"N), just south of the Venice Lagoon, North-

Eastern Italy. The area has high spatial variability in soil characteristics due to its deltaic origins (Fig. 2.1).

Three sampling locations were chosen in the basin (sites A, B, and C, Fig. 2.1). At sites A and B both topsoil (0 to 0.4 m depth) and subsoil (0.4 to 0.8 m depth) were collected, while only the topsoil was cored at site C since the profile is uniform. The main physical and chemical properties of the samples were characterized. Soil texture was determined with a laser particle size analyzer (Mastersizer 2000, Malvern Instruments Ltd., Great Malvern, UK). Soil total carbon content and soil organic carbon (SOC) content were analyzed with a Vario Macro Cube CNS analyzer (Elementar Analysensysteme GmbH, Hanau, Germany). Cation exchange capacity (CEC) was measured at a pH value of 8.2 according to the BaCl extraction method (Sumner et al., 1996). Soil pH was measured with a 1:2 soil to water ratio with a pH-meter (S47K, Mettler Toledo, Greifensee, Switzerland). Particle density (ρ_r) was measured with an ethanol pycnometer (Blake and Hartge, 1986). Bulk density (ρ_b) was determined from undisturbed core samples. EC_e was measured according to Rhoades *et al.* (1999).

Soil samples show high variability in sand (from 174.7 to 905.2 $g \cdot kg^{-1}$), organic carbon content (from 15.4 to 147.8 $g \cdot kg^{-1}$), and EC_e values (from 0.61 to 6.38 $dS \cdot m^{-1}$). Five soil types were selected: a sandy soil with low SOC content and low EC_e, a silty-clay-loam with low SOC content and high EC_e, two loam and one clay-loam with medium-high SOC content. Main soil properties are listed in Table 2.1.

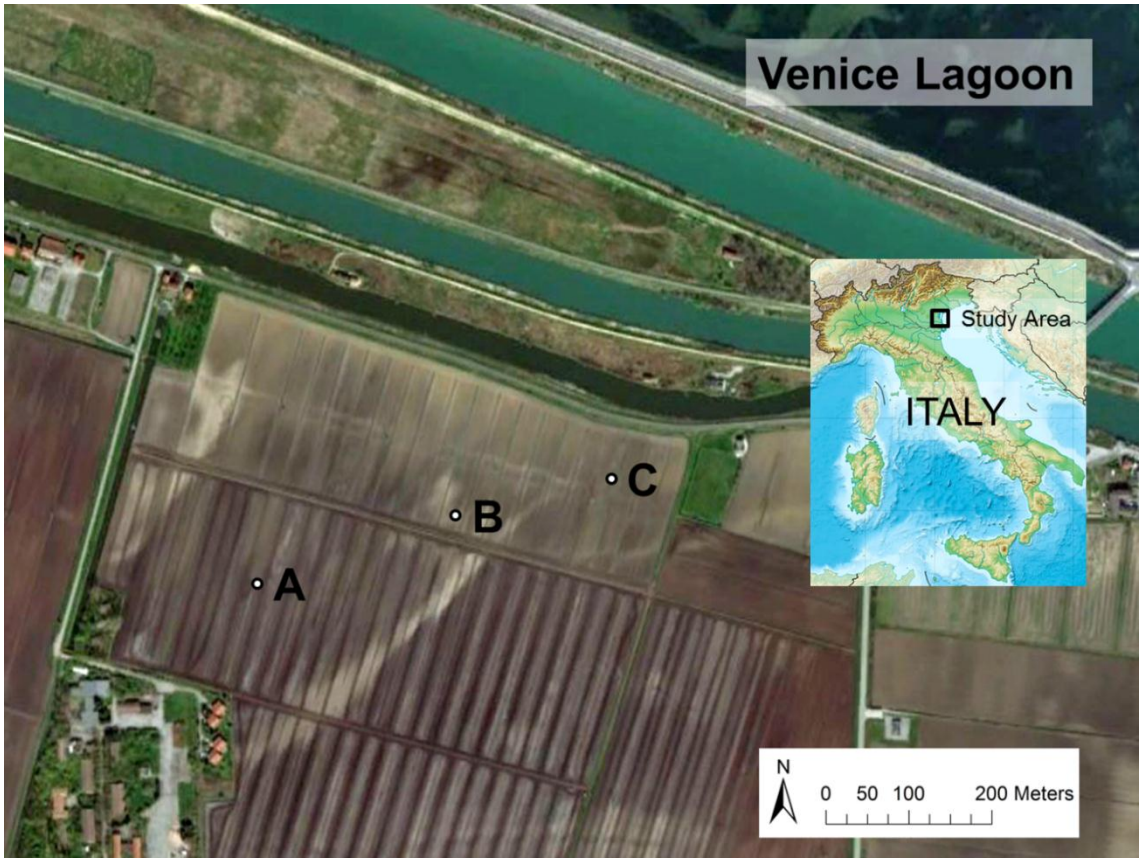

Figure 2.1. Aerial image of the study area at the southern edge of the Venice Lagoon, Italy. The sampling sites A, B, and C are marked.

Table 2.1. Texture, total and organic carbon content, cation exchange capacity, pH, particle density, bulk density, and conductivity of the saturated paste extract for the five soil samples collected in the Ca' Bianca sites and used in this study.

Soil Sample		Sand (%)	Silt (%)	Clay (%)	Total C (%)	SOC (%)	CEC ($meq \cdot g^{-1}$)	pH	ρ_r ($g \cdot cm^{-3}$)	ρ_b ($g \cdot cm^{-3}$)	EC_e ($dS \cdot m^{-1}$)
A	**Topsoil**	40.92	41.31	17.77	15.50	14.78	0.57	5.60	1.90	0.87	0.61
A	**Subsoil**	17.47	52.66	29.87	4.30	3.96	0.12	5.89	2.28	1.08	6.38
B	**Topsoil**	50.54	37.61	11.85	6.64	5.78	0.33	7.23	2.32	1.07	1.42
B	**Subsoil**	90.52	7.71	1.77	4.26	1.54	0.05	7.68	2.62	1.29	2.26
C	**Topsoil**	29.61	48.46	21.93	9.84	8.36	0.45	7.58	2.21	0.93	2.05

3.3. Experimental Settings

The 5TE probe was used in a mixture of soil (preliminarily air-dried and sifted at 2 mm) and saline solution (54.92% Cl^-; 30.82% Na^+; 7.68% SO_4^{2-}; 3.81% Mg^{2+}; 1.21% Ca^{2+}; 1.12% K^+; 0.44% $NaHCO_4$) to reproduce saline groundwater of the experimental site (Gattacceca et al., 2009). Soil samples were moistened to a relative saturation (S) of about 0, 0.35, 0.75, and 1.00 with a saline solution of 0, 5, 10, and 15 $dS \cdot m^{-1}$ (at 25 °C). The mixtures were prepared in a plastic container and then sealed and kept in a dark place at constant temperature 22 ± 1 °C for 48 hours. The soil was then packed uniformly in a $6 \times 10^{-4} \cdot m^3$ beaker to reproduce the field bulk density. Output values for ε_r, EC_a, and T were recorded by a datalogger (Em50, Decagon Devices) connected to the 5TE probe.

Electrical conductivity of the wetting solution (EC_w) differs from the electrical conductivity of the pore-water (EC_p) (Malicki and Walczak, 1999). Pore-water solution was extracted from a portion of the soil sample by vacuum displacement (Wolt and John, 1986) at −90 kPa and EC_p was measured with a S47K conductivity meter. EC_e was then measured on the remaining soil sample. Water content was determined gravimetrically (at 105 °C for 24 hours). Measures were replicated 3 times.

3.4. Calibration Procedure

A three-step procedure was implemented to calibrate the sensor output for the collected samples: (1) model calibration to convert ε_r and EC_a readings to θ or EC_p; (2) comparison and selection of the best models; (3) simultaneous calibration of the selected models for θ and EC_p and evaluation of their robustness by applying a bootstrap procedure.

3.4.1. Models to Convert ε_r Readings to θ

Dielectric permittivity can be converted to volumetric water content using empirical models (e.g., Topp et al., 1980). However temperature and soil electrical conductivity affect the dielectric permittivity measurements of ECH$_2$O sensors (Jones et al., 2005; Rosenbaum et al., 2011; Saito et al., 2009). In one of their latest studies, Rosenbaum *et al.* (2011) developed an empirical calibration to correct the temperature effect on ε_r measurements which performed very well in both liquid and soil media. Investigating the effect of temperature on ε_r, Bogena *et al*. (2010) concluded that in a T range from 5 °C and 40 °C, ε_r varies up to 8% with respect to the reference liquid used (ε_r = 40 at 25 °C). As all the calibration experiments presented in this work took place at a controlled temperature of 22 ± 1 °C, the effect of T on ε_r was considered negligible. On the other hand, ε_r is much more sensitive to electrical conductivity changes (Blonquist Jr. et al., 2005).

Polynomial model-types as that proposed by Topp *et al*. (1980) do not provide satisfactory θ estimates in the presence of high clay and organic contents or in saline soils, especially using sensors operating at low frequencies (Pardossi et al., 2009; Seyfried and Murdock, 2001). Indeed, application of the Topp model to the experimental data of Ca' Bianca provided a large average error (~0.11 $m^3 \cdot m^{-3}$).

Three models were tested to find a satisfactory empirical relationship between ε_r and θ data for each soil at different EC_w values, namely:

(a) logistic model:

$$\theta = \frac{\theta_{MAX}}{1 + e^{-(a+b\times\varepsilon_r)}} - U \tag{2.2}$$

(b) hyperbolic model:

$$\theta = \frac{\theta_{MAX} \times a \times \varepsilon_r}{\theta_{MAX} + a \times \varepsilon_r} \tag{2.3}$$

(c) logarithmic model:

$$\theta = a + b \times \ln(\varepsilon_r) \tag{2.4}$$

where θ_{MAX} is the volumetric content at saturation, a, b, and U are fitting parameters.

The three models were compared with the Akaike Information Criterion (AIC) (Akaike, 1974) and the one with the higher Akaike weight (W_{AIC}) (Burnham and Anderson, 2002)

was selected for the subsequent simultaneous calibration of θ and EC_p. The Akaike Information Criterion (AIC) is a measure of the goodness of fit of a specific model. It allows the direct comparison of different concurrent equations for model selection purposes. AIC accounts for the risk of over-parameterization as well as for the goodness of fit; several models can be ranked according to their AIC, with the one having the lower value being the best. From the AIC, the Akaike weight ($\Sigma W_{AIC} = 1$) can be computed, which represents the probability that a specific model is the best, given the data and the set of candidate models. Note that the fitting parameters showed a high dependence on EC_a and physico-chemical soil characteristics. To take this effect into account, the fitting parameters were expressed as a linear function of EC_a and other selected soil properties yielding a "general" calibration equation usable on the various soils of the study site.

3.4.2. Models to Convert ε_r and EC_a Readings to EC_p

Four models were tested: the first is the Malicki and Walczak (1999) model. They found that, when ε_r is higher than 6.2, the slope $\partial EC_a/\partial\varepsilon_r$ depends only on salinity but not on water content, nor bulk density, nor dielectric permittivity. They developed an empirical relationship linearly linking EC_a to ε_r for various values of EC_w, *i.e.*, $EC_a(\varepsilon_r, EC_w)$. The validity of the linear relationships holds above a "converging point" characterized by ε_{r0} = 6.2 and EC_{a0} = 0.08 dS·m^{-1}. EC_p was consequently defined as a function of $EC_a(\varepsilon_r, EC_w)$ and soil texture:

$$EC_p = \frac{EC_a - EC_{a0}}{(\varepsilon_r - \varepsilon_{r0}) \times l} \tag{2.5}$$

where l is the slope of the relation between $\partial EC_a/\partial\varepsilon_r$ and EC_w. This parameter depends on the sand content of the sample through the relation $l = l' + l'' \times sand(\%)$, with $l' = 5.7 \times 10^{-3}$ and $l'' = 7.1 \times 10^{-5}$.

On the basis of Equation (2.5), Hilhorst (2000) developed the following theoretical model:

$$EC_p = \frac{\varepsilon_p \times EC_a}{\varepsilon_r - \varepsilon_{EC_a=0}} \tag{2.6}$$

where ε_p is the real portion of the dielectric permittivity of the soil pore-water and $\varepsilon_{EC_a=0}$ is the real portion of the dielectric permittivity of the soil when bulk electrical conductivity is 0. $\varepsilon_{EC_a=0}$ is a soil-type dependent variable, even if Hilhorst recommended a value equal to 4.1 as a generic offset. Moreover, ε_p was calculated as (Hilhorst, 2000):

$$\varepsilon_p = 80.3 - 0.37 \times (T - 20) \tag{2.7}$$

where T is the soil temperature in degrees Celsius, 80.3 is the real part of the complex permittivity of the pore-water at 20 °C, and 0.37 is a temperature correction factor. Hilhorst considers the imaginary part of ε_r to be negligible, hence in his model $\varepsilon_r = \varepsilon'$. The Hilhorst model was proved to perform correctly only for low EC_p values. Hilhorst himself indicated an EC_p value of 3 $dS \cdot m^{-1}$ as the upper limit for the validity of his model when a capacitance sensor operating at 30 MHz is used.

The third tested model is the one proposed by Rhoades *et al.* (1989a) (hereafter simply referred as Rhoades). They expressed the pore-water electrical conductivity as:

$$EC_p = \frac{EC_a - EC_s}{\theta \times \pi} \tag{2.8}$$

where EC_s (the electrical conductivity of the solid phase) was shown to be dependent on soil texture and through a linear correlation with clay content (Amente et al., 2000; Rhoades et al., 1989a); π is a tortuosity factor that mainly depends on soil hydraulic properties and was defined by Rhoades *et al.* as:

$$\pi = c + d \times \theta \tag{2.9}$$

where the constants c and d can be estimated from the regression between EC_a and θ at constant EC_p (Rhoades et al., 1976).

Archie's law (1942) (hereafter simply referred as Archie) was developed to assess the conductivity of pore-water in clay-free rocks and sediments, and it has been therefore used in soils containing neither clay minerals nor organic matter. According to Archie EC_p can be derived as follows:

$$EC_p = k \times \frac{EC_a}{\phi^m \times S^n} \tag{2.10}$$

where Φ is the porosity (defined as $\Phi = 1 - \rho_b \times \rho_r^{-1} = \theta_{MAX}$), S the relative saturation (defined as $S = \theta \times \Phi^{-1}$), and k, m and n are fitting parameters. Allred *et al.* (2008)

showed that typical values of these three constants range from 0.5 to 2.5, from 1.3 to 2.5, and ~2 for *k*, *m*, and *n*, respectively.

Archie has been modified in order to be used also in soils containing clay minerals (Waxman and Smits, 1968) by simply considering the contribution of EC_s in Equation (2.10). Hence, EC_p was defined as:

$$EC_p = k \times \frac{EC_a - EC_s}{\phi^m \times S^n} \tag{2.11}$$

Despite the fact that Archie was originally developed for deep sediments in oil research, it has been successfully applied in shallow groundwater systems to trace salinity. An example of such implementation is given by Monego *et al.* (2010). It is worth noticing that Archie and Rhoades show a similar formulation, being equal when $m = 1$ and $n = 1$ (then $k = 1/\pi$).

The four models apply for $\theta > 0.1$ $m^3 \cdot m^{-3}$ (for Rhoades and Hilhorst), $\theta > 0.2$ $m^3 \cdot m^{-3}$ (for Malicki and Walczak), and $S > 0.3$ (for Archie).

The models were tested with the experimental (EC_a,ε_r) values and the chemical and physical properties of the five soil samples collected at Ca' Bianca. In a first step, the original formulations were tested by calculating the parameters according to the methodologies proposed by the authors. Next, the models were optimized by relating the calibration parameters to the physical and chemical characteristics of the soils. EC_p data at $S \approx 0.35$ were excluded from the optimization as it was impossible to collect a sufficient amount of solution with the extraction method used in this experiment. EC_p data at $S \approx 0$ were assumed equal to 0 $dS \cdot m^{-1}$ (Saito et al., 2008).

3.4.3. Simultaneous Calibration of Models for θ and EC_p

The model parameters for the simultaneous quantification of θ and EC_p were calibrated by minimizing the following objective function:

$$RSS_{tot} = \sum_{i=1}^{N}\left(EC_{p,i} - \hat{EC}_{p,i}\right)^2 + \sum_{j=1}^{M}\left(W_1 \times W_2 \times \left(\theta_j - \hat{\theta}_j\right)\right)^2 \quad (2.12)$$

where RSS_{tot} is the cumulative residual sum of squares, M and N are the total number of observed volumetric water content and pore-water electrical conductivity data, respectively, $EC_{p,i}$ and $\widehat{EC}_{p,i}$, θ_j and $\hat{\theta}_j$ are the observed and fitted EC_p and θ values, respectively, W_1 and W_2 are two weighting factors. The parameter W_1 allows more weight to be given to one of the two variables. The parameter W_2 ensures that a proportional weight is given to the two residual sums of squares (*RSS*), and that the effect of having different units for θ and EC_p is canceled. W_2 was calculated as suggested by Van Genuchten *et al.* (1991):

$$W_2 = \frac{M \times \sum_{i=1}^{N} EC_{p,i}}{N \times \sum_{j=1}^{M} \theta_j} \quad (2.13)$$

This weighted procedure prevents one data type (*i.e.*, EC_p or θ) from dominating the other, solely because of its higher numerical values.

In this study the limited dataset size (M = 80 and N = 55) did not allow a validation to be performed on an independent set of data. The models were thus validated through a bootstrap procedure (Efron, 1979). A Y number of iterations were carried out. At each iteration, a subset of 60 points out of 80 for θ and 42 out of 55 for EC_p were extracted, forming the calibration dataset. The remaining points were retained for validation.

At the end of the iterations, the root mean square error (RMSE=$\sqrt{\sum_{i=1}^{n}(x_i - \hat{x}_i)^2/n}$), which provides the goodness of fit, the median, and the 5th and 95th percentiles of the distribution of each parameter were retained for further analysis. The probability distribution function of RMSE was compared using the Kolmogorov-Smirnov (KS) test to assess the significance of difference in the model predictions.

The calibration procedure described above was performed using the Generalized Reduced Gradient (GRG) Nonlinear Solving Method (Frontline Systems, Inc., Incline Village, NV, USA).

4. Results and Discussion

4.1. Converting ε_r Readings to θ

Dependence of 5TE on bulk electrical conductivity was observed to be similar in all the tested soil samples. ε_r readings were greatly affected by EC_a: especially for high θ values, a small increase in EC_w significantly raised the dielectric output of the probe, indicating that dielectric readings carried out in highly conductive media must be corrected. This finding confirms the results by Rosenbaum *et al.* (2011) on the same probe and by Saito *et al.* (2008) on other Decagon dielectric probes operating at lower frequencies. An example of the non-linear response of ε_r at different EC_w and θ values is presented in Fig. 2.2(a). Starting from a relative saturation of 0.75, the response of the probe significantly diverged at salinity solution with EC_w>10 dS m^{-1}. Fig. 2.2(b) evidences also the direct effect of the EC_w on EC_a readings and how the effect was amplified at higher water content. This observation, confirmed by Schwank and Green (2007) and Rosenbaum *et al.* (2011), suggests investigating the effect of EC_a on θ estimation.

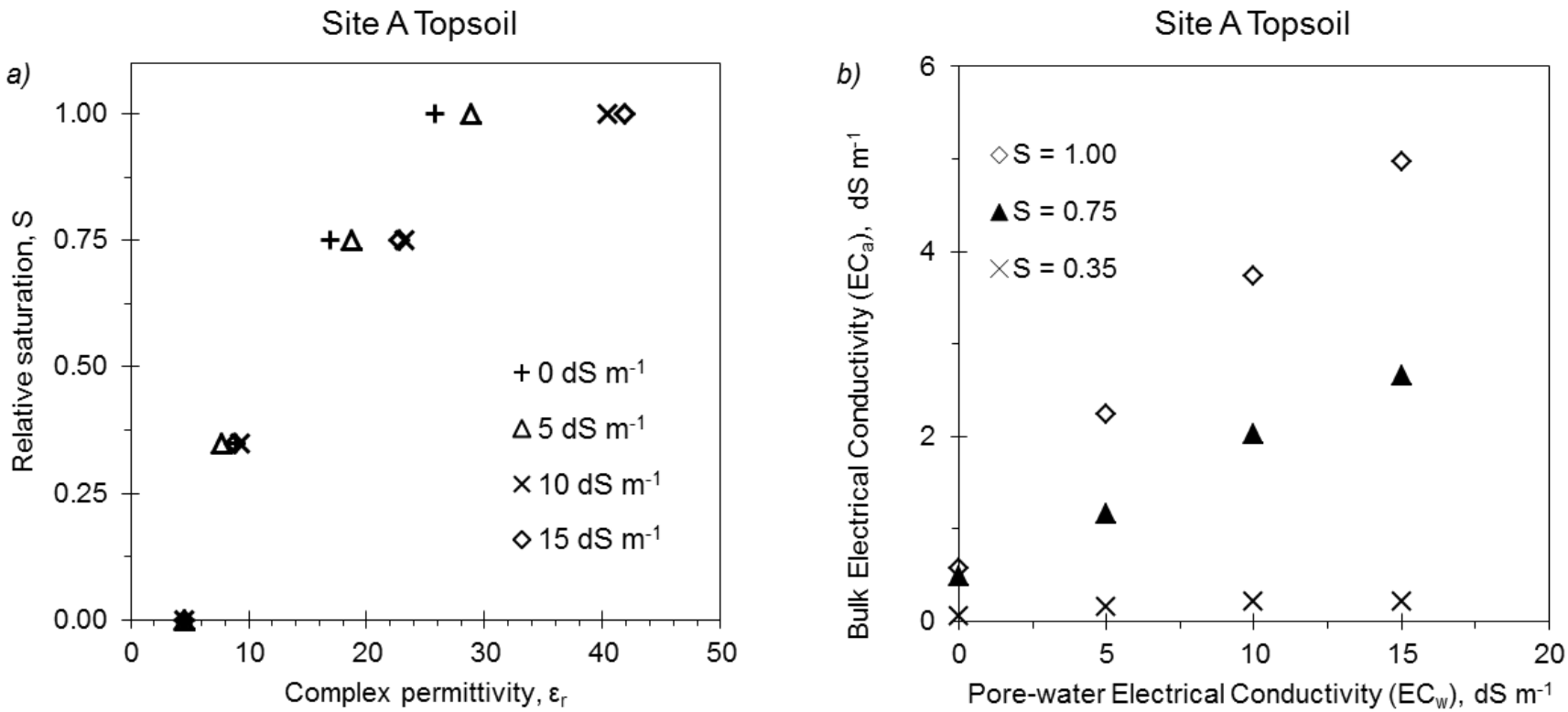

Figure 2.2. Site A, topsoil: (a) relative saturation vs. measured complex permittivity for four EC_w values of the wetting solution; (b) influence of EC_w on bulk electrical conductivity at various relative saturation levels.

Between the tested θ models, Equation (2.4) showed the best performances, with an Akaike weight W_{AIC} close to 1 (Table 2.2).

Table 2.2. Outcome of the θ model comparison according to Akaike information criterion (Burnham and Anderson, 2002): residual mean squares (RMS), total number of parameters (K—number of parameters of the model including the variance of the estimated residuals), Akaike Information Criterion (AIC), AIC differences (D_i), and Akaike weights (W_{AIC}).

Model	**RMS**	**K**	**AIC**	**D_i**	**W_{AIC}**
Hyperbolic	0.015	21	−301.61	104	2.11×10^{-23}
Logistic	0.002	42	−391.41	15	6.69×10^{-4}
Logarithmic	0.001	41	−406.03	0	1.000

Parameters *a* and *b* of the logarithmic model were found to be significantly correlated with the EC_a values at different water contents. Therefore the logarithmic model was reformulated as:

$$\theta = \left(a' + a'' \times EC_a\right) + \left(b' + b'' \times EC_a\right) \times \ln(\varepsilon_r) \tag{2.14}$$

where *a'*, *a''*, *b'*, and *b''* are empirical parameters. Calibration of Equation (2.14) highlighted a strong correlation between the terms $a' \times EC_a + a''$ and $b' \times EC_a + b''$. Consequently this latter term was assumed equal to $q \times (a' \times EC_a + a'')$, where *q* is a proportionality constant. Equation (2.14) could thus be reformulated as:

$$\theta = \left(a' + a'' \times EC_a\right) \times \left(1 + q \times \ln(\varepsilon_r)\right) \tag{2.15}$$

Equations (2.14) and (2.15) were compared with the AIC test. A $W_{AIC} = 0.99$ was obtained for Equation (2.15), indicating that this formulation of the logarithmic model is to be preferred over Equation (2.14), mainly for the reduced number of parameters.

To identify a "general" equation, *q* was set as a constant (=−0.766), whereas parameters *a'* and *a''* were related to soil properties (Table 2.3). Parameters *a'* and a'' were estimated according to the following empirical equations:

$$a' = -0.352 - 0.006 \times SOC(\%) \tag{2.16}$$

$$a'' = 0.020 - 0.009 \times \frac{clay(\%)}{sand(\%)} \tag{2.17}$$

Equation (2.15) allows correcting of the effect of dielectric losses due to the high electrical conductivity of the medium (Fares and Polyakov, 2006) due to high organic carbon content, salinity, and clay/sand ratio. The RMSE of Equation (2.15) was 0.038 $m^3 \cdot m^{-3}$.

4.2. Converting ε_r and EC_a Readings to EC_p

The parameters of models (2.5), (2.6), (2.8), and (2.11) showed significant correlations with soil properties (Table 2.3).

Table 2.3. Pearson linear correlation coefficients for some soil properties and the parameters in Equations (2.15) (logarithmic model), (2.5) (Malicki and Walczak), (2.6) (Hilhorst), (2.19) (Rhoades tortuosity), and (2.10) (Archie). Bold numbers indicate a significant linear relationship.

	Equation (2.15)		**Equation (2.5)**	**Equation (2.6)**	**Equation (2.19)**		**Equation (2.10)**	
	a'	***a''***	***l***	$\varepsilon_{ECa=0}$	***e***	***f***	***m***	***n***
Sand	*0.25*	*0.76*	**1.00**	*−0.60*	*−0.68*	*0.73*	*−0.79*	**1.00**
Clay	*−0.14*	*−0.8*	**−0.98**	*0.51*	*0.59*	*−0.62*	*0.66*	**−0.97**
Clay/Sand	*0.23*	**−0.89**	*−0.82*	*0.20*	*0.45*	*−0.43*	*0.31*	*−0.79*
SOC	**−0.98**	*0.30*	*−0.40*	**0.94**	*0.36*	*−0.48*	*0.78*	*−0.46*
$CaCO_3$	*0.26*	*0.58*	*0.85*	*−0.73*	**−0.95**	**0.96**	*−0.75*	*0.84*

The parameter *l* by Malicki and Walczak was confirmed to be mainly correlated to sand content. The calibrated parameters for Equation (2.5) are: EC_{a0} = 0.06 $dS \cdot m^{-1}$; ε_{r0} = 7.1; $l = 0.012 + 10^{-6} \times sand(\%)$ yielding RMSE = 2.52 $dS \cdot m^{-1}$. In the original paper by Malicki and Walczak *l* varied from 0.0083 to 0.0127 while in this experiment the range was narrower, from 0.0117 to 0.0124.

The $\varepsilon_{(ECa=0)}$ parameter by Hilhorst was expressed as a function of soil organic carbon content:

$$\varepsilon_{EC=0} = 4.851 + 0.203 \times SOC(\%) \quad (2.18)$$

According to Equation (2.18), $\varepsilon_{ECa=0}$ ranged from 5.16 to 7.85, values close to the interval found by Hilhorst (from 3.76 to 7.6 in soils and synthetic media). The calibrated model yielded RMSE = 2.34 $dS\ m^{-1}$.

Concerning the Rhoades and Archie models, the term EC_s was neglected as the 5TE probe registered EC_a = 0 in dry soil conditions. Please note that even if EC_s could sometimes be neglected (Corwin, 2008), other Authors demonstrated that it could assume a certain magnitude (Rhoades et al., 1989a).

In contrast to Equation (2.9) by Rhoades *et al.* (1976), π was found to be uncorrelated with soil water content. Nevertheless, π showed a linear correlation with soil porosity ($\pi = e + f \times \phi$), with *e* and *f* depending on $CaCO_3$ as follows:

$$\pi = \left(0.129 \times CaCO_3(\%) - 1.779\right) + \left(-0.232 \times CaCO_3(\%) + 3.989\right) \times \phi \tag{2.19}$$

In the tested samples π ranged from 0.22 to 0.71, whereas Rhoades *et al.* (1976) found a variation from 0.01 to 0.6. The inverse correlation of $CaCO_3$ with the tortuosity factor evidenced in the Ca' Bianca soils can be explained by the fact that here a low $CaCO_3$ content corresponds to high clay and SOC percentages. Indeed, the higher clay and SOC contents (more complicated geometric arrangement), the higher is soil tortuosity (Rhoades et al., 1989a). The "general" formulation of the Rhoades model provided RMSE = 0.90 dS m^{-1}.

Several formulations were attempted for Archie in order to decrease the number of parameters related to soil properties. Here, the parameters *k*, *m*, and *n* were alternately fixed and kept independent from the soil type. The formulation with *k* = 0.487 provided the best fitting according to the AIC test. With fixed *k*, *n* showed a significant correlation with sand content:

$$n = -0.669 + 0.035 \times sand(\%) \tag{2.20}$$

It is worth noticing that with higher sand contents (Fig. 2.3(a)) $n \cong 2.5$, which is close to *n* values suggested for sandy media (Allred et al., 2008). As shown in Table 2.3, *n* decreases with increasing clay values. For given *S* and EC_a values, it is clearly derived from Equation (2.10) that the smaller the *n* the higher is EC_p, *i.e.*, with a large percentage of clay the influence of "*the liquid phase pathway*" on the EC_a reading is reduced (Corwin, 2008; Rhoades et al., 1989a). A non-linear relationship was detected between *m* and soil organic carbon (Fig. 2.3(b)):

$$m = -0.018 \times SOC(\%) + \frac{4.350 \times SOC(\%)}{SOC(\%) + 0.966} \tag{2.21}$$

Values of *m* between 2.65 and 3.82 were derived. As reported by Archie, *m* becomes larger as the permeability of the porous medium decreases (increasing tortuosity). As shown in Fig. 2.3(b) the magnitude of *m* rises with SOC. High organic contents decrease soil bulk density, possibly increasing soil tortuosity (Barber, 1995). Archie calibration returned RMSE = 0.65 dS m^{-1}.

Comparison between the RMSE values computed for the four EC_p models showed that the "general" formulation of Archie provided the best estimates. Archie also had the highest W_{AIC} (~1.00). For the Malicki and Walczak, Hilhorst, and Rhoades models the W_{AIC} were close to zero.

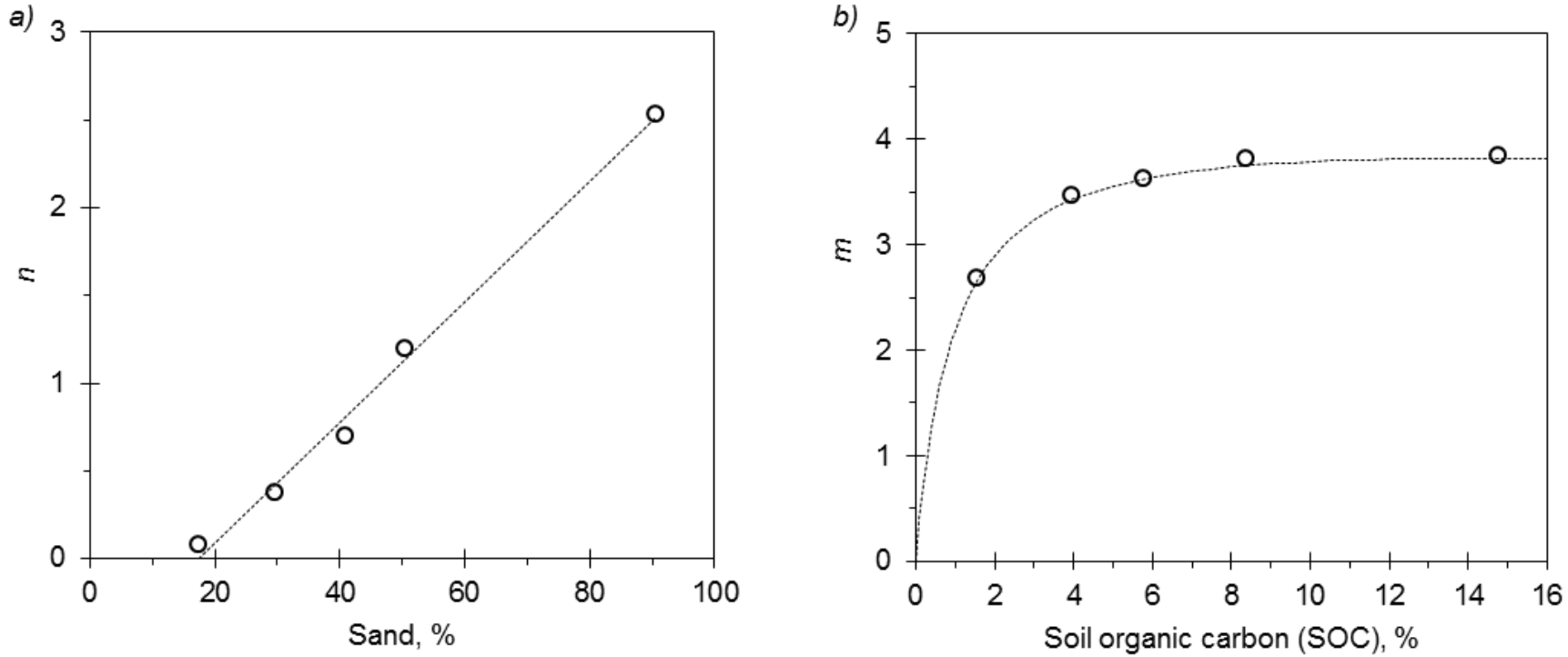

Figure 2.3. Archie model: relationships (a) *n vs.* sand content and (b) *m vs.* soil organic carbon. The dotted line represents the fit described by Equations (2.20) and (2.21), respectively. For the latter, RSS = 2.46×10^{-3} and RMSE = 0.04.

These results are also confirmed by the linear regressions between measured and estimated EC_p (Fig. 2.4). As displayed in this figure the models by Malicki and Walczak, and by Hilhorst did not show a good fitting, especially at high EC_p values, as already observed by (Hamed and Magnus Berndtsson, 2003; Persson, 2002).

The different performances of the four models at various salinity ranges were tested resampling observed and estimated EC_p 2,000 times, to compute average RMSEs and their confidence intervals at $p = 0.05$ as previously done by Giardini *et al.* (1998). The selected ranges were: (a) the 0–3 $dS \cdot m^{-1}$ and >3 $dS \cdot m^{-1}$; and (b) the 0–10 $dS \cdot m^{-1}$ and >10 $dS \cdot m^{-1}$.

At low EC_p range (*i.e.*, $EC_p < 3$ $dS \cdot m^{-1}$) Rhoades showed the smallest RMSE (0.57 $dS \cdot m^{-1}$), nevertheless its performance was not significantly different from those by Hilhorst (RMSE = 0.93 $dS \cdot m^{-1}$) and Archie (RMSE = 0.72 $dS \cdot m^{-1}$). On the contrary, the model by Malicki and Walczak provided significantly higher errors (RMSE = 1.69 $dS \cdot m^{-1}$).

Above 3 $dS \cdot m^{-1}$, the models by Malicki and Walczak and by Hilhorst significantly differentiated from the other two. In fact they generally overestimated EC_p in the range from 3 to 10 $dS \cdot m^{-1}$ with RMSE equal to 2.16 and 1.43 $dS \cdot m^{-1}$, respectively. On the other hand they underestimated EC_p when the pore-water was very conductive (*i.e.*, $EC_p > 10$ $dS \cdot m^{-1}$), with RMSE = 3.28 $dS \cdot m^{-1}$ and RMSE = 3.83 $dS \cdot m^{-1}$, respectively.

In their work, Malicki and Walczak used TDR probes at fairly high frequencies, reducing the influence of EC_a on ε_r. Moreover, their study was conducted using a wetting solution with a maximum conductivity of 11.7 $dS \cdot m^{-1}$. In the present work, calibrating the Malicki and Walczak model only for $EC_p < 10$ $dS \cdot m^{-1}$ would provide satisfactory estimations (RMSE = 1.00 $dS \cdot m^{-1}$). Moreover, the metrics of fitting regression would have shown a slope and intercept of 0.837 and 0.680, yielding very similar results to those obtained by Malicki and Walczak in their work. With some limitations, the model by Malicki and Walczak might therefore be used in capacitance applications as well as TDR (Malicki and Walczak, 1999) and frequency-domain reflectometry (Wilczek et al., 2012).

Hilhorst validated his model in a much lower EC_p range than the one used in this work. Hilhorst actually indicated the validity upper bound for the probe used in his work as 3 $dS \cdot m^{-1}$. Indeed, in the present study the model showed good performances in the 0–3

dS·m^{-1} range. Moreover, calibrating the model for EC_p <10 dS·m^{-1} would suitably yield a RMSE of 0.68 dS·m^{-1} with an observed-estimated relationship having a slope and an intercept of 0.957 and 0.127, respectively. Most likely, the higher operating frequency of 5TE compared to the capacitive probe used by Hilhorst (*i.e.*, 30 MHz) could have increased the range of model validity. However, as stated by Hilhorst, the model assumptions cease to be valid at higher salt concentrations as ε_p significantly deviates from that of free water (Equation (2.7)). From the experiment presented here this limit seems to be EC_p ~ 10 dS·m^{-1}.

The comparison of the error distribution at different EC_p ranges showed that Rhoades and Archie did not give significantly different performances. Nevertheless, the Rhoades model showed a larger RMSE at high EC_p values than at low ones (EC_p < 10 dS·m^{-1}: RMSE = 0.78 dS·m^{-1}; EC_p > 10 dS·m^{-1}: RMSE = 1.17 dS·m^{-1}). On the other hand, the Archie model showed a greater consistency over the two salinity ranges (EC_p < 10 dS·m^{-1}: RMSE = 0.69 dS·m^{-1}; EC_p > 10 dS·m^{-1}: RMSE = 0.54 dS·m^{-1}).

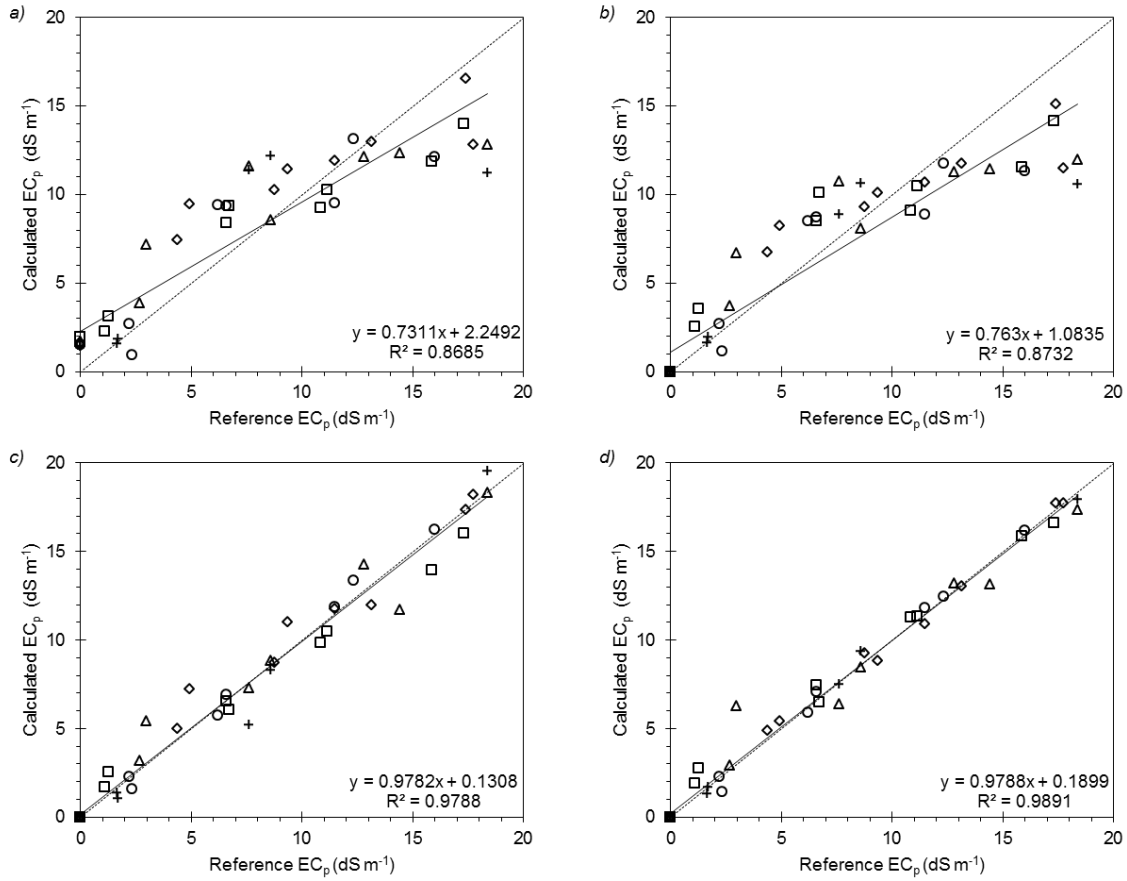

Figure 2.4. Comparison of calculated vs. reference pore-water electrical conductivity for the five soil samples using the "general" (a) Malicki and Walczak, (b) Hilhorst, (c) Rhoades, and (d) Archie models.; The symbols refer to: □ site A, topsoil; ◊ site A, subsoil; ○ site B, topsoil; + site B, subsoil; and Δ site C, topsoil.

4.3. Simultaneous Calibration of Models for θ and EC_p

As reported above, the "general" formulations of Rhoades and Archie showed overall similar performances. As already stated experimental θ values were used in the two equations. A simultaneous calibration was then done estimating EC_p and θ from EC_a and ε_r readings by substituting the "general" logarithmic θ model (Equation (2.15)) within Rhoades and Archie "general" models. The W_1 weight (Equation (2.12)) was set to 0.5, thus improving the EC_p estimation without notably worsening the θ evaluation.

The combined logarithmic θ model and Rhoades reads:

$$EC_p = \frac{EC_a}{\left(a'_{Rhoades} + a''_{Rhoades} \times EC_a\right) \times (1 - 0742 \times \ln(\varepsilon_r)) \times \pi_{Rhoades}} \tag{2.22}$$

with:

$$a'_{Rhoades} = -0.427 - 4.0 \cdot 10^{-5} \times SOC(\%) \tag{2.23}$$

$$a''_{Rhoades} = 0.024 - 0.008 \times \frac{clay(\%)}{sand(\%)} \tag{2.24}$$

$$\pi_{Rhoades} = \left(0.074 \times CaCO_3(\%) - 1.354\right) + \left(-0.132 \times CaCO_3(\%) + 3.232\right) \times \phi \tag{2.25}$$

where $a'_{Rhoades}$, $a''_{Rhoades}$, and $\pi_{Rhoades}$ are the fitting parameters defined in Equations (2.16), (2.17), and (2.19) during the independent calibration of θ and EC_p.

Similarly, the combined logarithmic θ model and Archie becomes:

$$EC_p = 0.466 \times \frac{EC_a}{\phi^{m_{Archie}} \times \left(\frac{\left(a'_{Archie} + a''_{Archie} \times EC_a\right) \times (1 - 0.738 \times \ln(\varepsilon_r))}{\phi} \right)^{n_{Archie}}} \tag{2.26}$$

with:

$$a'_{Archie} = -0.427 - 0.006 \times SOC(\%) \tag{2.27}$$

$$a''_{Archie} = 0.036 - 0.012 \times \frac{clay(\%)}{sand(\%)} \tag{2.28}$$

$$m_{Archie} = -2.8 \cdot 10^{-4} \times SOC(\%) + \frac{4.134 \times SOC(\%)}{SOC(\%) + 0.719} \tag{2.29}$$

$$n = -0.697 + 0.040 \times sand(\%) \tag{2.30}$$

where a'_{Archie}, a''_{Archie}, m_{Archie}, and n_{Archie} are the fitting parameters originally defined in Equations (2.16), (2.17), (2.21), and (2.20).

The calibration of Equation (2.22) yielded RSME values for θ and EC_p of 0.048 $m^3 \cdot m^{-3}$ and 0.77 $dS \cdot m^{-1}$, respectively. Better overall results were obtained by Equation (2.26): RMSE = 0.046 $m^3 \cdot m^{-3}$ and RMSE = 0.63 $dS \cdot m^{-1}$ for θ and EC_p, respectively. It is worth noting that the simultaneously calibrated parameters were very close to the independently calibrated ones.

A bootstrap validation was done on the simultaneous calibrations. A total of 5,000 iterations were operated for both Equations (2.22) and (2.26). Table 2.4 shows the variations of the slope and intercept of the fitting linear regression between observed and

predicted values. Soil water content was correctly predicted by both the equations: the slope and intercept medians of the observed-estimated relationships were fairly close to 1 and 0, respectively. EC_p predictions were less accurate, generally overestimated by Equation (2.22) and underestimated by Equation (2.26) (Table 2.4).

Table 2.4. Statistical analysis of the bootstrap validation outcome: median, 5th, and 95th percentile of slope and intercept distributions of the observed-predicted relationships for volumetric water content and pore-water electrical conductivity using Equations (2.22) and (2.26).

	Slope			Intercept		
	Median	**5% Limit**	**95% Limit**	**Median**	**5% Limit**	**95% Limit**
θ						
Rhoades (Equation (2.22))	0.97	0.89	1.02	0.01	−0.01	0.04
Archie (Equation (2.26))	0.98	0.91	1.04	0.01	−0.01	0.03
EC_p						
Rhoades (Equation (2.22))	1.15	0.98	1.31	0.13	−0.13	0.39
Archie (Equation (2.26))	0.93	0.88	1.03	0.32	0.11	0.53

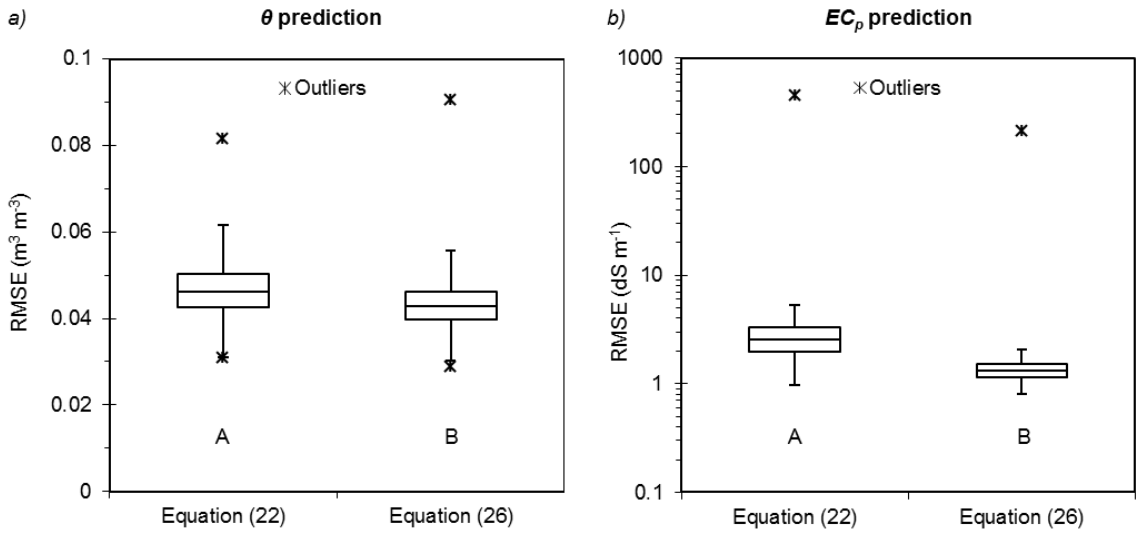

Figure 2.5. Comparison between the prediction performance of Equations (2.22) and (2.26) according to the Kolmogorov-Smirnov test. Boxplot for the RMSE values of (**a**) volumetric water content and (**b**) pore-water electrical conductivity. The letters A and B in the boxes indicate a significant difference ($p < 0.01$) between the RMSE distributions.

According to the Kolmogorov-Smirnov test, significant differences were observed between the two equations. The Archie-based model provided significantly lower RMSE values on the validation sets for both θ ($p < 0.01$) and EC_p ($p < 0.01$) (Fig. 2.5(a,b)). Equations (2.22) or (2.26) provided similar maximum errors for water content, with maximum RMSE of 0.08 $m^3 \cdot m^{-3}$ and 0.09 $m^3 \cdot m^{-3}$, respectively. On the other hand, Equation (2.22) produced a maximum EC_p error higher than that of Equation (2.26) (451.42 $dS \cdot m^{-1}$ *vs.* 211.26 $dS \cdot m^{-1}$). The overall more accurate prediction of the system implementing Archie can be justified by the more flexible functional form of the EC_p model allowed by the two exponential parameters.

5. Summary and Conclusions

Low-cost capacitance-resistance multiprobe sensors are becoming popular for agro-environmental studies. In order to obtain reliable results, robust models for soil water content and pore-water electrical conductivity must be calibrated in different soil and climatic conditions, especially when these instruments are used in coastal areas with contrasting soils and affected by saltwater contamination.

This experiment verifies the possibility of simultaneously quantifying water content and pore-water electrical conductivity from complex permittivity, bulk electrical conductivity, and soil temperature measurements performed by the ECH_2O-5TE (Decagon Devices, Inc.) probe. This result was achieved by improving empirical/theoretical reference models with the use of parameters dependent on physical and chemical soil properties, such as texture, soil organic carbon and soil carbonates. The improved models, in particular the one developed starting from Archie's law, prove to be reliable and robust over a wide range of water content (from dry to saturated conditions), salinity conditions (pore-water electrical conductivity from 0 to ~20 $dS \cdot m^{-1}$), and soil types (from sand with low SOC to clay-loam with high SOC).

Further studies performed in different soil and climatic environment coupled with improved dielectric sensors (e.g., with higher operating frequencies) will allow the accuracy of soil water content and pore-water salinity determination to be increased.

6. References

Akaike, H. 1974. A new look at the statistical model identification. Automatic Control, IEEE Transactions on 19:716-723.

Allred, B.J., Groom D., Reza Eshani, M. and J.J. Daniels. 2008. Resistivity methods. p. 85-108. *In* B.J. Allred, J.J. Daniels and M. Reza Ehsani (eds.) Handbook of agricultural geophysics. CRC Press, Taylor & Francis Group, New York, NY, USA.

Amente, G., J.M. Baker and C.F. Reece. 2000. Estimation of soil solution electrical conductivity from bulk soil electrical conductivity in sandy soils. Soil Sci. Soc. Am. J. 64:1931-1939.

Archie, G.E. 1942. The electrical resistivity log as an aid in determining some reservoir characteristics. Trans. AIME 5:54-62.

Barber, S.A. 1995. Soil nutrient bioavailability: A mechanistic approach. John Wiley & Sons Inc, New York, NY, USA.

Blake, G. and K. Hartge. 1986. Particle density. p. 377-382. *In* A. Klute (ed.) Methods of soil analysis. part 1. agron. monogr. 9. ASA, Madison, WI, USA.

Blonquist Jr., J.M., S.B. Jones and D.A. Robinson. 2005. Standardizing characterization of electromagnetic water content sensors: Part 2. evaluation of seven sensing systems. Vadose Zone Journal 4:1059-1069.

Bogena, H.R., M. Herbst, J.A. Huisman, U. Rosenbaum, A. Weuthen and H. Vereecken. 2010. Potential of wireless sensor networks for measuring soil water content variability. Vadose Zone Journal 9:1002-1113.

Burnham, K.P. and D.R. Anderson. 2002. Model selection and multi-model inference: A practical information-theoretic approach. Springer, New York, NY, USA.

Campbell, G.S. and W.C. Greenway. 2005. Moisture detection apparatus and method. 6904789. Date issued: 14 June, 2005.

Corwin, D. 2008. Past, present, and future trends of soil electrical conductivity measurements using geophysical methods. p. 17-44. *In* B.J. Allred, J.J. Daniels and Reza Eshani M. (eds.) Handbook of agricultural geophysics. CRC Press. Taylor & Francis Group, New York, NY, USA.

Dalton, F.N., W.N. Herkelrath, D.S. Rawlins and J.D. Rhoades. 1984. Time-domain reflectometry: Simultaneous measurement of soil water content and electrical conductivity with a single probe. Science 224:989-990.

Efron, B. 1979. Bootstrap methods: Another look at the jackknife. The Annals of Statistics 7:1-26.

Fares, A. and V. Polyakov. 2006. Advances in crop water management using capacitive water sensors. Adv. Agron. 90:43-77.

Friedman, S.P. 2005. Soil properties influencing apparent electrical conductivity: A review. Comput. Electron. Agric. 46:45-70.

Gattacceca, J.C., C. Vallet-Coulomb, A. Mayer, C. Claude, O. Radakovitch, E. Conchetto and B. Hamelin. 2009. Isotopic and geochemical characterization of salinization in the shallow aquifers of a reclaimed subsiding zone: The southern venice lagoon coastland. Journal of Hydrology 378:46-61.

Giardini, L., A. Berti and F. Morari. 1998. Simulation of two cropping systems with EPIC and CropSyst models. Ital.J.Agron 1:29-38.

Hamed, Y.P. and R. Magnus Berndtsson. 2003. Soil solution electrical conductivity measurements using different dielectric techniques. Soil Sci. Soc. Am. J. 67:1071-1078.

Heimovaara, T.J., A.G. Focke, W. Bouten and J.M. Verstraten. 1995. Assessing temporal variations in soil water composition with time domain reflectometry. Soil Sci. Soc. Am. J. 59:689-698.

Hilhorst, M.A. 2000. A pore water conductivity sensor. Soil Sci. Soc. Am. J. 64:1922-1925.

Jones, S.B., J.M. Blonquist Jr., D.A. Robinson, V.P. Rasmussen and D. Or. 2005. Standardizing characterization of electromagnetic water content sensors: Part 1. methodology. Vadose Zone Journal 4:1048-1058.

Keesstra, S.D., V. Geissen, K. Mosse, S. Piiranen, E. Scudiero, M. Leistra and L. van Schaik. 2012. Soil as a filter for groundwater quality. Current Opinion in Environmental Sustainability 4:507-516.

Kelleners, T.J., R.W.O. Soppe, D.A. Robinson, M.G. Schaap, J.E. Ayars and T.H. Skaggs. 2004a. Calibration of capacitance probe sensors using electric circuit theory. Soil Sci. Soc. Am. J. 68:430-439.

Kelleners, T., R. Soppe, J. Ayars and T. Skaggs. 2004b. Calibration of capacitance probe sensors in a saline silty clay soil. Soil Sci. Soc. Am. J 68:770-778.

Kizito, F., C.S. Campbell, G.S. Campbell, D.R. Cobos, B.L. Teare, B. Carter and J.W. Hopmans. 2008. Frequency, electrical conductivity and temperature analysis of a low-cost capacitance soil moisture sensor. Journal of Hydrology 352:367-378.

Malicki, M.A. and R.T. Walczak. 1999. Evaluating soil salinity status from bulk electrical conductivity and permittivity. Eur. J. Soil Sci. 50:505-514.

Monego, M., G. Cassiani, R. Deiana, M. Putti, G. Passadore and L. Altissimo. 2010. A tracer test in a shallow heterogeneous aquifer monitored via time-lapse surface electrical resistivity tomography. Geophysics 75:WA61.

Mualem, Y. and S.P. Friedman. 1991. Theoretical prediction of electrical conductivity in saturated and unsaturated soil. Water Resour. Res. 27:2771-2777.

Pardossi, A., L. Incrocci, G. Incrocci, F. Malorgio, P. Battista, L. Bacci, B. Rapi, P. Marzialetti, J. Hemming and J. Balendonck. 2009. Root zone sensors for irrigation management in intensive agriculture. Sensors 9:2809-2835.

Persson, M. 2002. Evaluating the linear dielectric constant-electrical conductivity model using time-domain reflectometry. Hydrological Sciences Journal 47:269-277.

Rhoades, J.D., F. Chanduvi and S.M. Lesch. 1999. Soil salinity assessment: Methods and interpretation of electrical conductivity measurements. Food & Agriculture Organization of the UN (FAO), Rome, Italy.

Rhoades, J.D., P.A.C. Raats and R.J. Prather. 1976. Effects of liquid-phase electrical conductivity, water content, and surface conductivity on bulk soil electrical conductivity. Soil Sci. Soc. Am. J. 40:651-655.

Rhoades, J., N. Manteghi, P. Shouse and W. Alves. 1989a. Soil electrical conductivity and soil salinity: New formulations and calibrations. Soil Sci. Soc. Am. J. 53:433-439.

Rhoades, J., N.A. Manteghi, P. Shouse and W. Alves. 1989b. Estimating soil salinity from saturated soil-paste electrical conductivity. Soil Sci. Soc. Am. J. 53:428-433.

Richards, L.A. and US Salinity Laboratory Staff. 1954. USDA handbook no. 60. diagnosis and improvement of saline and alkali soils. U.S. Government Printing Office, Washington, D.C., USA.

Rosenbaum, U., J.A. Huisman, J. Vrba, H. Vereecken and H.R. Bogena. 2011. Correction of temperature and electrical conductivity effects on dielectric permittivity measurements with ECH2O sensors. Vadose Zone Journal 10:582-593.

Saito, T., H. Fujimaki and M. Inoue. 2008. Calibration and simultaneous monitoring of soil water content and salinity with capacitance and four-electrode probes. American Journal of Environmental Sciences 4:683-692.

Saito, T.F., H. Yasuda and M. Hiroshi Inoue. 2009. Empirical temperature calibration of capacitance probes to measure soil water. Soil Sci. Soc. Am. J. 73:1931-1937.

Schwank, M. and T.R. Green. 2007. Simulated effects of soil temperature and salinity on capacitance sensor measurements. Sensors 7:548-577.

Seyfried, M. and M. Murdock. 2001. Response of a new soil water sensor to variable soil, water content, and temperature. Soil Science Society of America Journal 65:28-34.

Sumner, M.E., W.P. Miller, D.L. Sparks, A.L. Page, P.A. Helmke, R.H. Loeppert, P.N. Soltanpour, M.A. Tabatabai and C.T. Johnston. 1996. Cation exchange capacity and exchange coefficients. Methods of Soil Analysis.Part 3-Chemical Methods.1201-1229.

Topp, G.C., J.L. Davis and A.P. Annan. 1980. Electromagnetic determination of soil water content: Measurements in coaxial transmission lines. Water Resour. Res. 16:574-582.

Van Genuchten, M.T., F. Leij and S. Yates. 1991. The RETC code for quantifying the hydraulic functions of unsaturated soils. EPA: Ada, OK, USA.

Waxman, M. and L. Smits. 1968. 1863-A-electrical conductivities in oil-bearing shaly sands. Old SPE Journal 8:107-122.

Wilczek, A., A. Szypłowska, W. Skierucha, J. Cieśla, V. Pichler and G. Janik. 2012. Determination of soil pore water salinity using an FDR sensor working at various frequencies up to 500 MHz. Sensors 12:10890-10905.

Wolt, J.G. and G. John. 1986. A rapid routine method for obtaining soil solution using vacuum displacement. Soil Sci. Soc. Am. J. 50:602-605.

Chapter 3

Constrained Optimization of Spatial Sampling in a Salt-Contaminated Coastal Farmland Using EMI and Continuous Simulated Annealing

1. Introduction

The Venice Lagoon watershed is located in the eastern part of the Po river delta plain, Italy, and includes a very precarious coastal environment subject to both natural and anthropogenic changes with a significant and economically important fraction of the coastal farmland presently below the mean sea level. In the hydrogeological context of the Venice Lagoon coastland, a large risk of saltwater contamination characterizes the southernmost area because of the geomorphological setting of the coastal plain. Saltwater intrusion is connected to the natural geomorphological features of this area, i.e. the presence of sandy paleochannels. The time and space behavior of salt contamination is influenced by other anthropogenic factors, such as the activity of several pumping stations used to keep the area drained, groundwater withdrawals, irrigation and freshwater releases during the summer dry months (De Franco et al., 2009). Due to its deltaic origins the Venice Lagoon coastland is characterized by a high soil spatial variability, having a profound influence on a variety of issues such as soil quality assessment, solute transport in the vadose zone, and site-specific crop management (Corwin et al., 2010). If the sparsely sampled primary soil variables (e.g. soil salinity, texture) and more intensive ancillary data are spatially correlated, then the additional information from the ancillary data can be used to improve the estimate precision of the primary variable (Morari et al., 2009). Intensive grids of ancillary data, including ground penetrating radar, aerial photography, and apparent soil electrical conductivity (EC_a), can be used to characterize soil spatial variability. In agricultural studies EC_a is by far the most commonly used ancillary data (Corwin and Lesch, 2005). This is because EC_a measurements are reliable, fairly easy to take, and relatively inexpensive (Blackmer et al., 1995; Mulla, 1997). EC_a intensive surveys have been used to characterize salinity (Rhoades et al., 1999b), nutrients (Kaffka et al., 2005), texture (Triantafilis and Lesch, 2005), bulk density related (Rhoades et al., 1999a), and many other soil properties (Corwin and Lesch, 2005).

The optimization of soil sampling schemes based on spatial measurements of EC_a has proven to facilitate modeling the relationships between primary soil variables and EC_a (Corwin et al., 2010).

The objective of this chapter is to optimize a soil sampling scheme according to field geometry and EC_a spatial variability.

2. Materials and Methods

2.1. The study site

The site is located at Ca' Bianca (12°13'55.218"E; 45°10'57.862"N), right south of the Venice Lagoon, approximately 5 km from the Adriatic Sea (Fig. 3.1). The area was occupied in the 19th century by swamps and was reclaimed at the beginning of the past century. At present it lies entirely below mean sea level, mostly between 2 and 4 m below asl, and is mainly cultivated with maize. Geomorphological investigations at the basin scale have shown that fluvial and deltaic sedimentations constitute the outcropping deposits. The area is well known to be affected by saltwater contamination down to about 20 m depth with the presence of a first confined fresh-water aquifer 45-50 m below asl (Viezzoli et al., 2010).

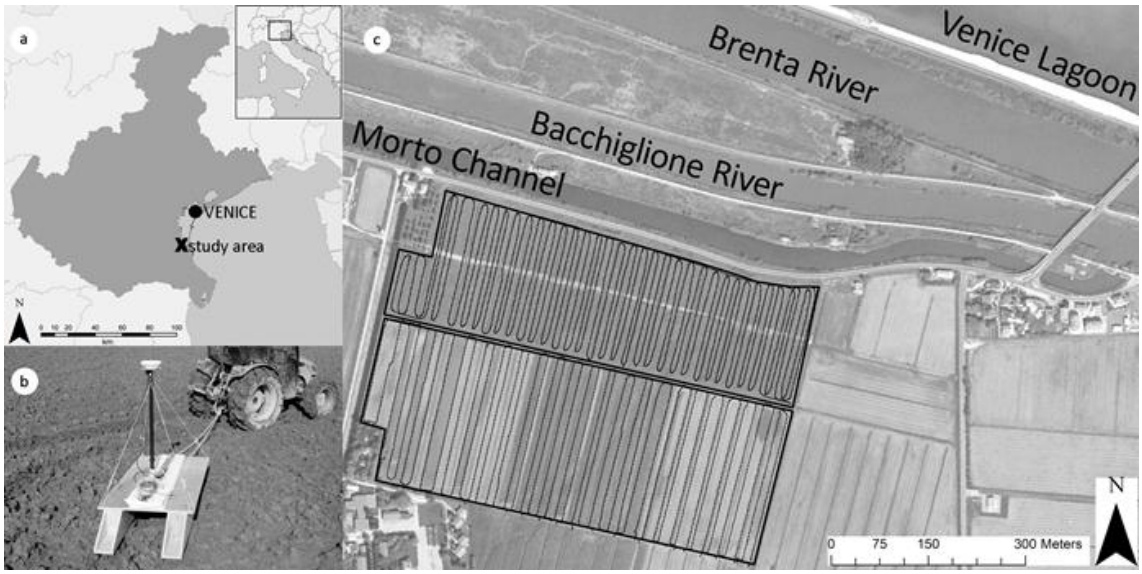

Figure 3.1. The study area: a) location with respect to the Venice Lagoon; b) the mobile EMI equipment used in this study; c) transects (dots) of the measurements of electro-magnetic induction.

2.2. *EC_a Survey*

Apparent electrical conductivity (*EC_a*) at three different investigation depths was measured in April 2010 with two electromagnetic conductivity-meters (CMD-1 and CMD-4. GF Instruments, Brno, Czech Republic) (Fig. 3.1.c).

Alike all EMI instruments, the CMD probes are equipped with two coils, one at each end of the instrument (Fig. 3.2.a). The head coil produces a (primary) local electromagnetic field (H_p) by inducing circular eddy-current loops in the soil. The electrical conductivity in the vicinity of the loops is proportional to the magnitude of these loops. A second electromagnetic field (H_i) is consequently generated by each current loop. The magnitude of such field is proportional to the value of the current that generated it. The tail coil then intercepts a fraction of the induced electromagnetic field (H_a) from each loop. The sum of these induced signals is then amplified and transformed into a voltage output, which is related to a depth-weighted *EC_a*. The secondary field will differ from the primary field in terms of amplitude and phase, as an effect of soil properties, spacing and orientation of the coils, frequency of the primary field (i.e. 10 KHz in the CMD probes), and distance from the soil surface (Hendrickx and Kachanoski, 2002). Normally, EMI equipment can measure *EC_a* at two configurations, one with the coils parallel ("low" or "horizontal") and one with the coils perpendicular ("high" or "vertical") to the soil surface. As shown in Fig. 3.2.b, when EMI are used in the low configurations, the readings mainly refer to a less deep soil increment than when used in the high configuration. Depth range and resolution are closely related: the increasing depth range decreases resolution and vice versa.

The CMD-1 probe, in continuous measurement mode with GPS on a mobile platform (Fig. 3.1.b), was used in both Low and High configurations with 0.5 s time acquisition interval, respectively with 0-0.75 m (*EC_a Low*) and 0-1.5 m (*EC_a* High) investigation depth. The CMD-4 probe was only used in the High position allowing measuring *EC_a* in the 0 - 6.00 m soil increment (*EC_a 6*).

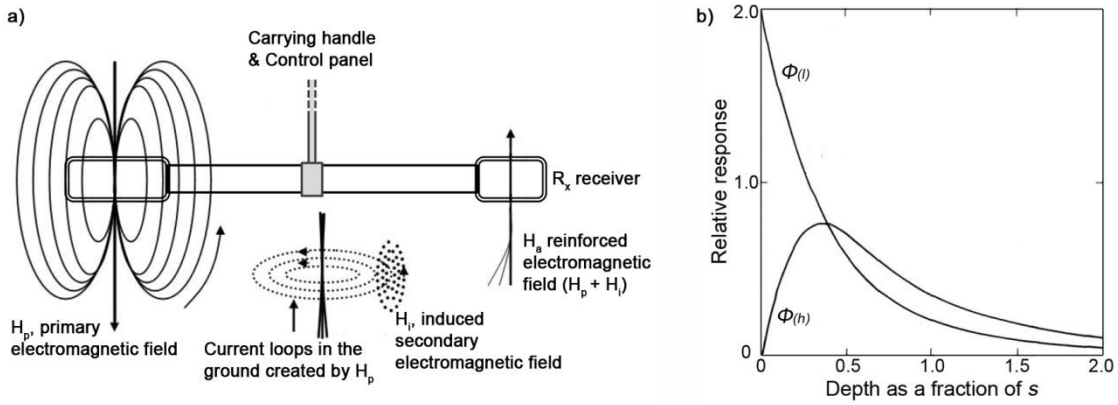

Figure 3.2. a) schematic of the operation of the CMD probes. Modified from Corwin et al. (2012); b) relative contribution of the secondary magnetic field for high/vertical ($\Phi_{(h)}$) and low/horizontal ($\Phi_{(l)}$) coils as a function of soil depth (*s* = intercoil spacing). Modified from McNeill (1980).

EC_a surveys were conducted prior to maize sowing when volumetric water content in the first 0.4 m profile was on average 35% and water table was approximately at 0.75-0.8 m. Negative values of EC_a *Low* were observed in the north-eastern corner of area probably due to electromagnetic disturbance of a nearby military base. These values were masked and not considered for spatial analyses. In total 17321, 20710 and 11608 data were recorded for EC_a *Low*, EC_a *High*, and EC_a *6* respectively.

2.3. *Spatial Simulated Annealing and Geostatistical Procedures*

Spatial simulated annealing (SSA) (Van Groenigen and Stein, 1998; Van Groenigen et al., 1999; Van Groenigen et al., 2000) was applied to optimize the sampling scheme of the study area in regard of its irregular shape and its unevenly distributed soil properties. A central concept in spatial SSA is the fitness function Φ(S) which has to be optimized to a global minimum. SSA proceeds by random perturbation of an initial set of those parameters (x and y coordinates) which describe Φ(S). Perturbations with a better fitness for Φ(S) are all accepted. To avoid local minimums of Φ(S), those perturbations that don't improve the function are also accepted with a probability of acceptance described by the Metropolis-criterion (Metropolis et al., 1953).As the optimization process

evolves, the maximum perturbation decreases, forcing the sampling scheme to "freeze" in its optimal configuration. The approach shows a wide flexibility in defining several optimization criteria with their corresponding fitness functions because different surveys may have different purposes (Castrignanò et al., 2008). The so-called MMSD (Minimization of the Means of the Shortest Distances)-criterion, which minimizes the expectation of the distance of an arbitrary point to its nearest observation point, has frequently been used in the past (Van Groenigen et al., 1999; Van Groenigen et al., 2000).

To densify the sampling scheme in areas with high heterogeneity, MWMSD (Minimization of the Weighted Means of the Shortest Distances)-criterion can be used. The MWMSD-criterion, a weighted version of the MMSD-criterion, introduces a location-dependent weighting function in Φ(S) as follows:

$$\phi_{MWMSD}(S) = \int_A w(\vec{x}) \| \vec{x} \quad V_s(\vec{x}) \| d\vec{x} \tag{3.1}$$

where: $\vec{x}$ denotes a two-dimensional coordinate vector; w($\vec{x}$) weighting function; V($\vec{x}$) the coordinate vector of the sampling point nearest to $\vec{x}$. The symbol $||$ is used as distance vector.

EMI surveys showed a high heterogeneity in EC_a values, which is accountable on both soil chemical and physical properties. The gradient of EC_a was chosen as weight to increase the sampling intensity in the areas of expected maximum variation. A multi-stage sampling design was applied to define the sampling scheme Two optimization criteria were used. The first (Minimization of the Mean of the Shortest Distance - MMSD) aims for an even distribution of sampling points over the entire survey area by minimizing the expectation of the distance between an arbitrarily chosen point and its nearest observation. Moreover, the preliminary creation of a sampling grid constrained on the sole field shape and boundaries aimed to create a basic sampling scheme that could cover for the spatial variability of many soil characteristics, even those not influencing EC_a readings. A number of 40 points were distributed according to MMSD. The second criterion (MWMSD) is a weighted version of the MMSD and uses the digital gradient of the grid-interpolated EC_a to calculate the optimal sampling density. Because the weights

are defined as the EC_a gradient, the method places more observations in the area of expected maximum variation. To take into account the variability along the soil profile, 40 points were distributed according to EC_a *Low* and the remaining to EC_a *High*. The sampling procedure used in this work was implemented in the free software SANOS (Van Groenigen and Stein, 1998). To be sure the absolute minimum in annealing simulation had been reached; the procedure was repeated seven times with a different initial seed, verifying that the point distributions on the maps actually remained the same.

Ordinary kriging was applied to interpolate EC_a data and reduce spike values due to measurement errors. The variogram study allowed also retrieving important information on the spatial structure of the soil parameter. Before applying univariate analysis, EC_a values were transformed and standardized into Gaussian values Y(x) using an *expansion into Hermite polynomials* (Wackernagel, 2003). After variogram modeling, ordinary kriging was applied and then the estimates were then back transformed to the raw variables.

3. Results and Discussion

Anisotropic variograms were observed for all the three EC measurements (Fig. 3.3). In particular, non-stationary variograms were shown along N0 and N45 directions, most likely due to the salinity intrusion from the rivers and cost. EC_a *6* was spatially correlated with both EC_a *Low* and EC_a *High*, approximately up to 25 m and 70 m respectively. Conversely EC_a *Low* and EC_a *High* resulted no spatially correlated.

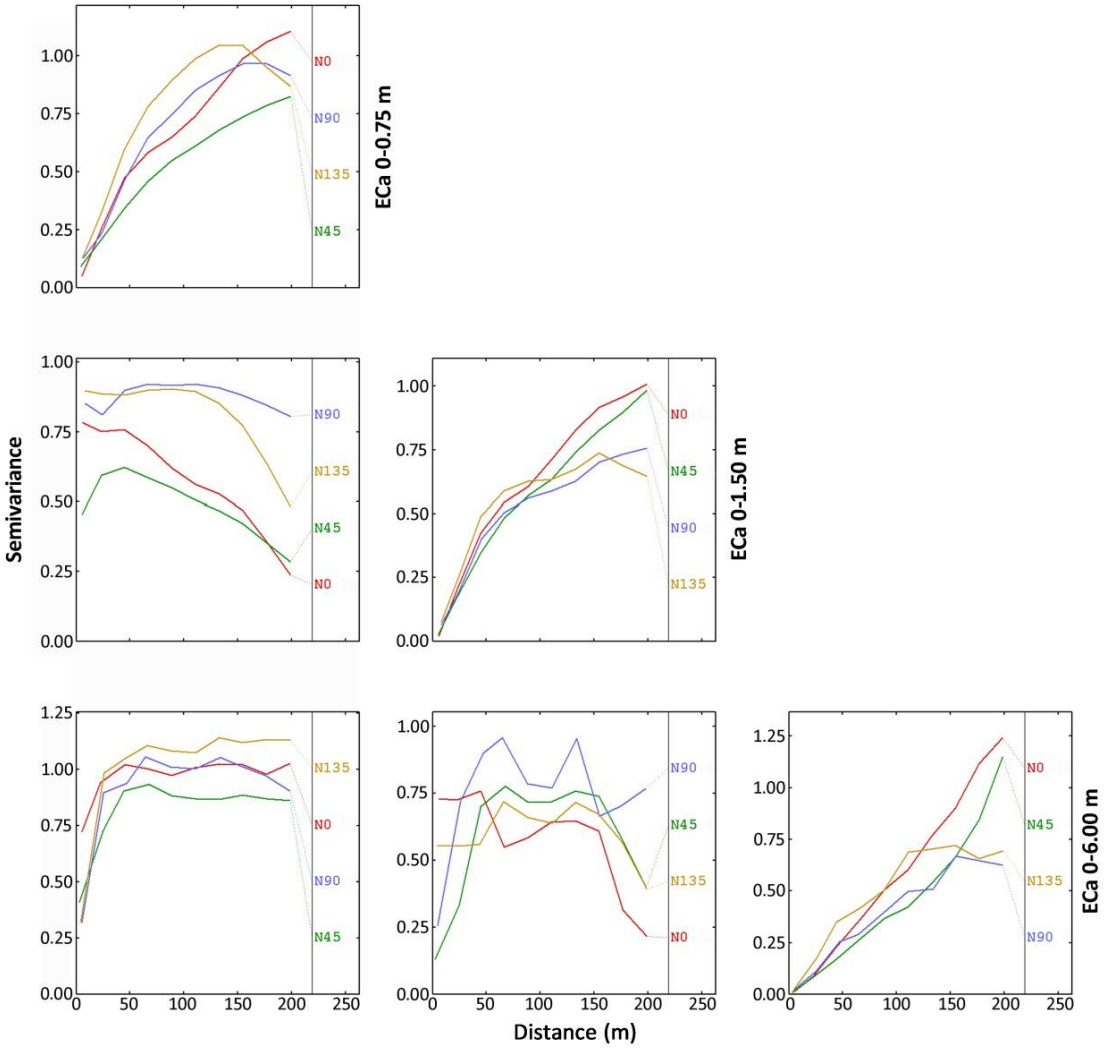

Figure 3.3. Direct variograms and cross-variograms between electrical conductivity at 0-0.75m, 0-1.50m, 0-6.00m in four different directions: N (N0), NE (N45), E (N45) and SE (N135)

Therefore, in order to represent the different structures of variability along the soil profile, sampling was optimized according to the gradient estimated in the kriging maps of EC_a *Low* and EC_a *High*. The EC_a *Low* variogram was fitted by a directional nested model including a nugget effect, a directional spherical model along N45 direction with a short-range of 150 m and a long-range of 1500 m and a directional spherical model along N135 direction with a short-range of 90 m and a long-range of 151 m. Also in the case of EC_a *High* a directional nested model was fitted including a directional spherical model along N10 direction with a short-range of 235 m and a long-range of 3300 m and a directional spherical model along N100 direction with a short-range of 120 m and a long-range to "infinity" (zonal anisotropy). Cross-correlation test was performed to evaluate the consistency of the variogram models. For both the variables $R^2 > 0.98$.

EC_a krigged maps show a large variability (Fig. 4) ranging from 0.04 to 2.06 dS m^{-1} and from 0.32 to 3.38 dS m^{-1} in the EC_a *Low* and EC_a *High* respectively. EC_a *High* map is characterized by higher values in the northern part with a positive gradient toward the rivers and lagoon. This trend suggests a direct effect of the saline intrusion on EC_a soil profiles. Both the maps show also a NW-SE band with low EC_a values that corresponds to one of the sandy paleochannels crossing the site.

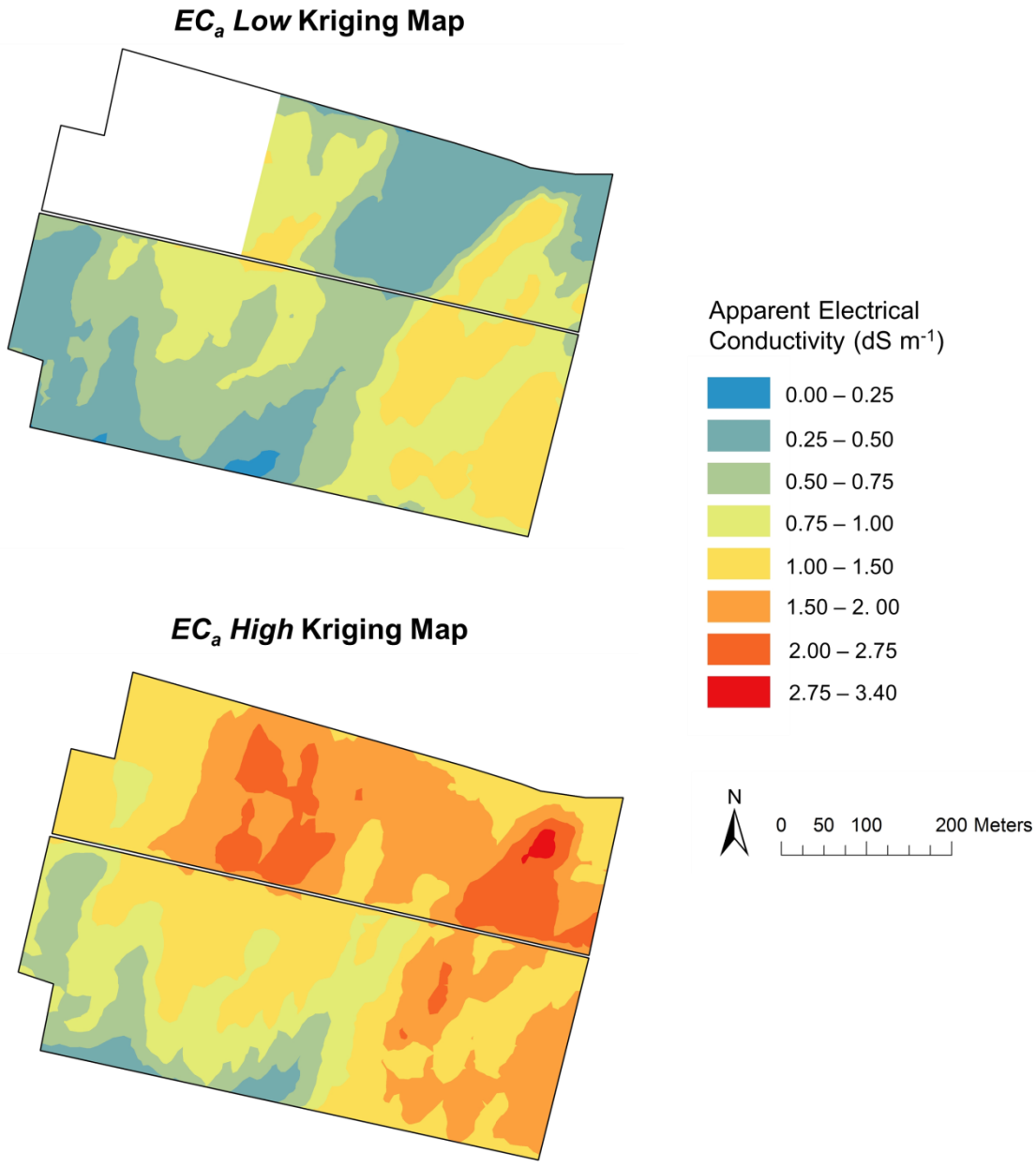

Figure 3.4. Kriging estimation maps for EC_a *Low* and EC_a *High*

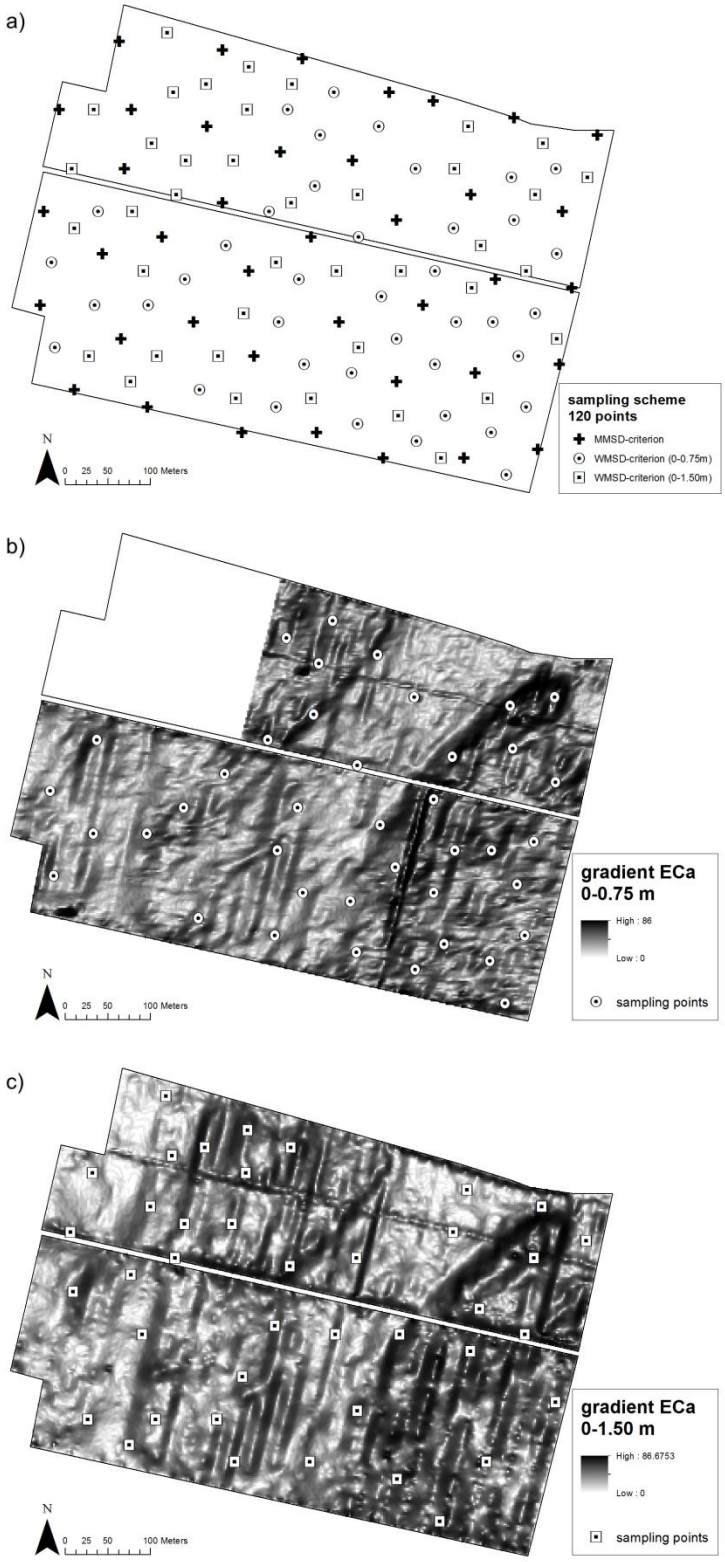

Figure 3.5. The optimized sampling scheme: (a) the 120 points altogether, (b) the 40 points found using the digital gradient of the grid-interpolated EC_a *Low*; (c) the 40 points found using the digital gradient of the grid-interpolated EC_a *High*.

Gradients maps (Figs. 3.5.b and 3.5.c) exhibit higher values along the boundaries of the paleochannels, especially in the northern part where soil salinity is expected to be higher. Conversely the SW area shows a low gradient in both of the maps. EC_a *Low* gradient could not be calculated in NW corner of the study site due to electromagnetic disturbance occurred during acquisition, nevertheless the same area showed in general a low gradient in EC_a *High*. A continuous NW-SE oriented line of filling subsoil added over a deep gas pipeline is also visible in the northern part of the maps. Fig. 3.5.a shows the optimized sampling scheme. The use of the MMSD-criterion to set 40 preliminary sampling points ensured a good coverage of the area. The first 40 points were placed in a grid-like design where the only irregularities of the grid are caused by the irregular shape of the site. MWMSD-criterion allowed allocating the remaining 80 points in areas with higher gradient. In particular the transaction zone along the paleochannels was sampled with higher density in both the EC_a gradient maps. Moreover few points were placed along the gas pipeline. The multistep approach allowed also covering even the NW corner where EC_a *Low* was not available placing 7 and 11 points according to MMSD and MWMSD criteria, respectively. It is clear that MWMSD-criterion cause the number of samples to increase in the sub-regions with higher priority (greater gradient).

4. Conclusions

The study site was characterized by a high degree of variability due to natural and anthropic phenomena. Characterizing soil properties would be particularly difficult in the site without the help of intensively surveyed ancillary data. As a matter of fact, the EC_a maps helped describing the site with high resolution, showing a wide range of apparent electrical conductivity values. The proposed multistep approach allowed considering this particular condition and optimizing the sampling scheme. EC_a maps have proven very effectively to drive the optimization procedure of sampling location, distinguishing between areas with different priority levels. Moreover, the selection of a first set of sampling locations on the base of the sole geometry of the study site should help minimizing biases due to those soil properties not correlated with EC_a.

In areas characterized by high soil spatial variability, the proposed methodology should help defining the relationship between intensively surveyed sensor data and soil properties.

5. References

Blackmer, T., J. Schepers and G. Meyer. 1995. Remote sensing to detect nitrogen deficiency in corn. In: Robert, P.C., Rust, R.H., Larson, W.E. (Eds.), Proceedings of Site-specific Management for Agricultural Systems. Second International Conference, March 1994, Minneapolis, MN, USA, pp. 505-512.

Castrignanò, A., F. Morari, C. Fiorentino, C. Pagliarin and S. Brenna. 2008. Constrained optimization of spatial sampling in skeletal soils using EMI data and continuous simulated annealing. *In* 1st global workshop on high resolution digital soil sensing & mapping, Sydney, Australia. 5-8 February 2008 2008.

Corwin, D.L., S.M. Lesch, E. Segal, T.H. Skaggs and S.A. Bradford. 2010. Comparison of sampling strategies for characterizing spatial variability with apparent soil electrical conductivity directed soil sampling. J. Environ. Eng. Geophys. 15:147-162.

Corwin, D. and S. Lesch. 2005. Apparent soil electrical conductivity measurements in agriculture. Comput. Electron. Agric. 46:11-43.

Corwin, D., S. Lesch and D. Lobell. 2012. Laboratory and field measurements. p. 295-341. *In* W. Wallender and K. Tanji (eds.) Agricultural salinity assessment and management. ASCE manual and reports on engineering practice no. 71 2nd ed. ASCE, Reston, VA, USA.

De Franco, R., G. Biella, L. Tosi, P. Teatini, A. Lozej, B. Chiozzotto, M. Giada, F. Rizzetto, C. Claude and A. Mayer. 2009. Monitoring the saltwater intrusion by time lapse electrical resistivity tomography: The Chioggia test site (Venice Lagoon, Italy). J. Appl. Geophys. 69:117-130.

Hendrickx, J. and R. Kachanoski. 2002. Solute content and concentration - indirect measurement of solute concentration: Nonintrusive electromagnetic induction. p. 1297-1306. *In* J.H. Dane and G.C. Topp (eds.) Methods of soil analysis, part 4—Physical methods. SSSA Book Series No. 5 ed. SSSA, Madison, WI, USA.

Kaffka, S., S. Lesch, K. Bali and D. Corwin. 2005. Site-specific management in salt-affected sugar beet fields using electromagnetic induction. Comput. Electron. Agric. 46:329-350.

McNeill, J. 1980. Electromagnetic terrain conductivity measurement at low induction numbers. Geonics Limited Mississauga, Ontario, Canada.

Metropolis, N., A. Rosembluth, M. Rosembluth and A. Teller. 1953. Equation os state calculations by very fast computing machines. J. Chem. Phys. 21:1087-1092.

Morari, F., A. Castrignanņ and C. Pagliarin. 2009. Application of multivariate geostatistics in delineating management zones within a gravelly vineyard using geo-electrical sensors. Comput. Electron. Agric. 68:97-107.

Mulla, D.J. 1997. Geostatistics, remote sensing and precision farming. p. 1-18. *In* J.V. Lake, G.R. Bock and J.A. Goode (eds.) Precision agriculture: Spatial and temporal variability of environmental quality. John Wiley & Sons Ltd, Chichester, UK.

Rhoades, J.D., F. Chanduvi and S.M. Lesch. 1999a. Soil salinity assessment: Methods and interpretation of electrical conductivity measurements. Food & Agriculture Organization of the UN (FAO), Rome, Italy.

Rhoades, J., D. Corwin and S. Lesch. 1999b. Geospatial measurements of soil electrical conductivity to assess soil salinity and diffuse salt loading from irrigation. p. 197-215. *In* D.L. Corwin, K. Loague and T.R. Ellsworth (eds.) Assessment of non-point source pollution in the vadose zone, geophysical monograph., 108. American Geophysical Union, Washington, DC, USA.

Triantafilis, J. and S. Lesch. 2005. Mapping clay content variation using electromagnetic induction techniques. Comput. Electron. Agric. 46:203-237.

Van Groenigen, J.W. and A. Stein. 1998. Constrained optimization of spatial sampling using continuous simulated annealing. J. Environ. Qual. 27:1078-1086.

Van Groenigen, J.W., G. Pieters and A. Stein. 2000. Optimizing spatial sampling for multivariate contamination in urban areas. Environmetrics 11:227-244.

Van Groenigen, J.W., W. Siderius and A. Stein. 1999. Constrained optimisation of soil sampling for minimization of the kriging variance. Geoderma 87:239-259.

Viezzoli, A., L. Tosi, P. Teatini and S. Silvestri. 2010. Surface water–groundwater exchange in transitional coastal environments by airborne electromagnetics: The Venice Lagoon example. Geophys. Res. Lett. 37:L01402.

Wackernagel, H. 2003. Multivariate geostatistics. Springer, Berlin, Germany.

Chapter 4

Identifying Site-Specific Management Units in an Area Affected by Saltwater Intrusion

1. Introduction

The southern margin of the Venice lagoon is nowadays a highly heterogeneous and precarious environment subject to both natural changes and anthropogenic pressure (Carbognin et al., 2006; De Franco et al., 2009).The area is part of the greater Po River alluvial delta plain, which is characterized by high spatial geomorphologic variability. The area is featured with highly permeable sandy drifts consisting on ancient river forks (i.e. paleochannels) (Carbognin and Tosi, 2003; Rizzetto et al., 2002; Rizzetto et al., 2003). Due to the presence of peat, the area has been subsiding remarkably since it was reclaimed for agricultural purposes at the beginning of the 20th century (Carbognin et al., 2005a; Gambolati et al., 2005; Teatini et al., 2007). Furthermore, saltwater intrusion represents here one of the main threats to crop production (Carbognin et al., 2005b; De Franco et al., 2009; Viezzoli et al., 2010) because this area lies well below sea level and the continuous drainage helps raising the saltwater-freshwater interface close to the soil surface (Bear, 1988).

Contrasting soil scenarios can lead to very different production outputs, in particular originating specific kinds of crop stress that are impractical to be effectively managed with a unique strategy (Robert, 2002). On the other hand, site-specific crop management (i.e. application of resources when, where, and in the amount needed) could be the best option in order to manage crops and soils according to field spatial variability (Larson and Robert, 1991; Van Uffelen et al., 1997). In particular, the use of Site-Specific Management Units (SSMUs, i.e. portions of field that is managed the same in order to achieve the same goal) has proved to be a reliable solution for the management issues in many heterogeneous farmlands (Robert, 2002).

Yield spatial variation is affected by a large range of factors, such as topographic, edaphic, biological, meteorological, and anthropogenic factors. For practical reasons, only a limited portion of these factors can be managed in order to increase crop productivity. Indeed, as suggested by (Corwin and Lesch, 2010), a simplified and effective way of designing SSMUs is to analyze the effect of a single factor class (e.g. edaphic factors) on yield spatial variability. As a matter of fact, the extent of yield variation specifically

related to changes in soil properties can be considerably large (Corwin et al., 2003; Vitharana et al., 2008).

In order to characterize the spatial variability of a vast group of soil properties (Corwin and Lesch, 2005) intensive and relatively inexpensive spatial measurements of soil apparent electrical conductivity (EC_a) are commonly used. EC_a can in fact be correlated to many soil properties, including soil salinity, water content, texture, organic carbon content, and bulk density (Corwin and Lesch, 2005). Unfortunately, in many cases EC_a measurements cannot sufficiently describe the spatial distribution of all the soil properties influencing yield: often a singular or a small group of soil properties are "dominant" in the contribution to the conduction of electricity in the soil (Corwin, 2008; Johnson et al., 2005). In such cases other types of ancillary data could be used to complement the EC_a survey data. Several types of sensors have recently been used to provide ancillary data in order to characterize large areas on the basis of a limited number of soil samples (Adamchuk et al., 2004; Mulder et al., 2011; Viscarra Rossel et al., 2011), including optical and radiometric sensors, which are closely related to soil color and water content (Post et al., 2000).

Some recent studies on the delineation of SSMUs driven by ancillary data from soil-proximal sensors can be found in (Corwin et al., 2003), (Li et al., 2007a; Li et al., 2007b), (Vitharana et al., 2008), (Johnson et al., 2008), (Roberts et al., 2012), and (Morari et al., 2009).

The objectives of this study were to: (*i*) investigate the effect of the spatial variability of soil salinity and other soil properties on maize yield in a field at the southern margin of the Lagoon of Venice; (*ii*) evaluate the use of proximal sensors for characterizing the spatial distribution of soil properties; and (*iii*) develop a protocol for SSMU delineation based on low-cost and intensively proximal sensed data.

2. Materials and Methods

2.1. Study site description

The study site (Fig. 4.1) was a ca. 21 ha field located at Chioggia, Venice, Italy (45°10'57"N; 12°13'55"E; -1 to -3.3 m below asl) along the southern edge of the Venice Lagoon. The soil at the study area is mainly silt-clay (*Molli-Gleyic Cambisols*) with the presence of peat and sandy drifts (i.e. paleochannels). In particular, two well preserved paleochannels (i.e. western and eastern) cross the study site (Fig. 4.1) and could potentially act as preferential pathway in saltwater intrusion (Donnici et al., 2011). A pumping station controls the water table level, which is generally maintained at <-0.6 m during the summer season in order to promote sub-irrigation. The experiment was carried out in 2010 and 2011. In the two years the same maize (*Zea mais* L.) variety (PR32P26, Pioneer Hi-Bred Italia, Gadesco Pieve Delmona, Italy) was cultivated. Soil tillage was an autumn ploughing at 30 cm, followed by standard seedbed preparation operations. Maize was fertilized with a base-dressing of 64 N kg ha^{-1} and 94 kg P_2O_5 ha^{-1} and a top-dressing of 184 kg N ha^{-1} (urea).

Meteorological data were recorded by a nearby automatic station (ARPAV, *Regional Agency for Environmental Protection, Veneto*). Rainfall was contrasting in the two cropping seasons: 2010 (April 22nd – September 10th) was very rainy (total rainfall: 0.539 m), whereas 2011 (April 4th – September 2nd) was fairly dry (total rainfall: 0.200 m). The two years were characterized by similar average temperature (2010, 21.12 °C; 2011, 20.70 °C) and average daily relative humidity (2010, 76.03%; 2011, 72.41%). Potential evapotranspiration (ET_0) was calculated with the Penmann-Monteith equation using the dual-crop coefficient approach (Allen et al., 1998). ET_0 was higher in the 2011 cropping season (total: 0.599 m; average: 3.7 mm day^{-1}) than 2010 (total: 0.497 m; average: 3.5 mm day^{-1}).

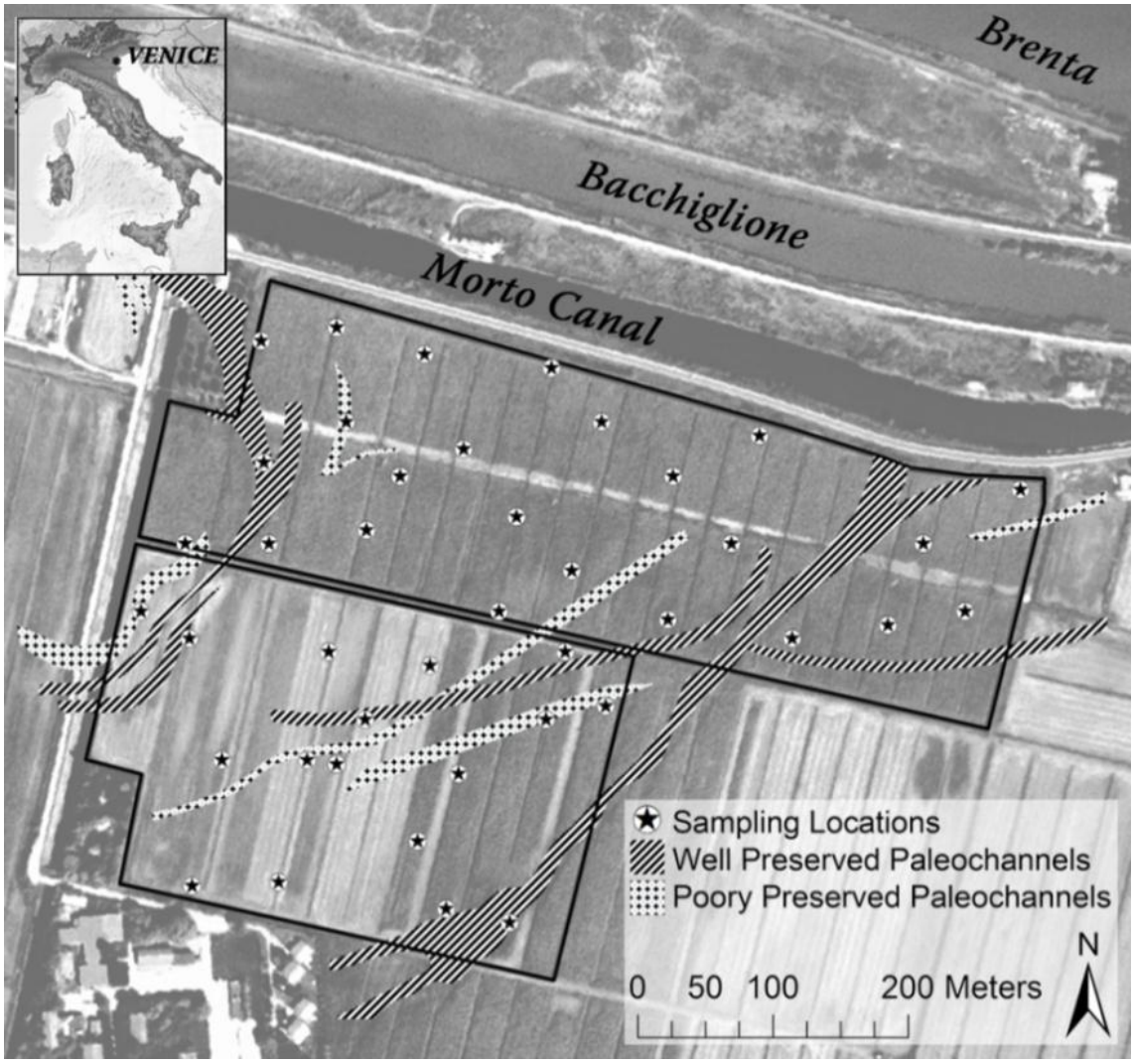

Figure 4.1. Map of the study area with highlights on local poorly and well preserved paleochannels (after (Donnici et al., 2011)), and soil sampling points location.

2.2. EC_a-directed soil sampling and soil analyses

The EC_a-directed soil sampling scheme discussed in chapter 3 was followed. Both undisturbed and disturbed soil samples were collected in May 2010 in 41 randomly selected points of the original sampling scheme. Disturbed samples were taken at 4 depth increments: 0-0.15, 0.15-0.45, 0.45-0.8, and 0.8-1.2 m. Undisturbed cores were extracted with a hydraulic sampler from the first 1-m profile and then analyzed at 0-0.15, 0.15-0.45, 0.45-0.8, and 0.8-1.00 m for bulk density (ρ_b, Mg m^{-3}). Disturbed

samples were analyzed for several physical-chemical properties. Soil electrical conductivity ($EC_{1:2}$, dS m^{-1}) and pH of a soil-water extract (ratio 1:2) (Ministero delle Politiche Agricole e Forestali, 1998) with an *EC*-pH-meter (S47K SevenMulti, Mettler Toledo, Greifensee, Switzerland). $EC_{1:2}$ measurements can be converted into the commonly used electrical conductivity of saturated paste extract (EC_e) values according to the following equation, which was calibrated for a subset of the soil samples used in this study:

$$EC_e = 6.29 \times EC_{1:2} - 0.96 \quad (4.1)$$

Texture was determined with a laser particle size analyzer (Mastersizer 2000, Malvern Instruments Ltd, Great Malvern, United Kingdom). Total C, soil organic carbon (SOC), and total N and S (%) were determined using the Vario Macro Cube CNS analyzer (Elementar Analysensysteme GmbH, Hanau, Germany). Inorganic carbon was converted to percentage of $CaCO_3$. The C:N ratio was calculated from SOC and total N.

Furthermore, in spring 2012, a micro elevation (*Z*, m) survey was carried out with the Trimble FM 1000 CNH (Trimble Navigation Ltd., Sunnyvale, CA, USA) real time kinematic (RTK) system at 1147 locations across the study site with a vertical accuracy of ± 0.02 m.

2.3. Apparent electrical conductivity and bare-soil reflectance data

In spring 2011 EC_a readings were acquired with an electromagnetic induction (EMI) sensor (CMD-1, GF Instruments, Brno, Czech Republic). According to the geometrical configuration of the probe the CMD-1 allows two depths of investigation, *Low* and *High* configurations, corresponding to 0-0.75 m (EC_a *Low*) and 0-1.5 m (EC_a *High*) soil depths, respectively. The CMD-1 probe was connected to a DGPS and mounted on a mobile platform, with 0.5 s time acquisition interval, collecting 18053 and 20470 measures across the study site for EC_a *Low* and EC_a *High*. On the same day, gravimetric water content (θ_g) was also assessed in the soil profile at the 41 sampling locations. Even though θ_g is time dependent, its spatial patterns can be assumed fairly constant

throughout the growing seasons (Engman, 1999), thus θ_g data could represent the relative level of plant-available water (Corwin et al., 2003).

The reflectance of bare-soil at 590 nm (VIS) and at 880 nm (NIR) was measured with a handheld active spectrometer (APS1-CropCircle, Holland Scientific, Lincoln, NE, USA) linked with a DGPS, with 1 s time acquisition interval, at 10214 locations across the site, in spring 2012. The well-known normalized difference vegetation index (NDVI) (Rouse et al., 1973) was calculated for bare-soil, as follows:

$$NDVI = \frac{NIR - VIS}{NIR + VIS} \tag{4.2}$$

2.4. Yield data

This study will discuss the 2010 and 2011 maize grain yield data. Maize yield (expressed as with 14% moisture) was measured with a combine harvester equipped with a yield monitor (Agrocom, Claas, Harsewinkel, Germany) and a DGPS. The harvester had an 8 meters header and registered contiguous yield measurements every 5 m (i.e. yield data cells = 40 m^2). Yield data were collected during the 2010 and 2011 harvests. Raw data were corrected setting a lower threshold of 2 Mg ha^{-1}. The operation eliminated nearly all near-zero readings that were mainly due to field-edge effects.

2.5. Data analysis and statistics

Data analysis aimed to validate the SSMU delineation procedure (Fig. 4.2). Firstly, soil data was used to define a yield response model at the 41 locations according to (Corwin et al., 2003), allowing identifying those soil properties significantly influencing yield spatial variability. Secondly, soil proximal-sensing measurements were calibrated (Lesch and Corwin, 2008) against the selected soil properties. Finally proximal-sensing maps were used to delineate SSMUs (Fridgen et al., 2004), which were then validated according to soil and yield spatial variability.

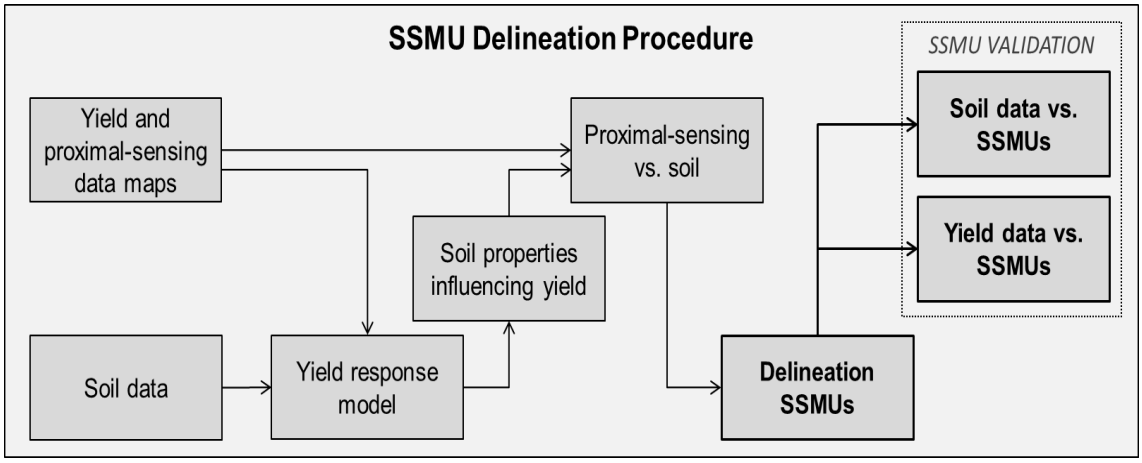

Figure 4.2. Schematics of the workflow for the Site-Specific Management Units (SSMUs) delineation.

2.5.1. Interpolation of elevation and proximal-sensing data

Elevation and proximal-sensing data did not exactly overlay with the soil sampling locations; consequently, such data were interpolated in order to estimate their value at the 41 locations. The spatial correlation structure of each dataset (δ_i) was modeled with isotropic exponential semivariograms:

$$v(\delta_i) = (\eta + \sigma) \times \left(1 - \exp\left(\frac{h}{r}\right)\right) \quad (4.3)$$

where η represents the nugget variance, σ the spatial variance component (partial sill), h the lag distance, and r the range parameter. The non-normally distributed datasets were normalized with the *normal score transformation* (Deutsch and Journel, 1992). The interpolations were made by *Ordinary Kriging* using ArcMap 10.0 (ESRI, Redlands, CA, USA). The goodness of the interpolations were tested with *leave-one-out* cross validations.

2.5.2. Spatial linear models

Ordinary least square (OLS) multiple linear regressions (MLRs) can reliably estimate a spatially distributed random variable when the regression residuals are spatially uncorrelated (Lesch et al., 1995; Lesch and Corwin, 2008; Schabenberger and Gotway,

2004). As a matter of fact MLRs represent a special case of models geostatistical mixed linear models; a more general family of models that include many well-known geostatistical techniques, such as universal kriging (Lesch and Corwin, 2008).

The soil properties were preliminarily tested for multicollinearity, which was observed between clay and sand and silt, between total C and SOC and total S. The suitable explanatory variables for the yield model were therefore Z, $EC_{1:2}$, θ_g, clay, ρ_b, pH, SOC, and $CaCO_3$. The yield response model was calibrated, allowing both linear and quadratic relationships between yield and soil properties (Corwin et al., 2003). The above described approach was performed for each of the individual depth increments and for the weighted average of increasing-depth soil profiles. Best model performances were obtained considering the averaged 0-0.8 m profile, suggesting that such depth was the most representative of the maize root zone in the study site. Multiple linear regressions between proximal-sensing data (i.e. EC_a and bare-soil reflectance) and the significant soil properties were then carried out.

The MLR residuals were examined for outliers, normal distribution (*Shapiro-Wilk Normality Test*; (Shapiro and Wilk, 1965)) and spatial autocorrelation (*Moran's I Test for Residual Spatial Autocorrelation*; (Cliff and Ord, 1981)). The regression models showing a significant residual spatial autocorrelation were then recalculated using the "spdep" (Bivand et al., 2011) library in R (Team, 2012) with the maximum-likelihood approach (Lesch and Corwin, 2008), in order to avoid biased parameter estimates (Cressie, 1993).

2.5.3. Delineation of the Site-Specific Management Units

The SSMUs design was done according to the spatial variability of EC_a and reflectance maps. The management units were delineated using a fuzzy c-means unsupervised clustering algorithm (Odeh et al., 1992) implemented in the Management Zone Analyst (MZA) software (Fridgen et al., 2004). The c-means algorithm aims to identify a continuous group of ancillary data values, minimizing the sum of square distances of all the data points from the cluster centroid. The fuzzy element allows one location to belong to different clusters at different degrees. This membership sharing is controlled

by a weighting exponent that is conventionally set to a value of 1.35 (Odeh et al., 1992). MZA was used with the same settings seen in (Morari et al., 2009), for a range of SSMUs between 4 and 7. The optimum number of SSMU was identified according to the minimization of the fuzziness performance index (FPI) and the normalized classification entropy index (NCE) (Odeh et al., 1992). FPI ($0 \leq FPI \leq 1$) is a measure of the amount of membership-sharing that occurs among management zones. The larger the FPI value, the strongest sharing of membership between the selected SSMUs. NCE ($0 \leq NCE \leq 1$) models the degree of disorganization created by dividing the data set into SSMUs. The lower the NCE value the higher the amount of organization between management zones.

The SSMU delineation was finally validated comparing the differences in soil properties between management units, and the differences in maize production in the SSMUs in 2010 and 2011. The comparison was done with the analysis of variance (ANOVA). Spatial correlations among the residuals were modeled using the "spdep" library in R with a generalized linear model approach.

3. Results and Discussion

3.1. Elevation, soil proximal-sensing, and yield spatial characterization

Elevation, soil-proximal sensing, and yield data showed high variability across the study site (Table 4.1). The semivariogram models specifications and cross-validation statistics for elevation and proximal-sensing data are shown in table 4.2. In general the semivariograms were characterized by very low nugget values. The cross-validations showed very low estimation errors, with slopes of the observed-predicted relationship very close to one and low root mean square errors. EC_a *Low* showed very similar spatial patterns with EC_a *High*. Analogously, VIS and NIR were comparable to NDVI. The maps for *Z*, EC_a *Low*, NDVI and yield in the two years are reported in Figs. 4.3, 4.4, and 4.5.

Table 4.1. Yield, proximal sensing, and elevation data† mean and range statistics.

	Number of sites	Mean	Minimum	Maximum	Standard deviation	Standard error	Coefficient of variation	Skewness	Kurtosis
Z	1147	-2.52	-3.33	-1.01	0.50	0.015	-0.20	0.64‡	-0.54
EC_a Low	18053	0.65	0.12	1.75	0.32	0.002	0.49	0.66‡	-0.52
EC_a High	20470	1.07	0.31	2.78	0.43	0.003	0.40	0.54‡	-0.54
NIR	10214	0.40	0.03	0.8	0.09	0.001	0.23	0.56‡	0.61‡
VIS	10214	0.23	0.02	0.54	0.08	0.001	0.35	0.98‡	0.65‡
NDVI	10214	0.28	0.15	0.42	0.07	0.001	0.23	0.04	-1.02
Yield 2010	2896	5.78	2.00	11.97	2.40	0.045	0.42	0.38‡	-0.74
Yield 2011	2973	8.76	2.00	14.99	3.28	0.060	0.37	-0.23	-0.85

† *EC_a Low*, apparent electrical conductivity for the 0-0.75 m increment; *EC_a High*, apparent electrical conductivity for the 0-1.5 m increment; NIR, near infrared band reflectance; VIS, visible band reflectance; NDVI, normalized difference vegetative index; *Z*, elevation.

‡ Significant. Skewness is significant if skewness divided by standard error of skewness (SES) > 2. Kurtosis is significant if kurtosis divided by standard error of kurtosis (SEK) > 2. SEK and KEW were calculated according to Tabachnick et al. (2001).

Table 4.2. Semivariogram models specifications‡ and Kriging summary statistics for elevation and proximal-sensing data†.

	Semivariogram model specifications				Kriging statistics	
	η^2	σ^2	*h* (m)	*r* (m)	Cross-validation	RMSE
Z	0.00	1.33	20.00	246.40	-0.03 + 0.99 × observed	0.078
EC_a Low	0.00	1.04	18.00	170.95	0.02 + 1.00 × observed	0.014
EC_a High	0.05	1.12	18.00	202.53	0.01 + 0.99 × observed	0.034
VIS	0.34	0.80	18.00	203.38	0.01 + 0.94 × observed	0.017
NIR	0.39	0.73	18.00	227.52	0.04 + 0.90 × observed	0.028
NDVI	0.04	0.99	18.00	81.34	1.00 × observed	0.004

† *Z*, elevation; *EC_a Low*, apparent electrical conductivity for the 0-0.75 m increment; *EC_a High*, apparent electrical conductivity for the 0-1.5 m increment; NIR, near infrared band reflectance; VIS, visible band reflectance; NDVI, normalized difference vegetative index.

‡ η^2, nugget variance; σ^2, spatial variance component (partial sill); *h*, lag; *r*, range.

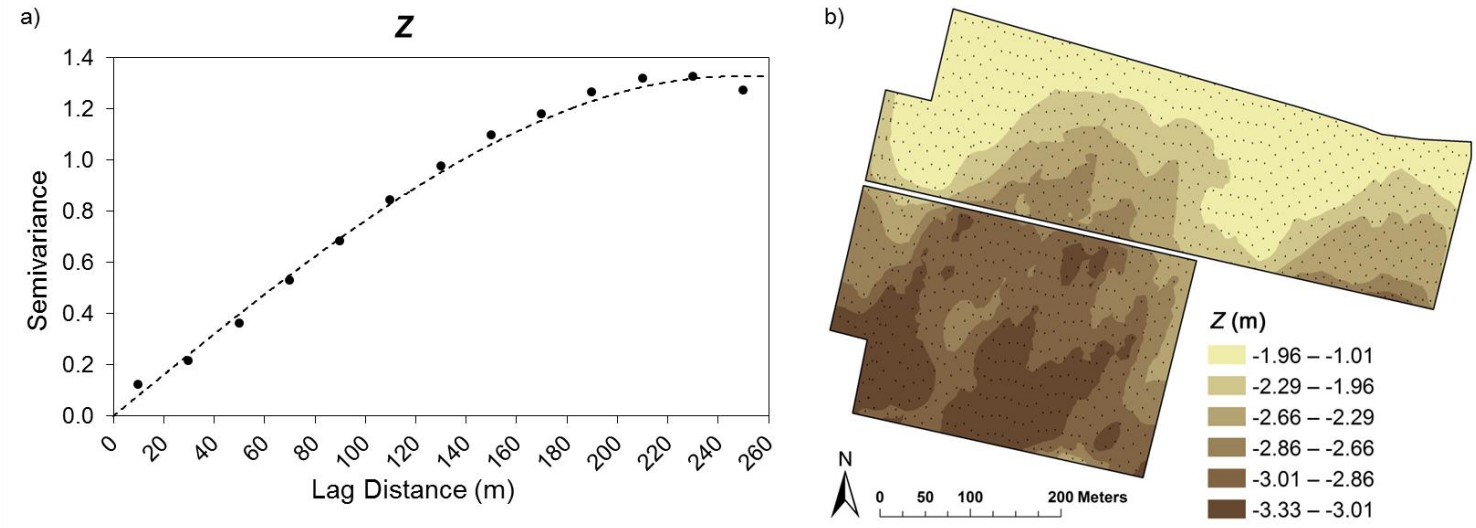

Figure 4.3. *a*) Isotropic semivariogram and *b*) kriged map for *Z*. The dots in the maps represent the survey grids.

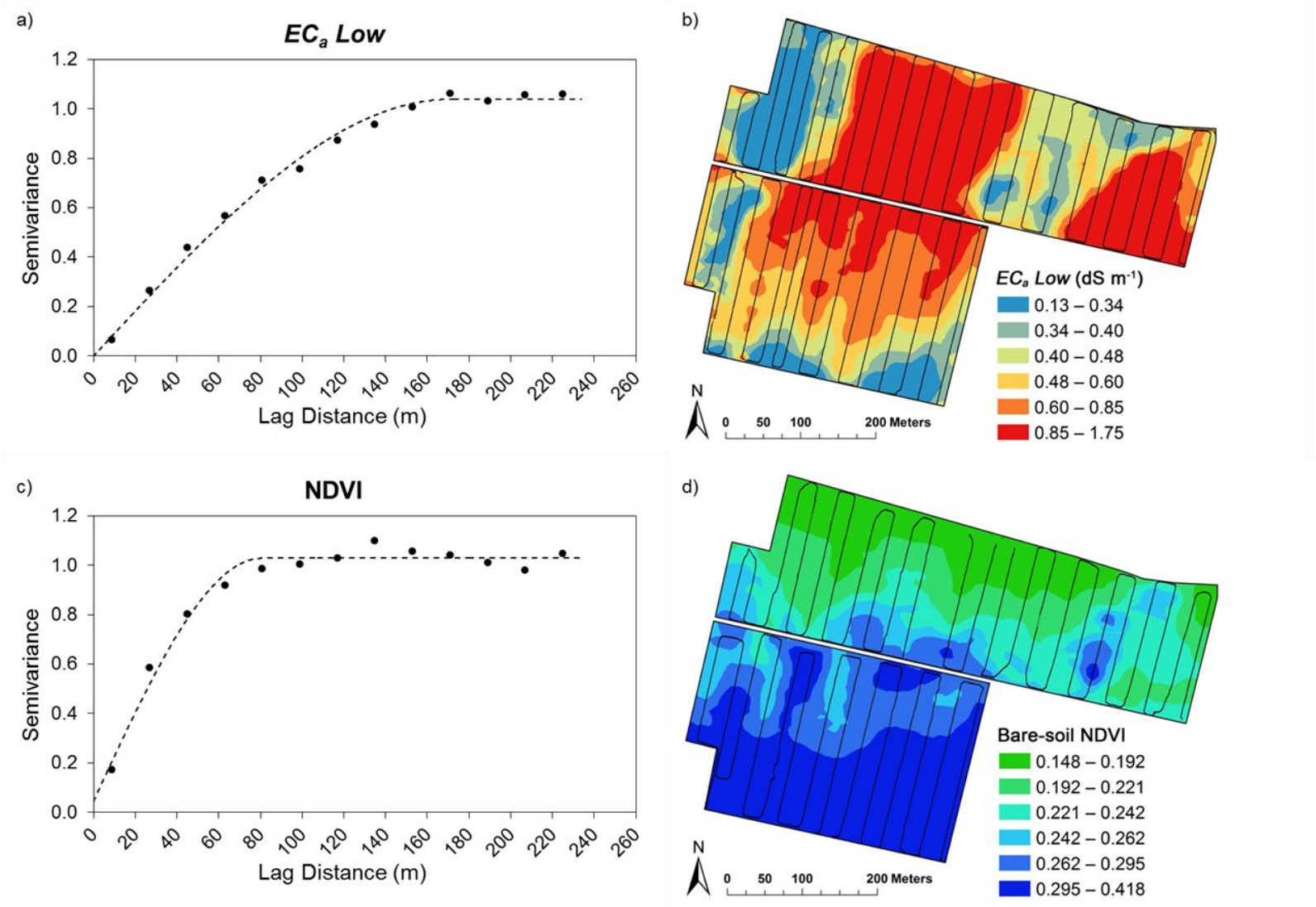

Figure 4.4. Isotropic semivariograms (*a* and *c*) and kriged maps (*b* and *d*) for EC_a *Low* and NDVI. The dots in the maps represent the survey grids.

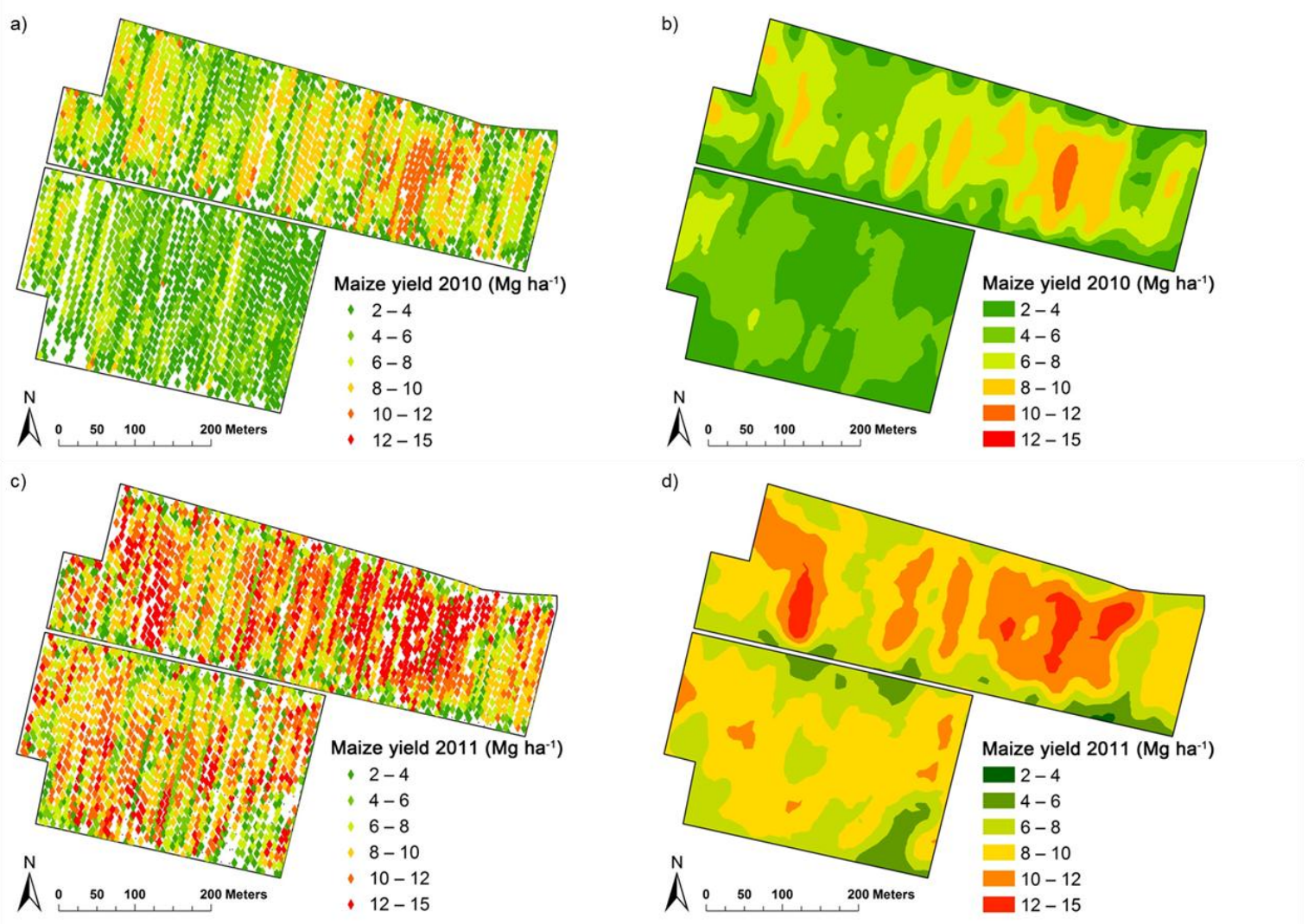

Figure 4.5. 2010 and 2011 yield points (*a* and *c*) and interpolated maps (*b* and *d*).

Elevation is highest in the northern part of the study area, ranging between ca. -2.5 and -1 m asl, and gradually decreases towards the southern part, with a minimum of -3.3 m asl. The EC_a maps showed the lowest values in the paleochannels (<0.50 dS m^{-1}), whereas higher EC_a values were observed in the other zones, especially in the northern part, suggesting drastic differences in soil. The reflectance maps showed similar patterns with the DEM map. In particular NDVI generally ranged between 0.148 and 0.242 in the northern part of the study area, whereas it increased gradually in the southern area with a maximum of 0.418.

Yield data in 2010 was considerably lower than in 2011 as it was compromised by a heavy wind-hail storm occurred on the 13th of August (ca. 0.06 m of rainfall). Consequently the 2010 yield data at the 41 sampling location was not used to fit the maize yield response model. However as the two yield maps showed similar spatial patterns, the 2010 yield data was anyway used for comparison at larger scale (i.e. comparison between SSMUs). In both years the highest yield values were observed in the paleochannels at the northern part of the study. Low yield was observed in the two years in areas either characterized by high EC_a values (in the northern part) or high NDVI values (in the southern part).

3.2. An overview on the soil data

The data for tested soil properties in the 0-0.8m soil increment (table 4.3) will be briefly described in this section, with a particular attention to the soil properties considered for the yield response model (i.e. Z, $EC_{1:2}$, θ_g, clay, ρ_b, pH, SOC, and $CaCO_3$). Correlations between soil properties are shown in table 4.4. All properties were normally distributed, with exception of pH, total carbon, and SOC.

Soil texture was very coarse in the paleochannels, except in the upper part of the eastern paleochannel where finer texture (loam) was observed. Outside the paleochannels, clay decreased gradually from high contents in the North (silty-clay loam) to lower values observed in the very South of the study area (sandy loam). On average, the soils were characterized by mid-high salinity (Abrol et al., 1988). Higher salinity values (>2 dS m^{-1}) were observed in correspondence of high EC_a values. Soil pH values varied drastically

in the area, from < 5.5 in the southern part of the site, to slightly-medium alkaline (>7.5), associated with the well preserved paleochannels and with high clay contents. SOC content, which strongly influenced several physical properties, was generally very high (average: 9.8 %). In mineral soils, organic matter is generally found in higher quantities in soils with fine texture (Lugato et al., 2009). Nevertheless, in organic soils such the ones found in the study area spatial variability of SOC and texture can be unrelated (Shimada et al., 2001). The northern part of the study site, where clay content was the highest, was generally characterized by relatively low SOC content (< 4 %), whereas the well preserved paleochannels showed slightly larger content (<9%). The saline areas and most of the southern part were characterized by high SOC content, generally in the 11-22 % range. As a consequence, higher bulk density values (ρ_b>1.2 Mg m^{-3}) were observed in sandy soil, whereas low ρ_b values (ρ_b<0.7 Mg m^{-3}) were observed in soils with high SOC and clay contents.

Table 4.3. Soil topographic and physicochemical properties mean and range statistics of the average over the 0 to 0.8 m depth increment at the 41 sampling locations.

Soil properties†	Mean	Minimum	Maximum	Standard deviation	Standard error	Coefficient of variation	Skewness	Kurtosis
Z, m	-2.58	-3.15	-1.40	0.39	0.06	-0.15	0.96‡	0.75
$EC_{1:2}$, dS m^{-1}	1.14	0.21	3.30	0.72	0.11	0.63	1.05‡	0.90
θ_g, kg kg^{-1}	0.27	0.08	0.44	0.09	0.01	0.31	-0.06	-0.15
Sand, %	44.09	14.77	73.09	14.87	2.32	0.34	0.42	-0.49
Silt, %	39.74	19.86	56.32	9.09	1.42	0.23	-0.72	-0.13
Clay, %	16.17	6.03	31.38	6.43	1.00	0.40	0.22	-0.44
ρ_b, Mg m^{-3}	0.90	0.51	1.44	0.21	0.03	0.24	0.30	-0.48
pH	7.04	4.45	7.99	0.85	0.13	0.12	-1.54	1.86‡
Total C, %	11.03	3.97	22.22	4.70	0.73	0.43	0.89‡	0.36
$CaCO_3$, %	9.99	0.29	27.07	7.27	1.14	0.73	0.49	-0.79
SOC, %	9.83	1.92	22.19	5.14	0.80	0.52	0.88‡	0.57
Total N, %	0.75	0.22	1.54	0.33	0.05	0.44	0.68	0.14
C:N	12.49	6.26	16.72	2.04	0.32	0.16	-0.72	1.19
Total S, %	0.52	0.11	1.20	0.26	0.04	0.51	0.64	-0.13

† *Z*, elevation; $EC_{1:2}$, electrical conductivity of a soil extract with a soil to water ratio of 1:2; θ_g, gravimetric water content; ρ_b, bulk density; SOC, soil organic carbon; C:N, SOC on total N ratio.

‡ Significant. Skewness is significant if skewness divided by standard error of skewness (SES) > 2. Kurtosis is significant if kurtosis divided by standard error of kurtosis (SEK) > 2. SEK and KEW were calculated according to Tabachnick et al. (2001).

Table 4.4. Correlation matrix for the soil properties† considered in this study. Bold numbers are significant (test for $|r|= 0$) at the $P \leq 0.05$ level; df=39.

	Z	$EC_{1:2}$	θ_g	Sand	Silt	Clay	ρ_b	pH	Tot. C	SOC	$CaCO_3$	Tot. N	C:N	Tot. S
Z	--													
$EC_{1:2}$	-0.09	--												
θ_g	-0.19	**0.64**	--											
Sand	-0.22	-0.23	**-0.35**	--										
Silt	0.14	0.26	**0.42**	**-0.97**	--									
Clay	**0.32**	0.16	0.21	**-0.94**	**0.83**	--								
ρ_b	0.24	**-0.36**	**-0.72**	**0.43**	**-0.50**	-0.29	--							
pH	**0.57**	-0.08	**-0.36**	0.11	-0.16	-0.04	**0.38**	--						
Tot. C	**-0.34**	0.20	**0.31**	0.04	-0.04	-0.05	-0.20	**-0.67**	--					
SOC	**-0.40**	0.21	**0.40**	0.01	0.01	-0.02	-0.28	**-0.73**	**0.98**	--				
$CaCO_3$	**0.57**	-0.17	**-0.56**	0.18	-0.22	-0.10	**0.54**	**0.70**	**-0.49**	**-0.62**	--			
Tot. N	**-0.39**	0.23	**0.39**	-0.03	0.04	0.00	-0.29	**-0.72**	**0.98**	**0.98**	**-0.61**	--		
C:N	**-0.53**	0.13	0.28	**0.37**	**-0.32**	**-0.42**	-0.18	**-0.51**	**0.56**	**0.62**	**-0.65**	**0.56**	--	
Tot. S	-0.29	0.20	0.29	-0.01	0.02	-0.01	-0.24	**-0.61**	**0.95**	**0.93**	**-0.48**	**0.94**	**0.49**	--

† Z, elevation; $EC_{1:2}$, electrical conductivity of a soil extract with a soil to water ratio of 1:2; θ_g, gravimetric water content; ρ_b, bulk density; SOC, soil organic carbon; C:N, SOC on total N ratio.

The relationships between soil properties, yield, and soil proximal-sensing data are shown in in table 4.5. No significant correlations were observed between soil properties and the 2010 yield. Conversely the 2011 yield positively correlated with clay content and negatively with soil salinity and with all the soil properties related to organic matter content. Although soil organic matter is generally known to be beneficial for soil quality (Baldock and Nelson, 2000), high contents of acidic peat can represent a very inhospitable medium for most crops (Andriesse, 1988). Moreover, the organic soils in the study site lay very close to the saline groundwater as they are more affected by subsidation than the mineral soils (Gambolati et al., 2005; Schothorst, 1977).

EC_a *Low* and *High* showed similar correlations with soil properties. EC_a was positively correlated with soil salinity and gravimetric water content, as commonly observed in similar studies (Corwin and Lesch, 2005). Soil bulk density and sand content were negatively correlated with EC_a; confirming that soils with low SOC and clay contents exibit greater resistance to the electrical current (see chapter II).

Significant correlations were observed also between elevation, texture, pH and properties related to organic matter content with optical properties in confirming results from other Authors (Chang et al., 2001; Gomez et al., 2008; Singh et al., 2004; Torrent and Barron, 1993; Viscarra Rossel et al., 2006). Correlations coefficients between VIS and NIR with soil properties were of opposite sign than those (ordinarily of higher significance) of NDVI.

Table 4.5. Pearson correlation coefficients calculated for studied soil properties and average yield, with ancillary data§ and yield.

Soil property†	Yield 2010	Yield 2011		*EC_a Low*		*EC_a High*		VIS		NIR		NDVI	
Z	-0.18	0.24		-0.12		-0.12		**0.72**	**	**0.61**	**	**-0.77**	**
$EC_{1:2}$	-0.19	**-0.34**	*	**0.52**	**	**0.49**	**	-0.18		-0.27		-0.06	
θ_g	-0.29	-0.16		**0.66**	**	**0.64**	**	-0.24		-0.30		0.05	
Sand	-0.01	-0.28		-0.29		**-0.31**	*	**-0.38**	*	-0.27		**0.43**	**
Silt	0.03	0.19		0.30		**0.31**	*	0.28		0.17		**-0.35**	*
Clay	-0.01	**0.36**	*	0.24		0.27		**0.48**	**	**0.38**	*	**-0.51**	**
ρ_b	-0.19	-0.18		**-0.46**	**	**-0.53**	**	0.14		0.15		-0.12	
pH	-0.29	0.23		-0.15		-0.15		**0.55**	**	**0.45**	**	**-0.66**	**
Total C	0.22	**-0.38**	*	0.09		0.08		**-0.42**	**	**-0.36**	*	**0.45**	**
$CaCO_3$	-0.28	0.01		**-0.40**	**	**-0.38**	*	**0.55**	**	**0.48**	**	**-0.52**	**
SOC	0.24	**-0.36**	*	0.15		0.12		**-0.51**	**	**-0.45**	**	**0.52**	**
Total N	0.24	**-0.33**	*	0.20		0.18		**-0.45**	**	**-0.38**	*	**0.46**	**
C:N	0.20	**-0.33**	*	0.15		0.09		**-0.73**	**	**-0.65**	**	**0.68**	**
Total S	0.22	**-0.35**	*	0.11		0.08		**-0.38**	*	**-0.33**	*	**0.40**	*
Yield 2010	---	0.10		0.05		0.13		-0.18		0.25		-0.23	
Yield 2011	0.10	---		0.01		0.11		**0.48**	**	-0.30		**0.45**	**

***** Significant (test for $|r|= 0$) at the $P \leq 0.05$ level; df=39

****** Significant (test for $|r| = 0$) at the $P \leq 0.01$ level; df=39

† Average over the root zone (0-0.8 m). Z, elevation; $EC_{1:2}$, electrical conductivity of a soil extract with a soil to water ratio of 1:2; θ_g, gravimetric water content; ρ_b, bulk density; SOC, soil organic carbon; C:N, SOC on total N ratio

3.3. Yield response model

Equation (4.4) shows the OLS MLR yield response model that best described maize production spatial variability in the study site:

$$Y = 18.70 - 0.48 \times EC_{1:2}{}^{2} - 3.62 \times \rho_b{}^{2} - 0.18 \times SOC - 0.71 \times clay + 0.02 \times clay^{2} + \varepsilon \qquad (4.4)$$

where Y is the estimated 2011 yield and ε is the random error component (Lesch and Corwin, 2008), which was confirmed to be normally distributed and spatially independent. Table 4.6 shows the regression summary for equation (4.4); all the soil parameters were significant ($P<0.05$).

Table 4.6. Ordinary least-squares backward stepwise regression statistics for the yield response model (Equation (4.4))†

Significant regressor variables‡	Coefficients	Standard Error	t	P > |t|
Intercept	18.70	3.19	5.86	<0.001
$EC_{1:2}{}^{2}$	-0.48	0.18	-2.62	0.013
$\rho_b{}^{2}$	-3.62	1.15	-3.15	0.003
SOC	-0.18	0.08	-2.24	0.032
Clay	-0.71	0.33	-2.14	0.039
$Clay^{2}$	0.02	0.01	2.64	0.012
Analysis of variance				
	Df	Sum of Square	Mean square	*F* ratio	*P* > *F*
Model	5	228.45	45.69	7.88	<0.001
Residual	35	202.84	5.80		
Corrected total	40	431.29			

† Dependent variable = average yield (Mg ha^{-1}), number of data points 41, root mean square error = 2.22 Mg ha^{-1}. R^2=0.530, and adjusted R^2=0.463

‡ Average over the root zone (0-0.8 m). $EC_{1:2}$, electrical conductivity of a soil extract with a soil to water ratio of 1:2; *SOC*, soil organic carbon; ρ_b, soil bulk density

According to equation (4.4), increasing values of soil salinity, bulk density, and soil organic carbon content would decrease yield; on the other hand yield would increase with increasing clay content values. The *one-at-a-time* sensitivity analysis reported in table 4.7 indicates clay as the most significant soil property influencing yield in 2011. The sensitivity analysis was carried out by calculating the yield variation due to an individual change of the mean value of the soil properties by 1 standard deviation.

Table 4.7. Degree of predicted yield sensitivity to 1 standard deviation (SD) change in each soil property of equation (4.4).

Parameter sensitivity†	Calculated yield	Percentage change	$EC_{1:2}$	ρ_b	*SOC*	*Clay*
	Mg ha^{-1}	%	dS m^{-1}	kg m^{-3}	%	%
Baseline (Eq. 4.4)	8.43	---	1.14	0.90	9.83	16.17
$EC_{1:2}$ + 1 SD	7.40	12.16	1.86	0.90	9.83	16.17
ρ_b + 1 SD	6.87	18.50	1.14	1.11	9.83	16.17
SOC + 1 SD	7.51	10.93	1.14	0.90	14.97	16.17
Clay + 1 SD	10.03	19.05	1.14	0.90	9.83	22.60

† Average over the root zone (0-0.8 m). $EC_{1:2}$, electrical conductivity of a soil extract with a soil to water ratio of 1:2; ρ_b, soil bulk density; *SOC*, soil organic carbon.

Fig. 4.6 compares the observed and predicted maize yield values. The model described about the 53% of the total yield variability, suggesting that other factors (other than the investigated soil properties) influenced yield in 2011. Moreover, the robustness of this type of yield response models is limited because of the noise in the yield data, which is commonly biased by combine dynamics (Corwin et al., 2003; Simbahan et al., 2004). In fact, the 8m-wide yield data cells (i.e. width of harvester header) often overlapped across the whole site, as the study area is crossed by N-S oriented draining canals, with a spacing of ca. 30 m. It is thus believed that the field layout biased the yield data, causing high differences between data points in neighboring harvest transect.

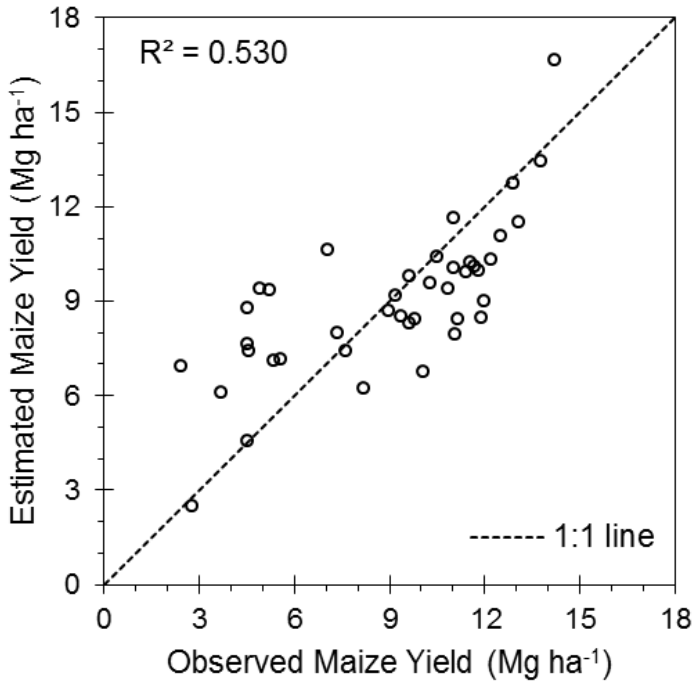

Figure 4.6. Observed vs. predicted maize yield estimates using equation (4.4). Dashed line is a 1:1 relationship.

3.4. Using EC_a and reflectance data to delineate SSMUs

The relations between $EC_{1:2}$, ρ_b, SOC, and clay with the proximal-sensing data were investigated to test if the latters could be used to represent soil spatial variability at the study site.

The sole EC_a was not sufficient to characterize the spatial variability of the four tested soil properties. Indeed EC_a readings could represent only $EC_{1:2}$ and ρ_b variability. Conversely, bare-soil reflectance significantly described SOC and clay. The regressions were similar for VIS and NIR, whereas the regression of NDVI was of opposite sign.

All the OLS MLRs were corrected using the maximum-likelihood approach as they showed spatial autocorrelation of the residuals. EC_a *Low* and NDVI described the spatial variability of the four selected soil properties with the highest significance and R^2.

As commonly done with EC_a data calibration (Lesch et al., 1992), the EC_a *Low* measurements were normalized to their natural logarithm:

$$\ln(EC_a Low) = -0.38 + 0.21 \times EC_{1:2} - 0.61 \times \rho_b + \varepsilon \quad (4.5)$$

with a R^2=0.415 (adjusted R^2=0.385). $EC_{1:2}$ and ρ_b were significant to the 0.004 and 0.018, respectively, whereas the intercept resulted non-significant. According to equation (4.5), high values of soil salinity and low values of soil bulk density would lead to high EC_a *Low* readings. Bulk density is known to correlate with EC_a readings (Corwin, 2008; Rhoades et al., 1999). As a matter of fact, in the study area, low ρ_b values can be observed in areas rich in peat and/or clay, which are known to facilitate the conduction of electricity in the soil (Anderson-Cook et al., 2002; Corwin and Lesch, 2005).

The NDVI regression was characterized by R^2=0.511 (adjusted R^2=0.485):

$$NDVI = 0.251 + 0.003 \times SOC - 0.003 \times clay + \varepsilon \quad (4.6)$$

The intercept and SOC and clay contents terms were significant to the 2×10^{-8}, 0.005, and 0.001 respectively. High SOC contents and low clay contents would increase the NDVI readings of a soil. The observed relationships between VIS and NIR with SOC and clay confirmed results reported by other Authors (Chang et al., 2001; Gomez et al., 2008; Singh et al., 2004; Torrent and Barron, 1993; Uno et al., 2005; Viscarra Rossel et al., 2006). Soil reflectance was in fact smaller for VIS than for NIR (Lillesand et al., 2004; Uno et al., 2005). Increasing SOC contents decreased both VIS and NIR reflectance (Uno et al., 2005). VIS decreased with a higher slope than NIR, increasing therefore NDVI.

The NCE and FPI indices (tables 4.8 and 4.9) indicated that the study site should be divided into five management units. The indices were in general very low (Brock et al., 2005; Morari et al., 2009) confirming that EC_a and bare-soil reflectance provide good ancillary information for SSMU delineation (Roberts et al., 2012). EC_a *Low* and NDVI provided the best values for both NCE and FPI. The concordance of the two indices is an indication of the goodness of the classification (Fridgen et al., 2004; Morari et al., 2009).

Table 4.8. Normalized classification entropy (NCE) index for the fuzzy c-means unsupervised clustering of selected couple of ancillary data†

Ancillary data		Number of SSMUs			
		4	5	6	7
EC_a Low	NDVI	0.031	0.029	0.030	0.039
EC_a Low	NIR	0.030	0.037	0.038	0.038
EC_a Low	VIS	0.032	0.030	0.031	0.036
EC_a High	NDVI	0.031	0.030	0.033	0.039
EC_a High	NIR	0.032	0.036	0.037	0.038
EC_a High	VIS	0.034	0.029	0.030	0.032

† *EC_a Low*, apparent electrical conductivity for the 0-0.75 m increment; *EC_a High*, apparent electrical conductivity for the 0-1.5 m increment; NIR, near infrared band reflectance; VIS, visible band reflectance ; NDVI, normalized difference vegetative index.

Table 4.9. Fuzziness performance index (FPI) for the fuzzy c-means unsupervised clustering of selected couple of ancillary data†.

Ancillary data		Number of SSMUs			
		4	5	6	7
EC_a Low	NDVI	0.056	0.048	0.048	0.062
EC_a Low	NIR	0.054	0.062	0.062	0.061
EC_a Low	VIS	0.058	0.050	0.050	0.057
EC_a High	NDVI	0.055	0.051	0.054	0.061
EC_a High	NIR	0.058	0.060	0.061	0.059
EC_a High	VIS	0.063	0.049	0.049	0.051

† *EC_a Low*, apparent electrical conductivity for the 0-0.75 m increment; *EC_a High*, apparent electrical conductivity for the 0-1.5 m increment; NIR, near infrared band reflectance; VIS, visible band reflectance ; NDVI, normalized difference vegetative index.

The *EC_a Low* and NDVI maps where therefore used to delineate five-SSMUs: hereafter named I, II, III, IV, and V (Fig. 4.7). With such design the forty-one soil sampling locations were grouped into subgroups of seven, nine, seven, nine, and nine points respectively for SSMU I, II, III, IV, and V.

SSMU I was characterized by fairly low *EC_a Low* (< 0.6 dS m^{-1}) and high NDVI (> 0.30) values. SSMU II identified most part of the well-preserved paleochannels, where clay content was very low, with soil showing very low *EC_a Low* (< 0.4 dS m^{-1}) values and NDVI in the 0.19 - 0.26 range. SSMU III was characterized by the highest *EC_a Low* values (> 0.8 dS m^{-1}). SSMU IV was located in the areas with low *EC_a Low* (< 0.6 dS m^{-1}) and low NDVI (< 0.1.9). Finally, fairly high *EC_a Low* (>0.6) and NDVI (> 0.24) values delineated SSMU V.

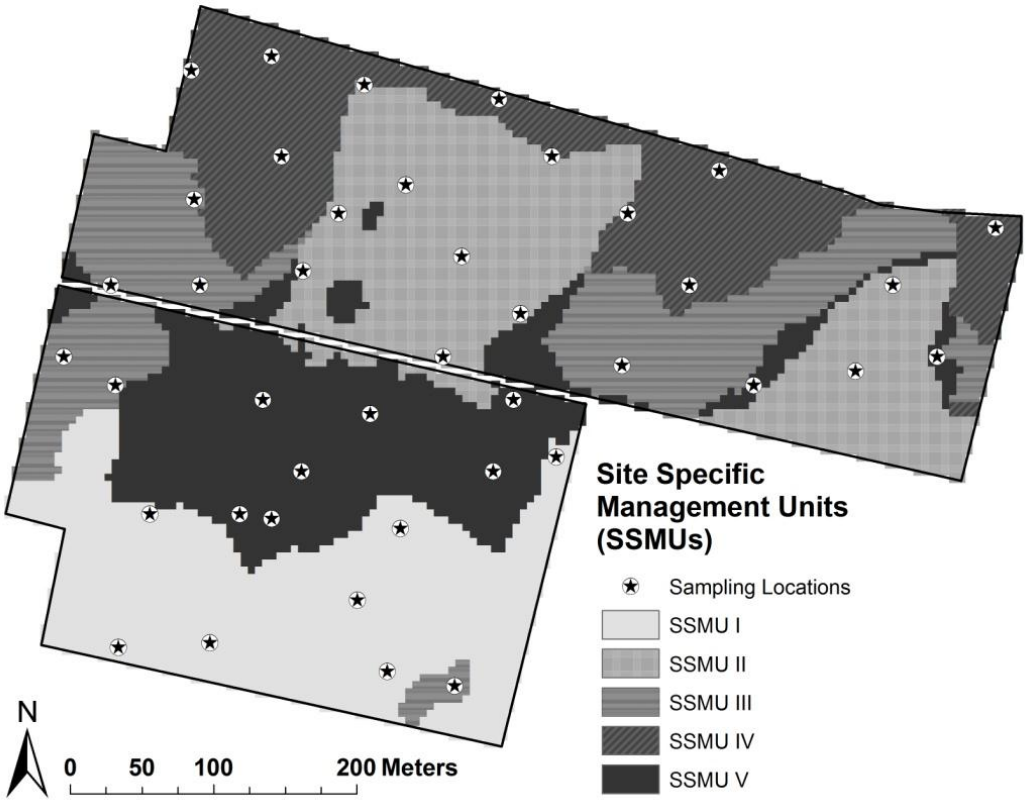

Figure 4.7. Delineation of Site-specific management units (SSMUs) using the fuzzy c-means unsupervised clustering algorithm on EC_a Low and NDVI; with sampling locations.

Fig. 4.8 depicts the value distribution of the soil properties selected in equation (4.4). The proposed SSMU delineation methodology helped identifying a very saline area (SSMU II), where the average $EC_{1:2}$=1.90 dS m^{-1} was almost twice as high as the average salinity observed in the other units (1.05, 0.64, 0.99, and 0.98 dS m^{-1} in SSMUs I, III, IV, and V, respectively). Maize is a crop moderately sensitive to soil salinity: according to the Maas and Hoffman salinity tolerance model (Maas and Hoffman, 1977) the threshold salinity value for optimal maize growth is 1.7 dS m^{-1} (measured as EC_e). Over such threshold maize yield theoretically decreases of 7.4 % per EC_e increment of 1 dS m^{-1}. According to the Maas and Hoffman model (Fig. 4.9), the average salinity values in all SSMUs were however above the critical threshold (EC_e, 1.7 dS m^{-1} ≈ $EC_{1:2}$, 0.42 dS m^{-1}) for maize. The model was recalculated converting EC_e into $EC_{1:2}$ after equation (4.1). For salinity over the threshold value, maize yield theoretically decreases of 46.6% per $EC_{1:2}$ increment of 1 dS m^{-1}.

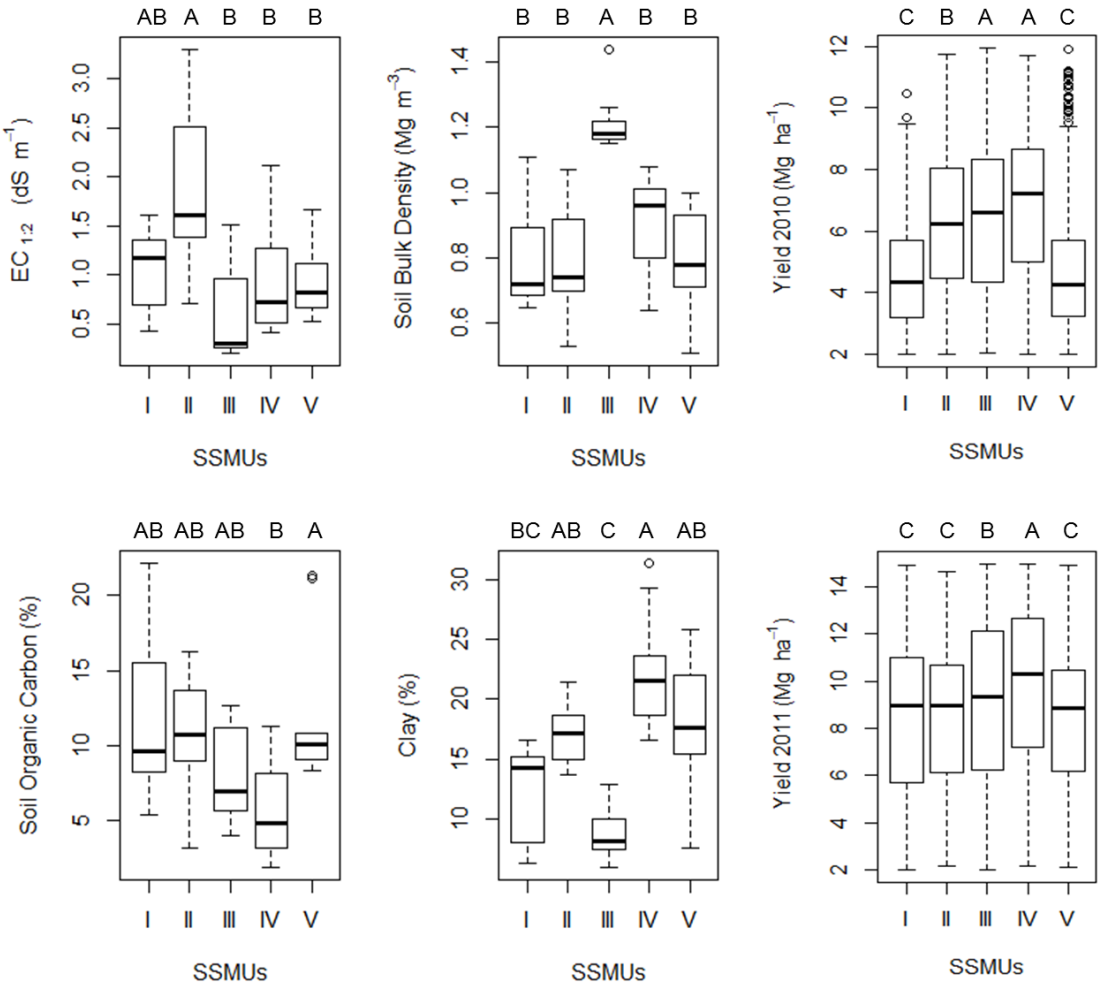

Figure 4.8. Boxplots for: $EC_{1:2}$, electrical conductivity of a soil extract with a soil to water ratio of 1:2; soil bulk density; soil organic carbon content; clay content; and the yield data of 2010 and 2011. The bold line crossing the rectangles represents the median value; circles represent outliers. Capital letters on top of the box-plots indicate a significant difference within SSMUs at the $p<0.05$ level.

SSMU II was characterized by the highest observed ρ_b values (average=1.22 Mg m^{-3}), the lowest observed clay content values (average=8.86 %), and low to mid-low soil salinity.

SSMU IV was characterized by mid-low salinity and the lowest observed SOC (5.80%) and highest clay (22.53%) average contents. It is worth noticing that the northern part of the eastern paleochannel, where texture was finer, was mainly confined also within SSMU IV.

SSMUs I, III, and V were the units with the highest observed SOC average contents (~12%), in particular SSMUs I and V were characterized by very high maximum SOC contents (SOC > 20 %), which were associated with the lowest observed pH values.

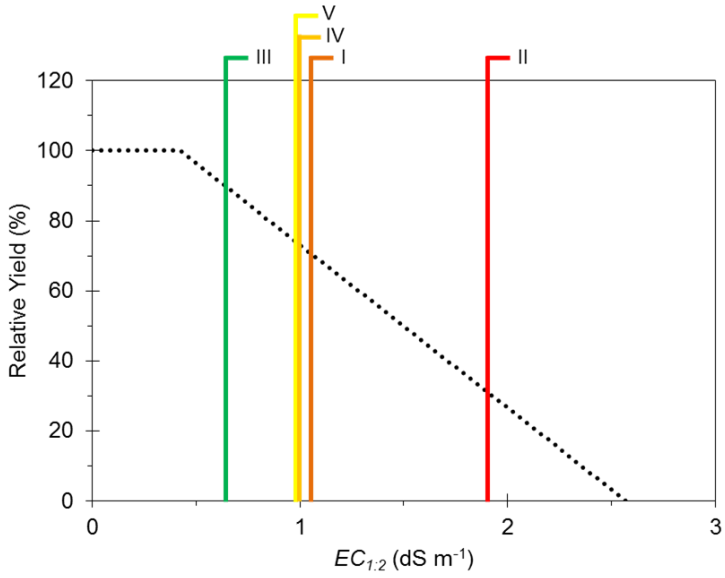

Figure 4.9. The average salinity values in the five management units over the (Maas and Hoffman, 1977) maize yield salinity response curve.

The yield data of 2010 and 2011 were classified according to the five management units. SSMUs I, II, III, IV, and V had 555, 659, 510, 588, and 584 yield data points assigned in 2010 and 595, 690, 506, 564, 618 in 2011.

In 2010 the SSMUs III and IV were identified as the most productive zones in the study site, suggesting that the low salinity and SOC contents observed in the paleochannels were favorable for maize in 2010. SSMU II, SSMU I and V were characterized by a lower average yield. The very shallow water table and high SOC contents, which in the southern portion of the study site are associated with pH values generally in the 4.5 – 5.5 range, could have increased the effect of soil salinity on yield reduction.

In 2011, the yield in SSMU III was significantly smaller than SSMU IV, suggesting that the low rainfall occurred in that year significantly reduced the yield in the areas of the

paleochannels with low clay and high ρ_b. The effect of salinity (SSMU II) seemed to be confirmed in 2011. As a matter of fact SSMU II showed an average yield almost as low as observed in units I and V, which were confirmed as the areas with the lowest maize production also in 2011.

4. Summary and Conclusions

Yield maps provide useful information on the spatial variability of crop productivity. Yield is affected by the combined effect of a large range of factors including edaphic, meteorological, biological, and anthropogenic factors. From a management point of view, many of these factors are unpractical to control and mitigate. Indeed, farmers generally limit their efforts trying to improve the sole effects of edaphic and biological (e.g. pests) factors. As edaphic factors are very consistent in time, long-term site-specific soil management is a reliable solution in areas characterized by high spatial variability (Corwin and Lesch, 2010; Hornung et al., 2006; Mzuku et al., 2005). Understanding which soil properties play a major role on limiting the spatial variability of yield is therefore essential. Soil salinity ($EC_{1:2}$), bulk density (ρ_b), and organic carbon (SOC) and clay contents were identified as the soil properties significantly influencing the spatial variability of maize yield, in a study site affected by saltwater intrusion at the southern edge of the Venice Lagoon, Italy. The spatial distribution of these soil properties could be significantly represented with intensive surveys of apparent electrical conductivity (for $EC_{1:2}$ and ρ_b) and bare-soil reflectance (for SOC and clay contents). Delineating Site-Specific Management Units (SSMUs) on the base of apparent electrical conductivity and bare-soil reflectance data allowed identifying areas of major agronomic interest: one homogeneous area with optimal maize yield and zones affected by high soil salinity, very coarse texture (i.e. sandy paleochannels), and two zones areas with both soil salinity and high organic carbon content. In particular, dry conditions led to a yield decrease in the very sandy portions of the paleochannels (SSMU III). This evidence suggests that water deficiency stress may occur in SSMU II in dry years.

Site-specific irrigation could definitely be the ideal solution in sandy and saline SSMU (Corwin et al., 2006) in order to exploit the potential of each zone and carry out a more sustainable use of soil.

5. References

Abrol, I., J.S.P. Yadav and F. Massoud. 1988. Salt-affected soils and their management. FAO. Food & Agriculture Org, Rome, Italy.

Adamchuk, V.I., J. Hummel, M. Morgan and S. Upadhyaya. 2004. On-the-go soil sensors for precision agriculture. Comput. Electron. Agric. 44:71-91.

Allen, R.G., L.S. Pereira, D. Raes and M. Smith. 1998. Crop evapotranspiration-guidelines for computing crop water requirements-FAO irrigation and drainage paper 56. FAO, Rome 300:6541.

Anderson-Cook, C.M., M. Alley, J. Roygard, R. Khosla, R. Noble and J. Doolittle. 2002. Differentiating soil types using electromagnetic conductivity and crop yield maps. Soil Sci. Soc. Am. J. 66:1562-1570.

Andriesse, J. 1988. Nature and management of tropical peat soils. FAO. Food & Agriculture Org, Rome, Italy.

Baldock, J.A. and P.N. Nelson. 2000. Soil organic matter. p. B25-B84. *In* M.E. Sumner (ed.) Baldock, J.A., and nelson, P.N. (2000) *soil organic matter*. in: . CRC press,, B25-B84. Handbook of soil science. CRC Press, Boca Raton, FL, USA.

Bear, J. 1988. Dynamics of fluids in porous media. Dover publications, New York, USA.

Bivand, R., L. Anselin, O. Berke, A. Bernat, M. Carvalho, Y. Chun, C. Dormann, S. Dray, R. Halbersma and N. Lewin-Koh. 2011. Spdep: Spatial dependence: Weighting schemes, statistics and models. R Package Version 0.5-31, URL Http://CRAN.R-Project.org/package=Spdep.

Brock, A., S. Brouder, G. Blumhoff and B. Hofmann. 2005. Defining yield-based management zones for corn–soybean rotations. Agron. J. 97:1115-1128.

Carbognin, L. and L. Tosi. 2003. Il progetto ISES per l'analisi dei processi di intrusione salina e subsidenza nei territori meridionali delle province di padova e venezia. Istituto Per Lo Studio Della Dinamica Delle Grandi Masse, CNR, Rome, Italy.

Carbognin, L., P. Teatini and L. Tosi. 2005a. Land subsidence in the venetian area: Known and recent aspects. Giornale Di Geologia Applicata 1:5-11.

Carbognin, L., F. Rizzetto, L. Tosi, P. Teatini and G. Gasparetto-Stori. 2005b. L'intrusione salina nel comprensorio lagunare veneziano. il bacino meridionale. Giornale Di Geologia Applicata 2:119-124.

Carbognin, L., G. Gambolati, M. Putti, F. Rizzetto, P. Teatini and L. Tosi. 2006. Soil contamination and land subsidence raise concern in the Venice watershed, Italy. Management of Natural Resources, Sustainable Development and Ecological Hazards. Vol.99: 691-700.

Chang, C.W., M.J. Mausbach, D.A. Laird and C.R. Hurburgh. 2001. Near-infrared reflectance spectroscopy–Principal components regression analyses of soil properties. Soil Sci. Soc. Am. J. 65:480-490.

Cliff, A.D. and J.K. Ord. 1981. Spatial processes: Models & applications. Pion London, .

Corwin, D. 2008. Past, present, and future trends of soil electrical conductivity measurements using geophysical methods. p. 17-44. *In* B.J. Allred, J.J. Daniels and Reza Eshani M. (eds.) Handbook of agricultural geophysics. CRC Press. Taylor & Francis Group, New York, NY, USA.

Corwin, D. and S. Lesch. 2010. Delineating site-specific management units with proximal sensors. Geostatistical Applications for Precision Agriculture139-165.

Corwin, D. and S. Lesch. 2005. Apparent soil electrical conductivity measurements in agriculture. Comput. Electron. Agric. 46:11-43.

Corwin, D., S. Lesch, J. Oster and S. Kaffka. 2006. Monitoring management-induced spatio–temporal changes in soil quality through soil sampling directed by apparent electrical conductivity. Geoderma 131:369-387.

Corwin, D., S. Lesch, P. Shouse, R. Soppe and J. Ayars. 2003. Identifying soil properties that influence cotton yield using soil sampling directed by apparent soil electrical conductivity. Agron. J. 95:352-364.

Cressie, N.A.C. 1993. Statistics for spatial data. John Wiley & Sons, New York, USA.

De Franco, R., G. Biella, L. Tosi, P. Teatini, A. Lozej, B. Chiozzotto, M. Giada, F. Rizzetto, C. Claude and A. Mayer. 2009. Monitoring the saltwater intrusion by time lapse electrical resistivity tomography: The chioggia test site (venice lagoon, italy). J. Appl. Geophys. 69:117-130.

Deutsch, C.V. and A.G. Journel. 1992. Geostatistical software library and user&s guide. Oxford university press, New York, NY, USA.

Donnici, S., F. Rizzetto, L. Tosi, E. Scudiero, F. Morari, R. Deiana, G. Cassiani and P. Teatini. 2011. Saltwater contamination in the venice lagoon margin, italy. 1: The influence of the geomorphological setting. p. 212. *In* S. Keesstra and G. Mol (eds.) Wageningen conference on applied soil science, Wageningen, The Netherlands. 18 - 22 September 2011 2011. Wageningen UR, Communication Services, Wageningen, The Netherlands.

Engman, E. 1999. Remote sensing in hydrology. p. 165-177. *In* D.L. Corwin, K. Loague and T.R. Ellsworth (eds.) Assessment of non-point source pollution in the vadose zone. Geophysical Monogr.108. ed. American Geophysical Union, Washington, DC, USA.

Fridgen, J.J., N.R. Kitchen, K.A. Sudduth, S.T. Drummond, W.J. Wiebold and C.W. Fraisse. 2004. Management zone analyst (MZA): Software for subfield management zone delineation. Agron. J. 96:100-108.

Gambolati, G., M. Putti, P. Teatini, M. Camporese, S. Ferraris, G.G. Stori, V. Nicoletti, S. Silvestri, F. Rizzetto and L. Tosi. 2005. Peat land oxidation enhances subsidence in the venice watershed. EOS Transactions, American Geophysical Union 86(23): 217‑224.

Gomez, C., R.A. Viscarra Rossel and A.B. McBratney. 2008. Soil organic carbon prediction by hyperspectral remote sensing and field vis-NIR spectroscopy: An australian case study. Geoderma 146:403-411.

Hornung, A., R. Khosla, R. Reich, D. Inman and D. Westfall. 2006. Comparison of site-specific management zones: Soil-color-based and yield-based. Agron. J. 98:407.

Johnson, C.K., R.A. Drijber, B.J. Wienhold and J.W. Doran. 2008. Productivity zones based on bulk soil electrical conductivity. p. 263-272. *In* B.J. Allred, J.J. Daniels and M. Reza Ehsani (eds.) Handbook of agricultural geophysics. CRC Press, Taylor & Francis Group, New York, NY, USA.

Johnson, C., R. Eigenberg, J. Doran, B. Wienhold, B. Eghball and B. Woodbury. 2005. Status of soil electrical conductivity studies by central state researchers. Trans. ASAE 48:979-989.

Larson, W. and P. Robert. 1991. Farming by soil. Soil Management for Sustainability.Soil and Water Conserv.Soc., Ankeny, IA, USA.

Lesch, S.M., J. Rhoades, L. Lund and D. Corwin. 1992. Mapping soil salinity using calibrated electromagnetic measurements. Soil Sci. Soc. Am. J. 56:540-548.

Lesch, S.M., D.J. Strauss and J.D. Rhoades. 1995. Spatial prediction of soil salinity using electromagnetic induction techniques 1. statistical prediction models: A comparison of multiple linear regression and cokriging. Water Resour. Res. 31:373-386.

Lesch, S. and D. Corwin. 2008. Prediction of spatial soil property information from ancillary sensor data using ordinary linear regression: Model derivations, residual assumptions and model validation tests. Geoderma 148:130-140.

Li, Y., Z. Shi and F. Li. 2007a. Delineation of site-specific management zones based on temporal and spatial variability of soil electrical conductivity. Pedosphere 17:156-164.

Li, Y., Z. Shi, F. Li and H.Y. Li. 2007b. Delineation of site-specific management zones using fuzzy clustering analysis in a coastal saline land. Comput. Electron. Agric. 56:174-186.

Lillesand, T.M., R.W. Kiefer and J.W. Chipman. 2004. Remote sensing and image interpretation. John Wiley & Sons Ltd, New York, NY, USA.

Lugato, E., F. Morari, S. Nardi, A. Berti and L. Giardini. 2009. Relationship between aggregate pore size distribution and organic–humic carbon in contrasting soils. Soil Tillage Res. 103:153-157.

Maas, E. and G. Hoffman. 1977. Crop salt tolerance\-current assessment. Journal of the Irrigation and Drainage Division 103:115-134.

Ministero delle Politiche Agricole e Forestali. 1998. Metodi di analisi fisica del suolo. Franco Angeli Editore, Milan, Italy.

Morari, F., A. Castrignanņ and C. Pagliarin. 2009. Application of multivariate geostatistics in delineating management zones within a gravelly vineyard using geo-electrical sensors. Comput. Electron. Agric. 68:97-107.

Mulder, V., S. De Bruin, M. Schaepman and T. Mayr. 2011. The use of remote sensing in soil and terrain mapping--A review. Geoderma.

Mzuku, M., R. Khosla, R. Reich, D. Inman, F. Smith and L. MacDonald. 2005. Spatial variability of measured soil properties across site-specific management zones. Soil Sci. Soc. Am. J. 69:1572-1579.

Odeh, I., A. McBratney and D. Chittleborough. 1992. Soil pattern recognition with fuzzy-c-means: Application to classification and soil-landform interrelationships. Soil Sci. Soc. Am. J. 56:505-516.

Post, D., A. Fimbres, A. Matthias, E. Sano, L. Accioly, A. Batchily and L. Ferreira. 2000. Predicting soil albedo from soil color and spectral reflectance data. Soil Sci. Soc. Am. J. 64:1027-1034.

Rhoades, J.D., F. Chanduvi and S.M. Lesch. 1999. Soil salinity assessment: Methods and interpretation of electrical conductivity measurements. Food & Agriculture Organization of the UN (FAO), Rome, Italy.

Rizzetto, F., L. Tosi, M. Bonardi, P. Gatti, A. Fornasiero, G. Gambolati, M. Putti and P. Teatini. 2002. Geomorphological evolution of the southern catchment of the venice lagoon (italy): The zennare basin. Scientific Research and Safeguarding of Venice, Corila Research Program: 2001 Results. Venice, Italy.

Rizzetto, F., L. Tosi, L. Carbognin, M. Bonardi, P. Teatini, E. Servat, W. Najem, C. Leduc and A. Shakeel. 2003. Geomorphic setting and related hydrogeological implications of the coastal plain south of the Venice Lagoon, Italy. IAHS Publ. Wallingford, UK.

Robert, P. 2002. Precision agriculture: A challenge for crop nutrition management. Plant Soil 247:143-149.

Roberts, D.F., R.B. Ferguson, N.R. Kitchen, V.I. Adamchuk and J.F. Shanahan. 2012. Relationships between soil-based management zones and canopy sensing for corn nitrogen management. Agron. J. 104:119-129.

Rouse, J., R. Haas, J. Schell and D. Deering. 1973. Monitoring vegetation systems in the great plains with ERTS. p. 309-317. *In* Third ERTS symposium, 1973. NASA SP-351, NASA, Washington, D.C., USA.

Schabenberger, O. and C.A. Gotway. 2004. Statistical methods for spatial data analysis. Chapman & Hall/CRC, CRC Press, Taylor & Francis Group, New York, NY, USA.

Schothorst, C. 1977. Subsidence of low moor peat soils in the western netherlands. Geoderma 17:265-291.

Shapiro, S.S. and M.B. Wilk. 1965. An analysis of variance test for normality (complete samples). Biometrika 52:591-611.

Shimada, S., H. Takahashi, A. Haraguchi and M. Kaneko. 2001. The carbon content characteristics of tropical peats in central Kalimantan, Indonesia: Estimating their spatial variability in density. Biogeochemistry 53:249-267.

Simbahan, G., A. Dobermann and J. Ping. 2004. Screening yield monitor data improves grain yield maps. Agron. J. 96:1091-1102.

Singh, D., I. Herlin, J.P. Berroir, E. Silva and M. Simoes Meirelles. 2004. An approach to correlate NDVI with soil color for erosion process using NOAA/AVHRR data. Advances in Space Research 33:328-332.

Tabachnick, B.G., L.S. Fidell and S.J. Osterlind. 2001. Using multivariate statistics. HarperCollins College Publisher. New York, NY, USA.

Team, R. 2012. R: A language and environment for statistical computing. R Foundation for Statistical Computing. Vienna, Austria.

Teatini, P., T. Strozzi, L. Tosi, U. Wegmüller, C. Werner and L. Carbognin. 2007. Assessing short-and long-time displacements in the Venice coastland by synthetic aperture radar interferometric point target analysis. Journal of Geophysical Research 112:F01012.

Torrent, J. and V. Barron. 1993. Laboratory measurement of soil color: Theory and practice. SSSA Special Publication 31:21-21. Madison, WI, USA.

Uno, Y., S. Prasher, R. Patel, I. Strachan, E. Pattey and Y. Karimi. 2005. Development of field-scale soil organic matter content estimation models in eastern canada using airborne hyperspectral imagery. Canadian Biosystems Engineering 47:1.9-1.14.

Van Uffelen, C., J. Verhagen and J. Bouma. 1997. Comparison of simulated crop yield patterns for site-specific management. Agricultural Systems 54:207-222.

Viezzoli, A., L. Tosi, P. Teatini and S. Silvestri. 2010. Surface water–groundwater exchange in transitional coastal environments by airborne electromagnetics: The venice lagoon example. Geophys. Res. Lett. 37:L01402.

Viscarra Rossel, R., V. Adamchuk, K. SUDDUTH, N. Mckenzie and C. Lobsey. 2011. Proximal soil sensing: An effective approach for soil measurements in space and time. Adv. Agron. 113:237-282.

Viscarra Rossel, R., D. Walvoort, A. McBratney, L. Janik and J. Skjemstad. 2006. Visible, near infrared, mid infrared or combined diffuse reflectance spectroscopy for simultaneous assessment of various soil properties. Geoderma 131:59-75.

Vitharana, U.W.A., M. Van Meirvenne, D. Simpson, L. Cockx and J. De Baerdemaeker. 2008. Key soil and topographic properties to delineate potential management classes for precision agriculture in the European loess area. Geoderma 143:206-215.

Chapter 5

General Conclusions

1. General Conclusions

Soil quality preservation and improvement are primary goals for remunerative sustainable agriculture. The southern margin of the Venice Lagoon is one of the most important agricultural basins in Veneto Region. Most of the agriculture in the area is directed to support dairy and beef farms. Nevertheless, the area is home of many remunerative *protected designation of origin* (*PDO*) and *protected geographical indication* (*PGI*) horticultural species, including the *Radicchio di Chioggia* (radicchio of Chioggia, *Cichorium intybus* L.), the *Cipolla Bianca di Chioggia* (white onion of Chioggia, *Allium cepa* L.); the *Carota di Chioggia* (carrot of Chioggia, *Daucus carota* L.); and the *Cicoria Catalogna Gigante di Chioggia* (giant puntarelle of Chioggia, *Cichorium intybus* L.). Therefore, if the current soil-quality issues (e.g. soil salinity, land subsidence) were not properly dealt with, agricultural activities in the area might be subject to severe economic losses in the future.

Conventional agricultural practices are not ideal at the southern edge of the Venice Lagoon as the area is characterized by high soil spatial heterogeneity. On the other hand, precision agriculture practices could be implemented allowing managing nutrients and water supply with a site-specific approach. Especially in areas affected by soil salinity or characterized very coarse texture the use of site-specific irrigation could increase soil quality and crop production: either applying enough water for salinity leaching, or for the plants to have optimal water content in the rootzone.

Soil water content and pore-water salinity can be monitored using dielectric and apparent electrical conductivity (EC_a) measures with low-cost capacitance-resistance sensors. Unfortunately, low-cost capacitance sensors are known to provide biased dielectric readings in conductive soils (e.g. saline soils, soils with high clay and organic carbon content). Moreover in order to estimate pore-water salinity from resistivity readings, its relationship with EC_a, soil type, and water must be understood and characterized. As seen in chapter 2, sensor-specific calibrations can guarantee accurate soil water content and pore-water electrical conductivity (EC_p) estimations even over contrasting soils and in very saline conditions. EC_p as presented in this dissertation is to be interpreted more as a function of the contribution of the soil solution in the conduction of electricity

through soil, rather than as a measure of its salinity, especially at very low water contents. In fact when soil dries and the biggest pores are emptied, the concentration of salts in the pore-water has been proved to increase. Nevertheless when the water content is high enough for the liquid phase to create a continuum pathway for electricity then pore-water salinity should then generally coincide with EC_p. Such limit has been pointed as roughly the 50% of the water content at field capacity (Corwin et al., 2012).

Farmers could therefore create affordable and reliable networks of rootzone sensors monitoring water content and salinity at some selected locations. Ideally the monitoring sites of such kind of networks should be chosen in order to represent large areas sharing similar edaphic characteristics.

In chapter 4 a methodology for Site-Specific Management Units delineation is presented and validated. Understanding soil spatial variability and identifying soil factors limiting crop production are key factors in the SSMU delineation. The only reasonable way of characterizing large areas is through the use of intensive proximal- and remote-sensing data surveys, which can be calibrated over a relative small number of soil samples. Spatial measures of EC_a are very commonly used with such aim. In this dissertation they were confirmed to be nearly essential for soil characterization, especially under saline conditions. Nevertheless, the use of EC_a could not be sufficient to represent a satisfactory number of soil properties. Therefore, the complementary use of other types of low-cost ancillary data (e.g. reflectance data or aerial imagery) should be common practice. This is particularly relevant in areas where the soil components influencing electricity conduction are not correlated as observed at the Ca' Bianca study site (see chapter 4).

EC_a-directed soil sampling scheme optimizations are a suggested practice as EC_a correlates to a large variety of soil properties. However, as seen in chapter 4, EC_a measurements do not always correlate with a sufficient number of soil properties. In this dissertation bare-soil reflectance was used to characterize the spatial variability of those soil properties not correlating with EC_a. Therefore it would be ideal to optimize sampling schemes also according to other ancillary data rather than the sole EC_a. In particular, as continuous simulated annealing allows multi-step scheme delineation, one step of the optimization could be carried out according to the spatial variability of complementary soil ancillary

data. Nevertheless, the selection of a first set of sampling locations on the base of the sole geometry of a study site should help minimizing biases due to those soil properties not correlated with EC_a.

The sampling scheme in chapter 3 was designed with the purpose of allocating a larger number of points were the spatial variability of EC_a was higher using EC_a-gradient maps as a weight for the optimizing criterion (i.e. Minimization of the Weighted Means of the Shortest Distances criterion) in the simulated annealing. As a consequence of that, many points were actually close or on the very borders of the SSMU delineated in chapter 4. The sampling scheme presented in chapter 3 was delineated in order to facilitate the kriging interpolations of soil properties (Van Groenigen and Stein, 1998). Different sampling scheme delineation criteria could be more effective for different porpoises, including representing at best the average values of soil properties within homogeneous areas. Indeed, other sampling scheme delineation techniques (i.e. response surface sampling design (Lesch, 2005)) allow selecting locations representing the centroid of zones sharing similar attributes. When using simulated annealing a similar approach could be followed substituting the EC_a-gradient maps with ones of reverse (i.e. complementary) values. The use of such weighting map would in fact allow densifying the sampling scheme in areas showing small spatial heterogeneity.

The area at the southern edge of the Venice Lagoon shares the same geomorphological settings characterizing the Ca' Bianca site. The methodologies presented in this dissertation could therefore be easily applied to other fields in the area.

The presence of large farms in this area should foster precision agriculture practices. Farmers are however missing the proper tools and knowledge to carry out accurate site-specific management. As a matter of fact, the acquisition of mobile equipment for EC_a surveys would be too expensive of an investment for a single farmer. As commonly done in other countries (e.g. USA) third-part professionals should offer the proximal-sensing survey service to farmers. Unfortunately such kind of service is not provided nowadays.

Site-specific irrigation may not however be the solution to all the issues affecting the land at the southern margin of the Venice Lagoon. Soil quality should be also preserved and improved carrying out less impacting agricultural practices, especially in the peaty areas.

Land subsidation is in fact going to be a major concern in the next decades, as peat is continuously oxidized because of heavy soil tillage. The consequent loss of soil organic matter decreases the depths of the vadose zone area, potentially magnifying the effects of salt accumulation in the soil profile.

2. References

Corwin, D., S. Lesch and D. Lobell. 2012. Laboratory and field measurements. p. 295-341. *In* W. Wallender and K. Tanji (eds.) Agricultural salinity assessment and management. ASCE manual and reports on engineering practice no. 71 2nd ed. ASCE, Reston, VA, USA.

Lesch, S. 2005. Sensor-directed response surface sampling designs for characterizing spatial variation in soil properties. Comput. Electron. Agric. 46:153-179.

Van Groenigen, J.W. and A. Stein. 1998. Constrained optimization of spatial sampling using continuous simulated annealing. J. Environ. Qual. 27:1078-1086.

Acknowledgements

I am particularly grateful to my supervisor, Prof. Francesco Morari, and my co-supervisors, Dr. Pietro Teatini and Prof. Antonio Berti, for helping me so much through my doctorate years. I was greatly inspired and motivated by their expertise, devotion, and enthusiasm for research.

I really want to thank Dr. Dennis L. Corwin and the USDA Soil Salinity Lab. staff for their support during my stay in Riverside, California. Dr. Corwin's profound knowledge and enthusiasm on apparent soil electrical conductivity field applications was very inspiring and helpful for my personal scientific formation. I also thank Dr. Corwin for co-supervising Chapter 4.

I am also truly thankful to Giovanni Favaron, Michele Ongarato, Dino Campaci, Roberto Pasqualotto, Dr. Riccarco Polese, Diego Mengardo, Dr. Dal Ferro Nicola, and Dr. Flavio Da Ronch for their help and support in the field activity; to Dr. Rita Deiana for her help in the EMI surveys; and to Dr. Gianluca Simonetti and Davide Piragnolo, for soil chemical and physical analyses.

My PhD research was funded the University of Padua research program "GEO-RISKS: Geological, morphological and hydrological processes: monitoring, modeling and impact in the north-eastern Italy", WP4.